# Novel Regulators of Glucagon Secretion from α-Cells

By

Troy Hutchens

Dissertation

Submitted to the Faculty of the

Graduate School of Vanderbilt University

in partial fulfillment of the requirements

for the degree of

DOCTOR OF PHILOSOPHY

in

Chemical and Physical Biology

December, 2015

Nashville, Tennessee

Approved:

Anne K. Kenworthy, Ph.D.

Jin Chen, MD, Ph.D.

Kevin D. Niswender, M.D., Ph.D.

David A. Jacobson, Ph.D.

David W. Piston, Ph.D.

**ACKNOWLEDGEMENTS**

Science is not a solitary endeavor. In the work described here and in my training I have been fortunate to have the support of a number of individuals and groups that deserve my thanks. Firstly, I would like to thank my mentor David W. Piston for his invaluable role in my training as a scientist. He has provided wonderful guidance for both my scientific and career pursuits. I would also like to thank all of the past and present members of the Piston lab, with whom I've had the pleasure of working with. Special thanks goes out to Alessandro Ustione, for being my go to source for technical advice and for being there whenever I needed to talk over my approach and my science. The Piston lab has been a truly great environment in which to spend my time as a graduate student.

I would also like to thank both the Vanderbilt Medical-Scientist Training Program and the Chemical and Physical Biology Program. The high level and operating efficiency of these programs speaks volumes about their leadership and administrative teams. Additionally, I would like to thank my thesis committee Anne K. Kenworthy, Jin Chen, Kevin D. Niswender, and David A. Jacobson for their thoughtful suggestions and guidance throughout my graduate school tenure.

Lastly, I would be remiss if I did not thank my wonderful wife Mary Hutchens. Without her love and support, my graduate school experience would not have been the same. Sharing in the graduate school experience, she understands the trials and tribulations that graduate school presents and has always been my closest confidante.

Financially, the work describe here has been supported by NIH grants DK098659 and DK098838 and the Iacocca Family Foundation. Flow Cytometry was performed utilizing the

Vanderbilt Medical Center Flow Cytometry Shared Resource Core, supported by NIH grants CA68485 and DK058404. Plasma hormones were analyzed by the Vanderbilt Hormone Assay and Analytical Services Core, supported by NIH grants DK059637 and DK020593. Additionally, the Vanderbilt Medical-Scientist Training Program is supported in part by NIH grant GM07347.

# TABLE OF CONTENTS

## LIST OF TABLES

**Table** **Page**

## LIST OF FIGURES

**Figure** **Page**

# CHAPTER 1
# INTRODUCTION

## 1.1 Introductory Comments

The work presented here focuses on the regulation of glucagon secretion from the islets of Langerhans. There is currently no consensus model for the action of the primary regulator of glucagon secretion, glucose. Rather, several competing models have emerged from the literature. The introduction provided in Chapter 1 is designed to provide the background necessary to understand the significance of glucose homeostasis, the roles that insulin and glucagon play in maintaining glucose homeostasis, and how these roles are disrupted in diabetes. This introduction is also designed to review current models of glucose-regulated glucagon secretion, important to understanding the relevance of the work presented in Chapters 2 and 3. Chapter 2 presents a new juxtacrine-mediated model of glucagon secretion through the EphA/ephrin-A signaling pathway. Chapter 3 reports on the regulation of glucagon secretion by an unknown factor secreted by brown adipose tissue. In my graduate career, I have had the pleasure of being involved with a number of smaller projects and collaborations. These projects represent diverse research foci, but necessitate similar quantitative and qualitative fluorescence imaging techniques and are discussed in Chapter 4. Chapter 5 is an informal discussion on the future directions of the projects discussed in the previous chapters.

## 1.2 Glucose Homeostasis

Glucose is a tightly regulated metabolic substrate. Despite large changes in glucose input (from fasting to ingestion of carbohydrate-rich meal) and glucose utilization (from resting to heavy exercise), blood glucose values are maintained within a narrow window (~4.0-9.0 mM / ~70-160 mg/dl) [1]. Maintenance of this narrow window of blood glucose values is physiologically vital, as deviations below and above these values can lead to significant organ dysfunction.

### 1.2.1 Hypoglycemia

Low blood glucose, or hypoglycemia, is injurious to the brain. Unlike other highly metabolically active tissues, the brain cannot utilize free fatty acids (FFA) due to their inability to cross the blood-brain barrier and thus, it is dependent on glucose as an energy source. Additionally, the brain has a very limited capacity to store glucose, so it is dependent on constant supply of glucose from plasma. Other potential energy sources, such as ketone bodies are not plentiful enough to be a viable energy source except under conditions of starvation when their availability is increased [2]. Functional brain failure (as characterized by the loss of cognitive function, aberrant behavior, seizures, and coma) occurs at plasma glucose concentrations of ~2.7 mM (~49 mg/dl) [3,4]. Neuronal death occurs at glucose concentrations of ~1 mM (~17 mg/dl) [3,4]. A number of mechanisms are thought to mediate the process of hypoglycemia-induced neuronal death, including activation of glutamate receptors following glutamate release, generation of reactive oxygen species, zinc release from neurons, increased poly(ADP-ribose) polymerase activity, and increases in mitochondrial permeability [4]. The observation of numerous overlapping and independent mechanisms to prevent hypoglycemia reflects the significance of its highly deleterious and immediate consequences.

### 1.2.2 Hyperglycemia

Elevated plasma glucose, or hyperglycemia, produces a different set of complications. Acutely, hyperglycemia can cause severe dehydration through osmotic diuresis which can lead to circulatory failure, coma, and death. Chronically, hyperglycemia results in tissue-specific dysfunctions which cause a number complications, including retinopathy, neuropathy and nephropathy [5]. These complications result in an increased risk of morbidity and mortality, as evidenced by diabetic patients with poorly controlled blood glucose. Hyperglycemia exposes all of the cells in the body to high levels of glucose. Most cells are able to cope with this increased extracellular glucose by decreasing glucose transport, thus keeping a relatively stable concentration of intracellular glucose. However, certain cell types including capillary endothelial cells in the retina, peripheral neurons and Schwann cells, and mesangial cells in the renal glomerulus are unable to decrease glucose transport, and thus develop high concentrations of intracellular glucose leading to glucose toxicity [6]. Numerous theories have been hypothesized to explain the molecular mechanisms underlying the adverse effects associated with hyperglycemia and glucose toxicity. Connecting these theories is the idea that increased glucose metabolism through various pathways (glycolysis, polyol/aldol reductase, hexosamine) results in a number of byproducts and signaling molecules (reactive oxygen species, advanced glycation endproducts, diacylglycerol, uridine diphosphate N-acetylglucosamine) that alter gene expression or protein function and ultimately result in cellular damage and dysfunction [5,6]. In addition to maintaining a steady supply of glucose, as required for brain function, there is also a survival advantage in preventing the buildup of

excess blood glucose, supporting the need for tight regulation of blood glucose within a narrow concentration window.

### 1.2.3 Regulation of Glucose Homeostasis

Given the biological importance of maintaining a narrow window of blood glucose concentrations, it is unsurprising that the regulation of glucose homeostasis has developed into a robust system with multiple redundant layers of regulation involving numerous interdependent organ systems [7–10]. The largest regulators of blood glucose concentration are the counter-regulatory hormones insulin and glucagon. These two hormones are responsible for maintaining euglycemia in response to glucose/carbohydrate ingestion and fasting (Figure 1-1). The ingestion of carbohydrates causes an increase in blood glucose that stimulates the release of insulin into the bloodstream which in turn results in a lowering of blood glucose. Conversely, maximal release of glucagon into the bloodstream occurs during fasting (when blood glucose is low) and acts to increase blood glucose and prevent hypoglycemia.

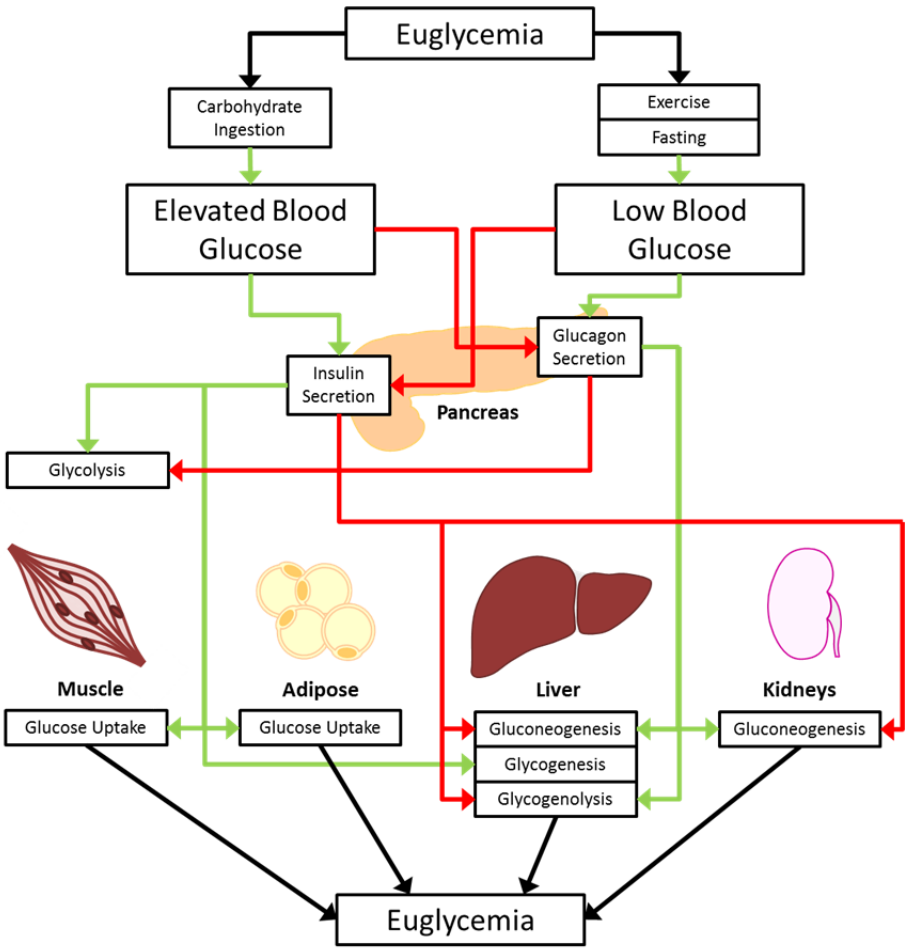


**Figure 1-1 Schematic of glucose homeostasis as regulated by insulin and glucagon.** Green represents activation and red represents inhibition of the processes described.

## 1.3 Insulin and Insulin Signaling

### 1.3.1 Insulin Biosynthesis

Insulin synthesis takes place in β-cells within the pancreatic islets of Langerhans (discussed in 1.6). Human insulin is a 51-amino acid peptide (5808 Da) dimer composed of an A-chain and a B-chain linked together by two disulfide bonds. The sequence and structure of insulin is highly conserved across vertebrates [11]. Initially, insulin starts out as a single 110-amino acid preproprotein known as a known as preproinsulin. The first 24-amino acid residues of preproinsulin form a signal peptide that traffics the peptide into the lumen of the rough

endoplasmic reticulum (RER) [12]. Upon entering the lumen of the RER, the 24-amino acid signal peptide is cleaved, producing proinsulin. Proinsulin is further processed in the RER, resulting in appropriate folding and formation of disulfide bonds between the A- and B-chains. Following trafficking through the cis- and trans-Golgi networks, proinsulin is selectively sorted into a regulated secretion pathway where it is packaged into secretory granules. Proinsulin is further processed by two endopeptidases known as propeptide convertase 1 and 2 that cleave proinsulin at 2 positions, releasing a peptide fragment known as C-peptide. An exoprotease (carboxypeptidase E) then cleaves a pairs of basic peptides from the C-terminal of the B-chain to produce mature insulin [12]. Within secretory granules, mature insulin forms stable hexamers through coordination with zinc ions [13]. Insulin secretory granules are then released through exocytosis in response to various regulatory stimuli (discussed in 1.7 and 1.8).

### 1.3.2 Action of Insulin

Insulin is a potent anabolic hormone responsible for a diverse set of physiologic effects. In addition to its role in the regulation of blood glucose levels, insulin produces a general anabolic effect on other macronutrients (peptides and lipids). Insulin inhibits proteolysis while promoting both the uptake of amino acids and protein synthesis. Additionally, insulin inhibits lipolysis while promoting the uptake of free fatty acids, lipid synthesis, and the esterification/storage of free fatty acids. Together, these effects result in the clearance of amino acids and triglycerides from the blood stream and the storage of both macronutrients. Here, I will focus on the similar roles that insulin plays in the regulation of blood glucose through inhibiting the production of new glucose (gluconeogenesis), inhibiting the release of

stored glucose (glycogenolysis) while promoting its uptake and storage (glycogenesis) (Figure 1-1).

### 1.3.3 Insulin Signaling Mechanisms

Canonical insulin signaling occurs through interaction between insulin and the insulin receptor (IR), though insulin is also capable of stimulating the insulin-like growth factor-1 (IGF-1) receptor at high concentrations [14]. The IR is a ~320 kDa tetramer, consisting of 2 α- and 2 β-subunits. The IR is widely expressed across a number of different tissues. However, with respect to glucose regulation, insulin primarily acts on muscle, adipose, liver, and kidney tissue. Insulin effects on other tissues are considered to be physiologically important, but are not directly related to glucose homeostasis [12]. The IR is a receptor tyrosine kinase (RTK). Similar to other RTKs, ligand binding results in autophosphorylation of the IR and a conformational change that increases the activity of the kinase domain [15]. The diverse signaling that occurs following IR activation can be separated into two major pathways; the phosphatidylinositol 3-kinase (PI3K) pathway and the mitogen-activated protein kinase (MAPK) pathway.

The majority of the metabolic actions of insulin signaling are mediated through the PI3K pathway. In the PI3K pathway, activated IR phosphorylates insulin-receptor substrate-1 (IRS-1), which in turn binds and activates PI3K. Activated PI3K stimulates the uptake of glucose and its storage as glycogen through a complex system of phosphorylations [16,17]. PI3K phosphorylates phosphatidylinositol (4,5)-bisphosphate ($PIP_2$) to generate phosphatidylinositol (3,4,5)-trisphosphate ($PIP_3$) . PIP3 binds to and activates protein kinase B (PKB), which phosphorylates and inactivates glycogen synthase kinase (GSK). Inactive GSK is incapable of phosphorylating

and inactivating glycogen synthase (GS), and thus GS catalyzes the conversion of glucose to glycogen [18]. This primarily occurs in muscle and in the liver. Activated PKB also stimulates the uptake of glucose in muscle and fat through the phosphorylation of TBC1 domain family member 4 (TBC1D4) which leads to the activation of Rab proteins that facilitate the translocation of glucose transporter type 4 (GLUT4) to the plasma membrane [19,20]. Once at the plasma membrane, GLUT4 facilitates the diffusion of glucose into cells along its concentration gradient. Once inside the cell, glucose is phosphorylated to glucose 6-phosphate by glucokinase (liver) or hexokinase (muscle), preventing its diffusion back outside the cell and ensuring an inward concentration gradient (Figure 1-2).

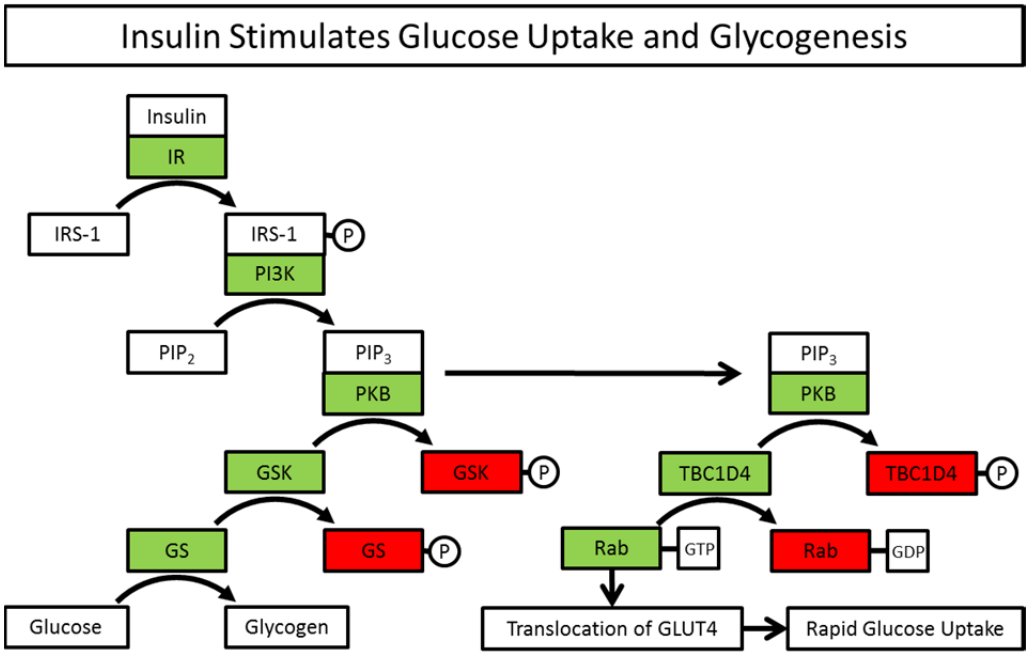


**Figure 1-2 Schematic depicting molecular mechanism of insulin-induced glucose uptake and stimulation of glycogenesis.** Green represents active and red represents inactive enzymes.

Insulin signaling inhibits gluconeogenesis and glycogenolysis directly, through inactivation of key enzymes involved in glucose metabolism and through the down regulation of their expression. Insulin signaling activates a phosphoprotein phosphatase-1 (PP1) that dephosphorylates the bifunctional enzyme phosphofructokinase 2/fructose bisphosphatase 2 (PFK2/FBP2). Dephosphorylation of PFK2/FBP2 leads to activation of PFK2 activity and a decrease in FBP2 activity. Together, this leads to increased production of fructose-2,6-bisphosphate (F26BP) from fructose-6-phosphate (F6P)that activates phosphofructokinase 1 (PFK1) and inhibits fructose bisphosphatase (FBP), stimulating glycolysis and inhibiting gluconeogenesis, respectively [21] (Figure 1-3).

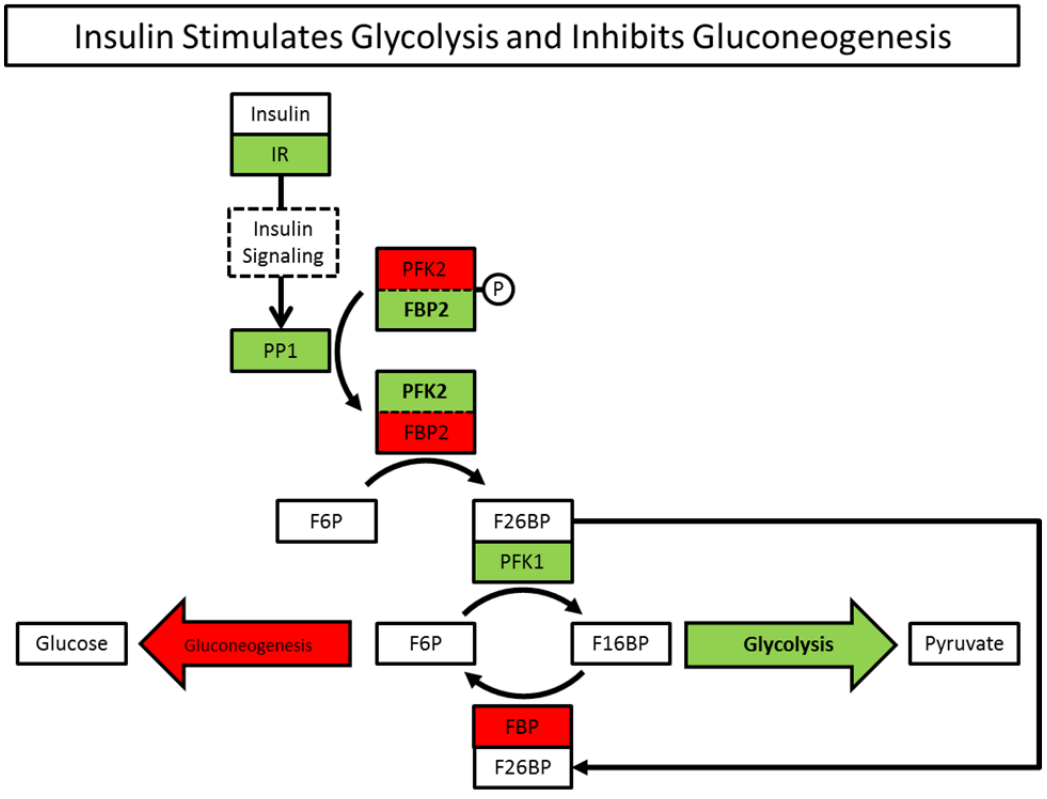


**Figure 1-3 Schematic depicting molecular mechanism of insulin-induced stimulation of glycolysis and inhibition of gluconeogenesis.** Green represents active and red represents inactive enzymes/processes.

Glycogenolysis is inhibited through insulin-mediated activation of PP1 and phosphodiesterase (PDE). PP1 dephosphorylates and inactivates both phosphorylase kinase (PK) and glycogen phosphorylase *a* (GP-a). PDE converts cyclic adenosine monophosphate (cAMP) to adenosine triphosphate (ATP) and prevents cAMP from binding to and activating protein kinase A (PKA), which mediates the phosphorylation and activation of PK. PK catalyzes the phosphorylation of glycogen phosphorylase *b* (GP-b) into GP-a. Thus, preventing the activation of PK prevents the phosphorylation and activation of GP-a, which is required for breaking down glycogen into glucose-1-phosphate (G1P) [12] (Figure 1-4). Also through the PI3K pathway, insulin signaling results in the down-regulation of phosphoenolpyruvate carboxykinase and glucose-6-phosphatase [22,23]. By inhibiting the expression of these key metabolic enzymes involved in gluconeogenesis and glycogenolysis, insulin signaling prevents further increases in blood glucose.

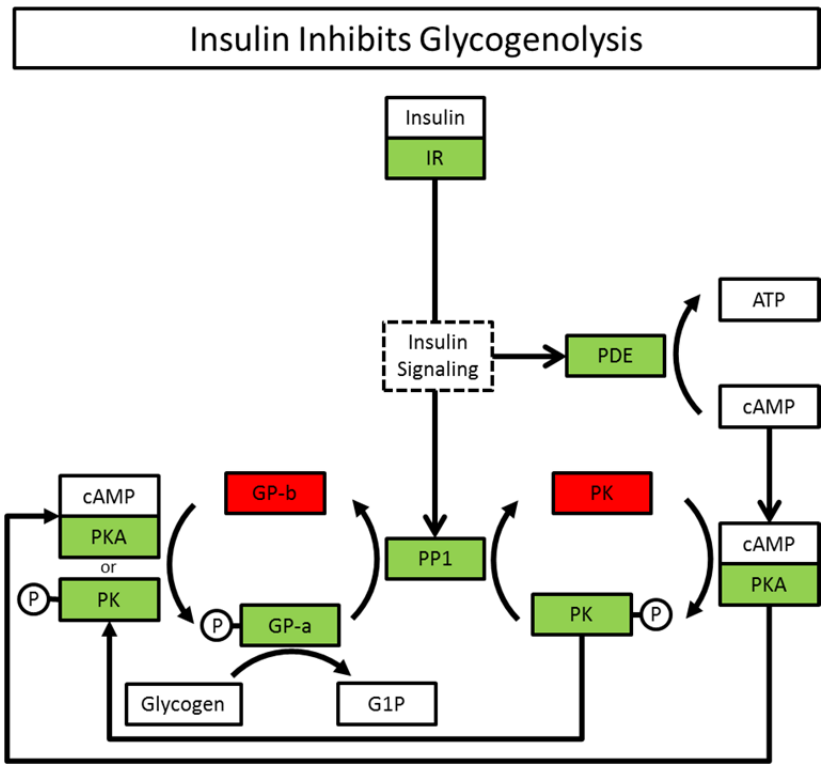


**Figure 1-4 Schematic depicting molecular mechanism of insulin-induced inhibition of glycogenolysis.** Green represents active and red represents inactive enzymes.

## 1.4 Glucagon and Glucagon Signaling

### 1.4.1 Glucagon Biosynthesis

Glucagon is primarily synthesized in α-cells within pancreatic islets of Langerhans (discussed in 1.6). Glucagon (29-amino acids, 3485 Da) is 1 of several distinct and active peptides that are derived from a preproprotein known as preproglucagon. Similar to insulin processing, preproglucagon is converted into proglucagon through the cleavage of a short signal peptide. Tissue-specific expression of propeptide convertase enzymes determine which product(s) is (are) generated from proglucagon. Propeptide convertase 2 plays a critical role generating glucagon from proglucagon in α-cells [24]. Alternative processing in other cell types results in the production of different active peptides [25]. Within intestinal L-cells and K-cells, proglucagon is

cleaved to generate glucagon-like peptide 1 (GLP1) and gastric inhibitory polypeptide (GIP), respectively. GLP1 and GIP are metabolic hormones known as incretins that play important roles in the regulation of glucose homeostasis (discussed in 1.2). Once packaged into secretory granules, glucagon is released through exocytosis in response to a number of physiologic states and stimuli.

### 1.4.2 Action of Glucagon

Counter-regulatory to insulin, the main role of glucagon is to maintain adequate blood glucose levels necessary to prevent the deleterious effects of hypoglycemia during fasting. Without continuous input from ingestion, the body quickly metabolizes the glucose available in the bloodstream and additional glucose must be introduced either from the release of free glucose from glycogen stores (glycogenolysis) or from new synthesis from glucagon precursors (gluconeogenesis). Glucagon acts on both of these pathways, promoting glycogenolysis and gluconeogenesis (Figure 1-1).

### 1.4.3 Glucagon Signaling Mechanisms

Glucagon acts through complex cell-specific signaling pathways to produce a variety of effects on a diverse set of target tissues. Glucagon-mediated regulation of blood glucose primarily occurs through the regulation of hepatic glycogenolysis and gluconeogenesis. Traditionally, glucagon was thought to solely act on the liver. However, glucagon has been shown to regulate a number of other processes in additional tissues, including kidney, intestinal smooth muscle, specific central nervous system (CNS) neurons, cardiac tissue, and adipose tissue; all of which

express the glucagon receptor. As the majority of glucagon's effects on glycogenolysis and gluconeogenesis occurs in the liver, this section will focus on the glucagon-mediated regulation of hepatic glucose metabolism. The glucagon receptor is a ~62 kDa G protein-coupled receptor (GPCR) that is coupled to a $G_s$ alpha subunit. Binding of glucagon to its receptor releases the $G_\alpha$ complex that activates adenylyl cyclase (AC) and stimulates the production of cAMP from ATP. cAMP binds to and activates PKA. PKA then mediates the glucagon-induced increase in both glycogenolysis and gluconeogenesis[21,26]. In glucagon-mediated stimulation of glycogenolysis, PKA initiates a phosphorylation cascade, phosphorylating and activating phosphorylase kinase which in turn phosphorylates inactive GP-b into active GP-a. GP-a then goes on to catalyze the release of G1P from glycogen (Figure 1-5).

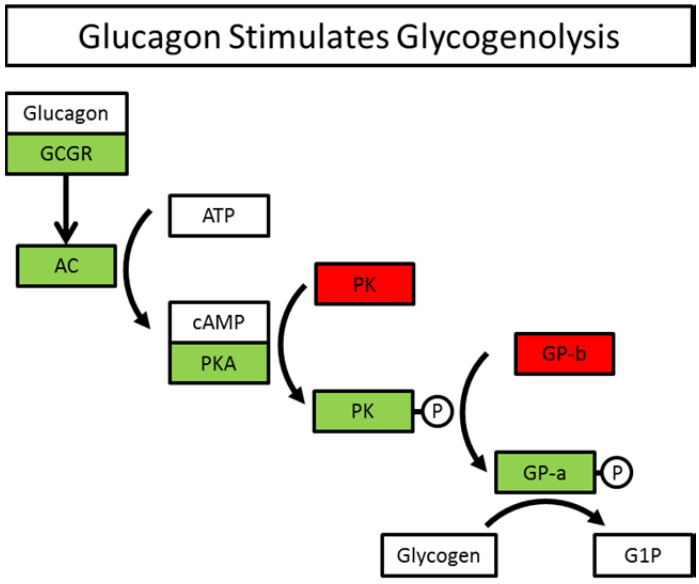


**Figure 1-5 Schematic depicting molecular mechanism of glucagon-induced stimulation of glycogenolysis.** Green represents active and red represents inactive enzymes.

In stimulating gluconeogenesis, PKA phosphorylates the bifunctional enzyme PFK2/FBP2. Phosphorylation of PFK2/FBP2 by PKA leads to inactivation of PFK2 activity and an increase in FBP2 activity. This leads to decreased production of F26BP, and thus F26BP does not activate PFK1. Inactive PFK1 is incapable of phosphorylating F6P to F16BP, leading to an inhibition of glycolysis. Additionally, low levels of F26BP are insufficient to inactivate FBP, thus FBP activity remains high and drives gluconeogenesis [21,26] (Figure 1-6).

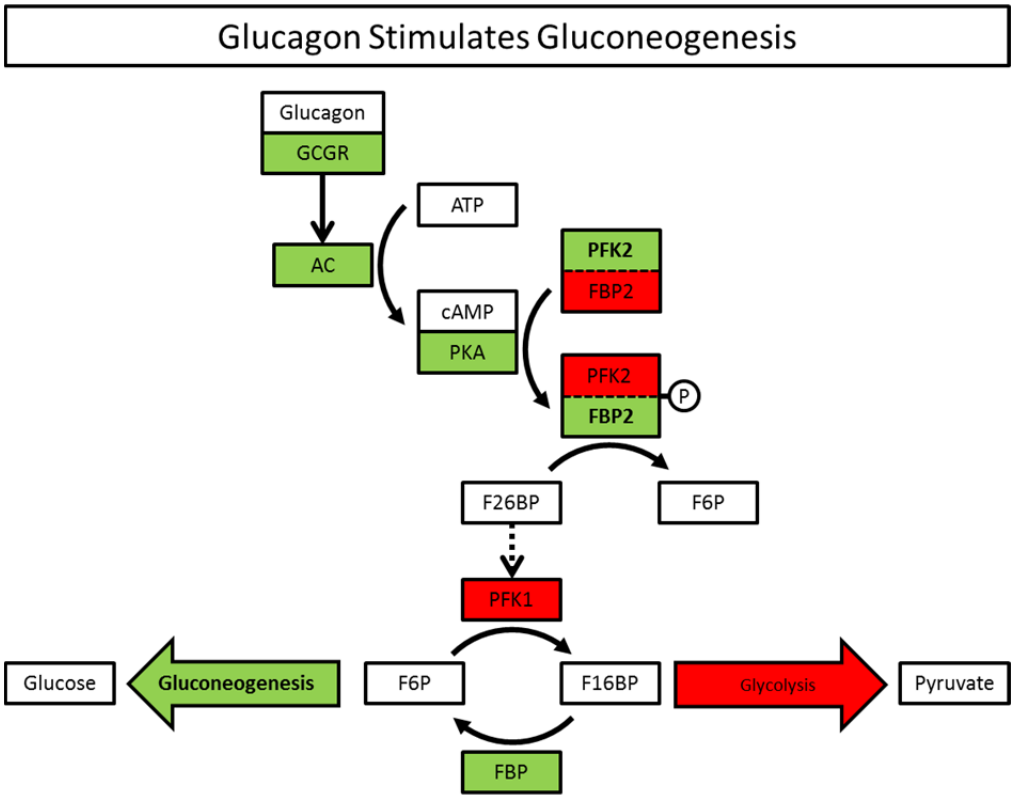


**Figure 1-6 Schematic depicting molecular mechanism of glucagon-induced stimulation of gluconeogenesis.** Green represents active and red represents inactive enzymes/processes.

### 1.5 Additional Regulators of Blood Glucose

In addition to insulin and glucagon which act as major regulators of glucose homeostasis, a number of other hormones are known to play smaller roles in the regulation of blood glucose. Cortisol, thyroxine, and epinephrine have been shown to raise blood glucose both in coordination with and independent of insulin and glucagon. Cortisol stimulates hepatic gluconeogenesis through the induction and maintenance gluconeogenic enzyme activity [27]. However, this increase in gluconeogenesis does not result in a large increase in blood glucose, as much of the newly synthesized glucose is stored as glycogen (glycogenesis). Additionally, cortisol inhibits glucose uptake through the inhibition of insulin-mediated translocation of GLUT4 and inhibits glucose utilization in peripheral tissues in favor of fatty acids [27]. Thyroxine stimulates glycogenolysis and enhances the absorption of sugars from the intestine, but also stimulates peripheral glucose utilization, resulting in only a moderate increase in blood glucose [28]. Epinephrine increases blood glucose through direct cAMP-mediated effects on glycogenolysis and gluconeogenesis that mirror glucagon signaling [27]. Epinephrine has also been shown to be a potent stimulator of glucagon secretion. Numerous other hormones and signaling pathways have been shown to have indirect effects of blood glucose levels by affecting changes in insulin and glucagon secretion (discussed in 1.8.1 and 1.9.3).

### 1.6 Pancreatic Islets of Langerhans

As mentioned above, the pancreatic islets of Langerhans are endocrine micro-organs that contain the α- and β-cells, and thus play a major role in the regulation of glucose homeostasis through the glucose-dependent release of insulin and glucagon. Islets are roughly spherical structures composed of clusters of multiple endocrine cell types that synthesize and secrete

unique hormones. The three major islet-cell types (α-, β-, and δ-cells) synthesize and secrete glucagon, insulin, and somatostatin, respectively. Other minor islet-cell types, that compose less than 5% of islet mass (PP/γ-cells and ε-cells) synthesize and secrete pancreatic polypeptide and ghrelin, respectively. Collectively, islets form the endocrine pancreas and are dispersed throughout the exocrine pancreas. Initially, islets were named for their appearance in histological slices, where collections of distinct round endocrine tissue was dotted like "islets" throughout a sea of exocrine tissue [29]. The diameter of islets varies from species to species (human = 55 ± 29 μM; mouse = 116 ± 80 μM), but does not correlate with organism size, indicating a possible size limit to functional islets [30]. Additionally, the composition of islet cell types varies from organism to organism. In humans, β-cells make up ~54%, α-cells make up ~35%, and δ-cells make up 11% of islet cell mass. In mice, β-cells make up ~75%, α-cells make up ~19%, and δ-cells make up 6% of islet cell mass [31]. There are also significant interspecies differences in islet cytoarchitecture (Figure 1-7). In humans, α-, β-, and δ-cells are dispersed throughout the islet; whereas in mice, α- and δ-cells form an outer mantel around a core of β-cells [32]. In both humans and mice, a higher density of islets can be found in the body and tail of the pancreas as compared to the head [33]. In rats, this gradient in islet distribution is accompanied by functional difference between islets located in the head and body/tail of the pancreas. Rat islets within the body/tail have a higher percentage of α-cell mass and display increase in the secretion of both insulin and glucagon [34]. In humans islets, there are no regional differences in islet-cell composition or hormone secretion [33]. As compared to neighboring exocrine tissue, endocrine islets are highly vascularized with a large and torturous capillary network that resembles the architecture of glomeruli. Islets, which only account for 1-2% of

the pancreas by mass, receive 5-15% of the pancreatic blood supply [35]. The unique microvasculature of islets has led to the development of several models that attempt to integrate islet cytoarchitecture and function through blood flow dynamics [36,37]. Further contributing the role that the microvasculature plays in islet function, there is the observation of a glucose-dependent increase in blood flow that is specific to islets and not observed in exocrine tissue [38].

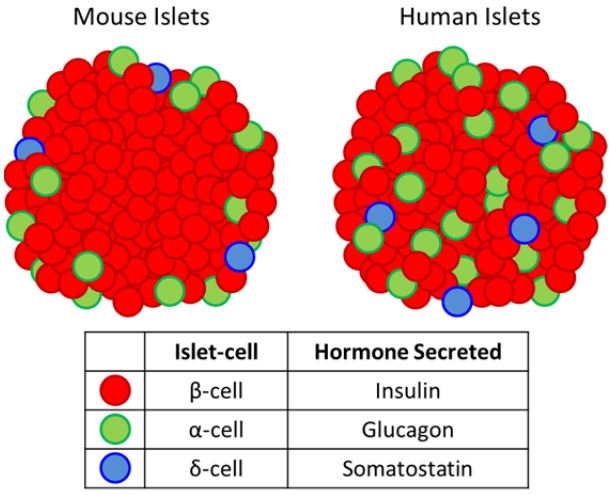


**Figure 1-7 Diagrams of mouse and human islets.** β-cells (green) secrete insulin, α-cells (red) secrete glucagon, and δ-cells (blue) secrete somatostatin. In mouse islets, α- and δ-cells are primarily located in the islet periphery, whereas in human islets, all three cell types are distributed throughout each islet, possibly in a pattern consistent with a clustering of smaller islets with a mouse-like islet-cell patterned architecture.

## 1.7 Glucose Regulation of Insulin Secretion

Insulin secretion is largely regulated directly by glucose concentrations. Insulin secretion from *ex vivo* islets, isolated from the pancreas and removed from hormonal and neuronal input, recapitulates the glucose-dependent changes in insulin secretion observed *in vivo* [39,40]. Both *in vivo* and *ex vivo*, low glucose concentrations inhibit insulin secretion and high glucose

concentrations stimulate insulin secretion (Figure 1-8). Unlike other stimulus-coupled secretory cells, glucose stimulation of β-cells does not occur through ligand activation of a membrane receptor and activation of signaling cascades. Rather, glucose must enter and be metabolized by β-cells to induce insulin secretion, and thus acts as a 'fuel' to drive insulin secretion.

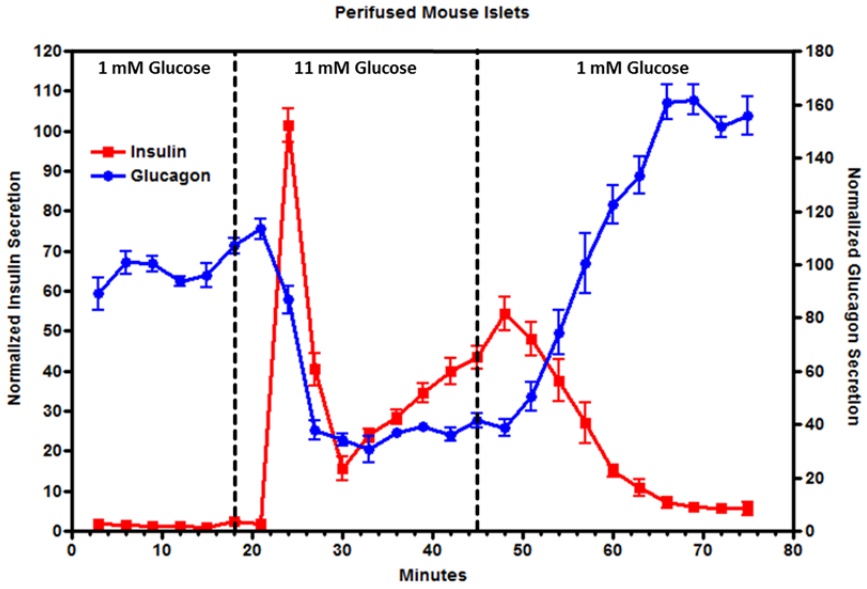


**Figure 1-8 Glucose-regulation of hormone secretion is preserved in perifused islets.** Stimulation with 1 mM glucose inhibits insulin secretion and facilitates glucagon secretion. Stimulation with 11 mM glucose stimulates insulin secretion and inhibits glucagon secretion. Insulin secretion is normalized to maximal insulin secretion observed in fraction 8. Glucagon secretion is normalized to the average glucagon secretion observed in fractions 1-7. Data are presented as the average of normalized data ± SEM; n = 6 mice.

### 1.7.1 Glucose-stimulated Insulin Secretion

Extracellular glucose is taken up by β-cells primarily through the low affinity (Km = ~17 mM) glucose transporter type 2 (GLUT2) in mice and the high affinity (Km = ~3-7 mM) glucose transporter type 1 in humans (GLUT1) [41,42]. Both glucose transporters allow for the rapid equilibration of extracellular and intracellular glucose at a faster rate than it can be utilized by the β-cell [43,44]. Once inside the β-cell, glucose is phosphorylated to glucose-6-phosphate (G6P)

by glucokinase, the rate limiting step in glucose utilization. Glucokinase is a low affinity (Km = ~6-10 mM) enzyme with a sharp sigmoidal dependence on substrate (glucose) concentration that is not negatively inhibited by its product (G6P), making glucokinase an ideal glucose sensor [45–47]. Under normal physiologic conditions, G6P is shuttled into the glycolysis pathway. Other pathways such as the pentose phosphate pathway, conversion to sorbitol, and glycogenesis play minor roles in β-cell glucose utilization [48,49]. In β-cells, glycolysis leads to an increase in intracellular the ATP to adenosine diphosphate (ADP) ratio. This increase in ATP/ADP leads to the closure of ATP-sensitive $K^+$ channels ($K_{ATP}$) through direct binding of ATP [50]. At low glucose, $K_{ATP}$ channels are open, allowing for the outflow of $K^+$ and resulting in a resting membrane potential of approximately -70 mV [51]. Glucose-induced increases in ATP/ADP leads to the closure of $K_{ATP}$ channels, which cause membrane depolarization and the opening of voltage-dependent L-type $Ca^{2+}$ channels. The influx of $Ca^{2+}$ through open $Ca^{2+}$ channels increases the concentration of intracellular calcium ($[Ca^{2+}]_i$) and triggers exocytosis of insulin secretory granules [52] (Figure 1-9).

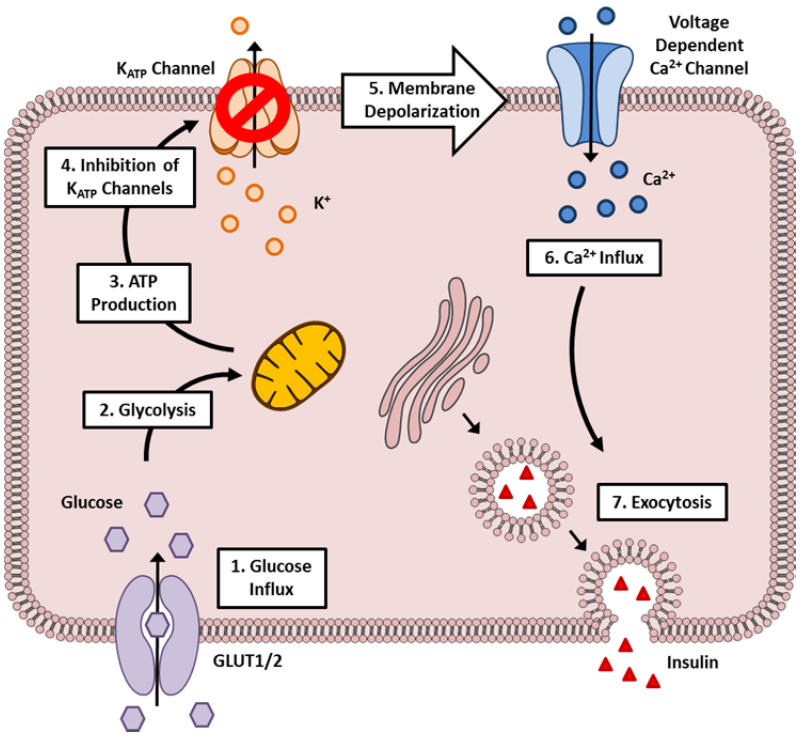


**Figure 1-9 Model of glucose-stimulation of insulin secretion from β-cells.** (1) Glucose influx through GLUT1/2 drives (2) glycolysis. Glycolysis end-products are further metabolized in the mitochondria to (3) produce additional ATP. An increase in the ATP/ADP ratio (4) inhibits $K_{ATP}$ channels, causing (5) membrane depolarization. Membrane depolarization triggers (6) $Ca^{2+}$ influx through voltage-dependent $Ca^{2+}$ channels. The increase in $[Ca^{2+}]_i$ triggers (7) the exocytosis of insulin secretory granules.

### 1.7.2 Biphasic Insulin Secretion

Rapid increases in glucose induce a characteristic biphasic insulin secretion response both *in vitro* and *in vivo* [53,54] (Figure 1-8). The first phase of insulin secretion is characterized by a sharp and robust peak of insulin secretion that quickly falls off. The second phase of insulin secretion is slower, less robust, but sustained insulin secretion. The existence of two separate populations of insulin secretory granules is thought by some to play a role in the two phases on insulin secretion [55]. The first phase of insulin secretion is thought to be supplied by a readily releasable pool of secretory granules already docked at the cell membrane and able to be secreted quickly. Whereas, the second phase is supported by secretory granules located more centrally within the β-cell and requiring transport to the membrane. However, it has been

noted that only a small fraction of the readily releasable pool actually contributes to insulin secretion. This suggests that additional factors, besides the presence of two separate pools of secretory granules, contribute to the biphasic insulin secretion profile. The change in $[Ca^{2+}]_i$ in response to rapid increases in glucose concentration is also biphasic, with a large initial increase in $[Ca^{2+}]_i$ immediately followed by a steady phase of $[Ca^{2+}]_i$ activity [56]. This $[Ca^{2+}]_i$ profile indicates that the source of the biphasic insulin secretion, or at least the first phase of insulin secretion is at or upstream of $Ca^{2+}$ influx rather than downstream at the level of exocytosis. However, the burst of $[Ca^{2+}]_i$ followed immediately by a steady but lower levels of $[Ca^{2+}]_i$ activity do not explain the nadir separating the first and second phases of insulin secretion, or the slow rise in insulin secretion observed at the start of the second phase [57]. One hypothesis to explain the discrepancies between the observed $[Ca^{2+}]_i$ activity and insulin secretion is an increased efficacy of the stimulating$[Ca^{2+}]_i$ signal [58,59]. In this model, the initial burst of $[Ca^{2+}]_i$ activity is responsible for the first peak of insulin secretion and the nadir, while the following steady $[Ca^{2+}]_i$ activity is accompanied by a transition of increasing efficacy of $[Ca^{2+}]_i$-induced insulin secretion, resulting in the slow rise in insulin secretion observed in the second phase.

### 1.7.3 Electrical, Calcium, and Insulin Secretion Oscillations

In addition to the $[Ca^{2+}]_i$ dynamics described above, β-cells display a number of other unique electrical attributes. Within the range of stimulatory glucose concentrations, the membrane potential of β-cells oscillates between cycles of depolarization and repolarization. Additional clusters of action potentials are often observed superimposed on these periods of depolarization. The balance between depolarization and repolarization is mediated by voltage-

dependent $Ca^{2+}$ channels and multiple types of $K^+$ channels. Depolarization and activation of voltage-dependent $Ca^{2+}$ channels occurs through the mechanisms described above. Repolarization following $Ca^{2+}$ influx occurs directly through activation of small conductance calcium-activated potassium channels [60] and through the reactivation of inwardly rectifying $K_{ATP}$ channels through a decrease in the ATP/ADP ratio caused by an increase in $Ca^{2+}$ ATPase activity [61]. Additionally, these changes in electrical and $[Ca^{2+}]_i$ activity are synchronized between β-cells within a single islet (Figure 1-10). Shared electrical and $[Ca^{2+}]_i$ activity occurs through active gap junctions that electrically and physically connect neighboring β-cells within an islet. β-cell gap junctions are formed by a homohexamer of connexin 36 (Cx36) proteins and allow ions and small molecules to freely pass between adjacent β-cells [62]. Cx36 gap junctions cause islet β-cells to behave as a syncytium of cells rather than a collection of individual cells. Electrical coupling between β-cells dampens the activity of individual β-cells that might otherwise be more readily excitable, preventing the unnecessary and potentially detrimental secretion of insulin secretion at low glucose [63]. The syncytial nature of β-cells acts to further define the distinction between the secretion "on" and secretion "off" states. The entrainment of $[Ca^{2+}]_i$ activity within an islet leads to corresponding synchronized pulses in insulin secretion from the same islet [64]. Pulsatile insulin secretions are also observed both *in vivo* within the portal vein and peripheral circulation and *ex vivo* in perifusion experiments with isolated islets [39,40]. Coordination between intrapancreatic ganglia and islet paracrine factors (discussed in 1.8.1) are believed to explain the synchronization of insulin pulsatility from the whole pancreas, whereas paracrine factors alone contribute to the pulsatility of insulin secretion from perifused *ex vivo* islets [65]. The pulsatile nature of insulin secretion is believed to play a role in preventing insulin

resistance through the downregulation of the insulin receptor and thus preventing the development of type 2 diabetes (discussed in 1.11.2) [66].

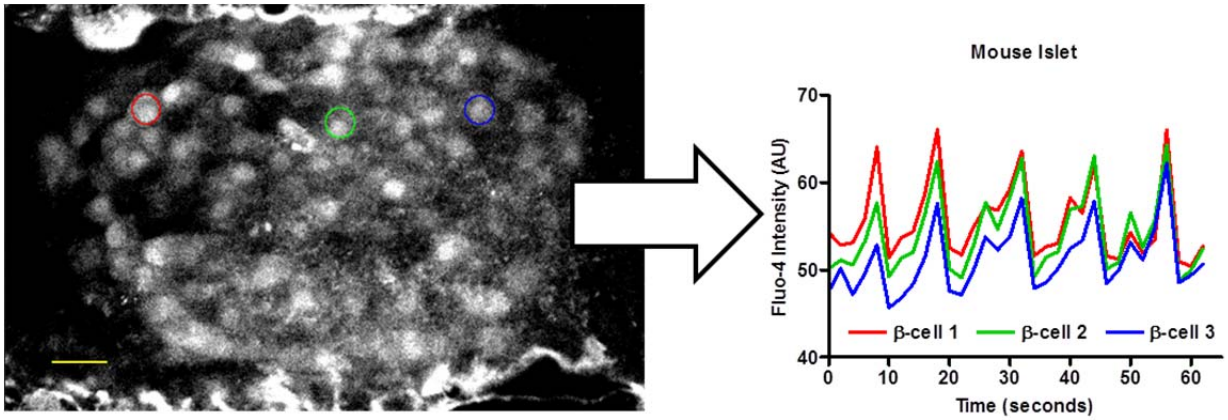


**Figure 1-10 Calcium oscillations are synchronized between nonadjacent β-cells within a single islet.** (Left) Single confocal section of a mouse islet loaded with $[Ca^{2+}]_i$ biosensor Fluo-4. Regions of interest are highlighted on three nonadjacent β-cells, labeling β-cell 1 (red) β-cell 2 (green) and β-cell 3 (blue). Scale bar represents 20 μM. (Right) Traces of Fluo-4 intensity, a marker for relative changes in $[Ca^{2+}]_i$, in the three regions of interest identified in the confocal section to the left.

## 1.8 Additional Modulators of Insulin Secretion

Additional modulators of insulin secretion can be separated into two categories; intra-islet and extra-islet modulators. The distinction between these categories is important, considering that a large portion of the research in islet biology and specific islet-cell function utilize isolated islets. In these *ex vivo* studies, isolated islets are removed from extra-islet modulations of hormone secretion, whereas intra-islet modulators of hormone secretion are maintained and must be taken into account. For example, a drug has been shown to affect insulin secretion may not act directly on β-cells, but may instead act on another islet-cell type, such as δ-cells, to modulate a process, such as somatostatin secretion, that indirectly modulates insulin secretion.

### 1.8.1 Paracrine and Autocrine Regulation of Insulin Secretion

Intra-islet modulators of insulin secretion can be further separated into secreted and non-secreted signaling pathways. Intra-islet secreted pathways include both autocrine and paracrine signaling. In endocrine signaling, a hormone is secreted from one location, enters the bloodstream, and acts at some distant location. Contrastingly in autocrine and paracrine signaling, the secreted signaling molecule acts directly on the cell that it was secreted from (autocrine) or on neighboring cells (paracrine). In addition to their endocrine effects on distant target tissues, islet cell hormones have been shown to have significant paracrine effects in modulating the secretion of other islet hormones. In regards to insulin secretion, somatostatin and glucagon have been shown to have opposing roles. Somatostatin, secreted by neighboring δ-cells, has been shown to inhibit insulin secretion by binding to somatostatin receptors expressed on β-cells and decreasing intracellular cAMP in β-cells [67]. Conversely, glucagon, secreted by neighboring α-cells, has been shown to stimulate insulin secretion, purportedly though binding to glucagon receptors expressed on β-cells and increasing intracellular cAMP in β-cells [68]. The role of autocrine insulin signaling on insulin secretion is highly contested. Historically, insulin was thought play a negative feedback role in its own secretion. However multiple studies have found that insulin signaling back onto β-cells results in an inhibition [69–71], a stimulation [72–74], or no effect on its own secretion[75–77] . Some of the confusion regarding the autocrine role of insulin may be due to additional autocrine regulation of insulin secretion by signaling molecules that are co-secreted with insulin, such as serotonin and dopamine. Serotonin is co-secreted with insulin and has been shown to modulate insulin secretion intracellularly and extracellularly. Intracellular serotonin is used as a substrate in the serotonylation and constitutive activation of small GTPases that stimulate insulin secretion.

Once secreted, extracellular serotonin acts on the 5-$HT_{1A}$ receptor to decrease intracellular cAMP and inhibit insulin secretion before being taken up by serotonin transporters [78]. Dopamine has been shown to play a similar role as a negative feedback for insulin/dopamine secretion. Dopamine is co-secreted with insulin and acts on β-cell dopamine receptors, primarily dopamine receptor D3 (DRD3), to disrupt $[Ca^{2+}]_i$ dynamics and inhibit insulin secretion [79].

### 1.8.2 Juxtacrine Regulation of Insulin Secretion

Unlike paracrine and autocrine signaling, where signal transmission is dependent on the secretion of a signaling molecule, juxtacrine signaling is transmitted through direct cell-cell contact and the interaction between membrane bound proteins on neighboring cells. Cell adhesion molecules including neural cell adhesion molecule (NCAM) and E-, N-, and T-cadherin are necessary for appropriate insulin secretion. $NCAM^{-/-}$ mice have defective insulin secretion with an increase in basal insulin secretion (low glucose) and a decrease in glucose-stimulated insulin secretion (high glucose) that is independent of changes in $[Ca^{2+}]_i$ or $K_{ATP}$ activity [80]. Down-regulation of E-cadherin leads to a reduction of glucose-stimulated insulin secretion from clustered pseudoislets formed from a cell culture β-cell model (MIN6B1) [81]. Additionally, blockade of E-cadherin through the use of an anti-E-cadherin antibody was shown to inhibit both $[Ca^{2+}]_i$ and insulin secretion from a similar pseudoislet model (MIN6) [82]. Blockade of E-cadherin was also shown to disrupt gap-junction communication between adjacent cells within pseudoislets, possibly contributing to the observed defect in insulin secretion [82]. Conditional knockout of N-cadherin within β-cells results in defective insulin secretion, ostensibly due to a

reduction in the number of insulin secretory granules per β-cell [83]. A similar role in the regulation of insulin secretion through the regulation of secretory granules has been suggested for T-cadherin. T-cadherin has been found to be physically associated with insulin secretory granules and T-cadherin$^{-/-}$ mice display a reduction in glucose-stimulated insulin secretion [84]. Maintaining appropriate cell-cell connections is required for appropriate insulin secretion. Thus, modulation of the expression and affinities of cell adhesion molecules expressed in islets represents a mechanism for the regulation of insulin secretion.

Insulin secretion has also been shown to be regulated by the widely expressed and robust EphA/ephrin-A signaling system [85] (Chapter 2). Both EphA receptors and ephrin-A ligands are expressed on the plasma membrane of β-cells. Signaling between EphA receptors and ephrin-A ligands is bidirectional, and often results in opposing actions [86]. The clustering of β-cells and direct cell-cell contacts within islets enables a constant state of signaling though the EphA/ephrin-A signaling pathways. It has been hypothesized that the balance between EphA forward signaling and ephrin-A reverse signaling is determined by a glucose-sensitive protein tyrosine phosphatase (PTP) that acts to dephosphorylate EphA receptors at high glucose and thus inhibit EphA forward signaling. In this model, EphA forward signaling predominates at low glucose, contributing to the inhibition of insulin secretion and ephrin-A reverse signaling predominates at high glucose, facilitating glucose-stimulation of insulin secretion [85]. Additionally, a defect in glucose-stimulated insulin secretion is observed in ephrin-A5$^{-/-}$ mice, indicating the importance of the signaling pathway in maintaining appropriate insulin secretion [85].

### 1.8.3 Extra-islet Modulators of Insulin Secretion

Isolated islets exposed to low and high glucose largely recapitulate the insulin secretion response observed *in vivo* in the fasting and fed states. However, insulin secretion from isolated islets discounts the fine-tuning and situational-specific modulation of insulin secretion from hormonal and neuronal sources. GLP1 and GIP are two gut-derived hormones known as incretins. GLP1 and GIP are secreted by L-cell (ileum and colon) and K-cells (duodenum and jejunum), respectively, in response to the ingestion of carbohydrates, proteins, and fats [87]. Both hormones act directly on β-cells through GPCRs to potentiate insulin secretion [88]. Due to the proximity of L- and K-cells to the gut lumen, it is proposed that they are able to directly sense nutrient availability and secrete GLP1 and GIP accordingly. This nutrient responsive secretion of GLP1 and GIP is believed to underlie the incretin effect, where oral ingestion of glucose leads to a larger increase in plasma insulin than intravenous administration of glucose with equivalent increases in blood glucose [89].

Islets also receive input from the autonomic nervous system. Parasympathetic stimulation through the vagus nerve results in an increase in insulin secretion [90]. This parasympathetic potentiation of insulin secretion occurs through the release of acetylcholine (ACh) and its action on β-cell muscarinic receptors (subtype 3) to increase $Na^+$ conductance and augment $Ca^{2+}$ influx through voltage-dependent $Ca^{2+}$ channels [91]. Additional parasympathetic stimulation may occur through vasoactive intestinal peptide (VIP), pituitary adenylate cyclase activating peptide (PACAP), and gastin-releasing peptide (GRP) [92]. Parasympathetic regulation of insulin secretion plays an important role in the fed state through CNS glucose sensing and activation of the parasympathetic system. Additionally, parasympathetic stimulation of insulin secretion can occur prior to changes in blood glucose, in anticipation of the ingestion of food

and the consequent increase in blood glucose. This is known as the cephalic phase of insulin secretion [93].

Sympathetic stimulation of β-cells by the catecholamine norepinephrine results in an inhibition of insulin secretion [90]. Following activation of $\alpha_2$-adrenoceptors on β-cells, norepinephrine-mediated inhibition of insulin secretion has been proposed to be mediated by a number of different signaling pathways. These pathways include hyperpolarization of the β-cell, a decrease in intracellular cAMP, and inhibition of exocytosis machinery [94,95]. Other catecholamines such as epinephrine (released from the adrenal medulla) and dopamine (released from β-cells and co-secreted with insulin) have similar roles in negatively regulation insulin secretion. Sympathetic regulation of insulin secretion is important during periods of activity when the demand for glucose production and utilization is high, and thus the secretion of insulin, which opposes these actions, is inhibited.

Arginine and other amino acids have been shown to stimulate insulin secretion [12,96]. Unlike glucose, cationic amino acids do not serve as a 'fuel' source to generate insulin secretion as they are poorly metabolized by β-cells [97,98]. Rather they are transported across the β-cell membrane as cations, resulting in β-cell depolarization independent of glucose concentrations [99,100].

**1.9 Glucose Regulation of Glucagon Secretion**

Due to the therapeutic success of insulin replacement therapy for the management of diabetes, the majority of diabetes and islet biology research has focused on insulin and β-cells. This has led to a detailed and well accepted model of glucose stimulation of insulin secretion (discussed

in 1.7). In recent years, it has become apparent that α-cells and glucagon dysfunction contribute significantly to the pathophysiology, and specifically the hyperglycemia, of diabetes. This has spurred research into α-cell function and glucagon regulation; however there is not yet a consensus model for the glucose regulation of glucagon secretion. In general, glucagon is secreted at low glucose and glucagon secretion is inhibited at high glucose (Figure 1-8). Current models of glucose regulation of glucagon secretion can be broadly separated into two categories; α-cell-intrinsic regulation of glucagon secretion and paracrine regulation of glucagon secretion. I will also present a new model of juxtacrine regulation of glucagon secretion that is complementary to both of these models (discussed in Chapter 2).

### 1.9.1 α-cell electrophysiology

α- and β-cells share many key mediators of glucose sensing and exocytosis, including glucose transporters, the glycolytic enzyme glucokinase, $K_{ATP}$ channels, and voltage-dependent $Ca^{2+}$ channels [101–104]. Despite these similarities, α- and β-cells display opposite secretion outcomes in response to elevations in glucose. In α-cell-intrinsic models of glucose regulation of glucagon secretion, the inhibition of glucagon secretion in response to glucose is attributed to unique α-cell electrophysiology. However, much of the electrophysiology of α-cells is highly debated. One generally agreed upon aspect of α-cell electrophysiology is observation that increases in $[Ca^{2+}]_i$ mediated by voltage-dependent $Ca^{2+}$ channels are required for glucagon secretion [105,106]. The role of $K_{ATP}$ channel activity in α-cells is controversial. Mice lacking functional $K_{ATP}$ channels ($Sur1^{-/-}$) have a defect in the glucagon secretory response at low glucose, indicating that $K_{ATP}$ channels play a key role in the secretion of glucagon [107]. Additionally, pharmacological

manipulation of $K_{ATP}$ channels indicates the presence of $K_{ATP}$ channels-dependent regulation of glucagon secretion [105]. Tolbutamide is a pharmacological agent that binds to and results in the closure of $K_{ATP}$ channels. Conflicting effects on glucagon secretion have been reported with tolbutamide treatment. These discrepancies may be explained in part due to a concentration dependent effect of tolbutamide. At concentrations between 0.1 and 1 μM, tolbutamide treatment results in increased glucagon secretion, whereas concentrations of 10 μM have been shown to inhibit glucagon secretion [105]. This increase in glucagon secretion is presumed to be due to an decrease in $K_{ATP}$ current and an increase in $[Ca^{2+}]_i$, both of which have been shown to be an effect of tolbutamide treatment in single α-cells [108]. Diazoxide, a pharmacological agent that opens $K_{ATP}$ channels, has been shown to have the opposite effect, resulting in a decrease in $K_{ATP}$ current, an increase in $[Ca^{2+}]_i$, and an inhibition of glucagon secretion [105,108]. Some of these same studies have argued that $K_{ATP}$ channel-dependent regulation of glucagon secretion is separate from glucose-dependent regulation of glucagon secretion. These studies found that glucose does not have a large effect on α-cell metabolism, $K_{ATP}$ current, or $[Ca^{2+}]_i$ [108], although other studies indicate that elevations in glucose result in an increase in both α-cell metabolism and $[Ca^{2+}]_i$ [109]. Discrepancies in glucose metabolism pathways and ATP products further support the minor or non-existent inactivation $K_{ATP}$ channel of α-cells as compared to β-cells. In α-cells, glucose metabolism follows an anaerobic pathway leading to less ATP generation as compared to β-cells, where glucose metabolism follows an aerobic pathway [49,110]. Based on these observations, two different models of α-cell-intrinsic regulation of glucagon secretion have emerged; one that focuses on the elevated secretion of glucagon at low glucose and one that focuses on the inhibition of glucagon secretion at high glucose.

### 1.9.2 α-cell-intrinsic Models of Glucose Regulation of Glucagon Secretion

The first model focuses on glucagon secretion at low glucose and assumes that glucose metabolism does not largely affect ATP/ADP or $K_{ATP}$ channels. In this model, low concentrations of glucose are capable of inducing glucagon secretion. This is supported by findings that the majority of $K_{ATP}$ channels are already inactivated at low glucose, indicating that very minor changes in ATP/ADP are capable of depolarizing the cell and resulting in glucagon secretion [111]. Additionally, α-cells are electrically active in the absence of glucose [112]. In α-cell-intrinsic models where glucose metabolism does not affect the activity of in $K_{ATP}$ channels, spontaneous depolarization of α-cells accounts for glucagon secretion observed at low glucose, but there is no identified mechanism to explain the inhibition of glucagon secretion observed with elevations in glucose.

The second model focuses on the inhibition of glucagon secretion with elevations in glucose. In this model, glucose metabolism and an increase in ATP/ADP inhibit $K_{ATP}$ channel activity. Further, the degree of $K_{ATP}$ channel inactivation is directly determined by glucose concentration and results in either depolarization and secretion events at low glucose or a fixed membrane potential and no secretion events at high glucose [112,113]. Thus, this α-cell-intrinsic model of glucose-inhibition of glucagon secretion is dependent on the inhibition of α-cell action potentials and resulting $Ca^{2+}$ influx. Differential expression of voltage-dependent ion channels between α- and β-cells could explain the different outcomes observed in the two cell types following $K_{ATP}$ channel inactivation. Many voltage-dependent ion channels, including those found in α-cells, exhibit a dual dependence on membrane potential, where short depolarizations result in increased activity and extended depolarizations result in channel inactivation [112]. Reactivation of extended depolarization-inactivated voltage-dependent ion

channels requires a return to a negative membrane potential. Thus, if high glucose concentrations maintain a constant inhibition of $K_{ATP}$ channels and prevent a return to a negative membrane potential these voltage-dependent ion channels might remain inactivated. This may also explain the reduction in α-cell action potential height with tolbutamide treatment, as inactivated voltage-dependent ion channels would not contribute to the magnitude of the action potential [113]. This dual dependence phenomenon is believed to be responsible for the glucose-inhibition of glucagon secretion in α-cell-intrinsic models (Figure 1-11). In support of α-cell-intrinsic regulation of glucagon secretion, glucose-inhibition of glucagon secretion is observed at glucose concentrations (~3-5 mM) that do not result in any changes in the secretion of potential paracrine inhibitors such as insulin [113]. However, newly identified juxtacrine regulation of glucagon secretion may also play a role in the inhibition of glucagon secretion at these glucose concentrations when paracrine regulation of glucagon secretion is inactive (discussed in Chapter 2).

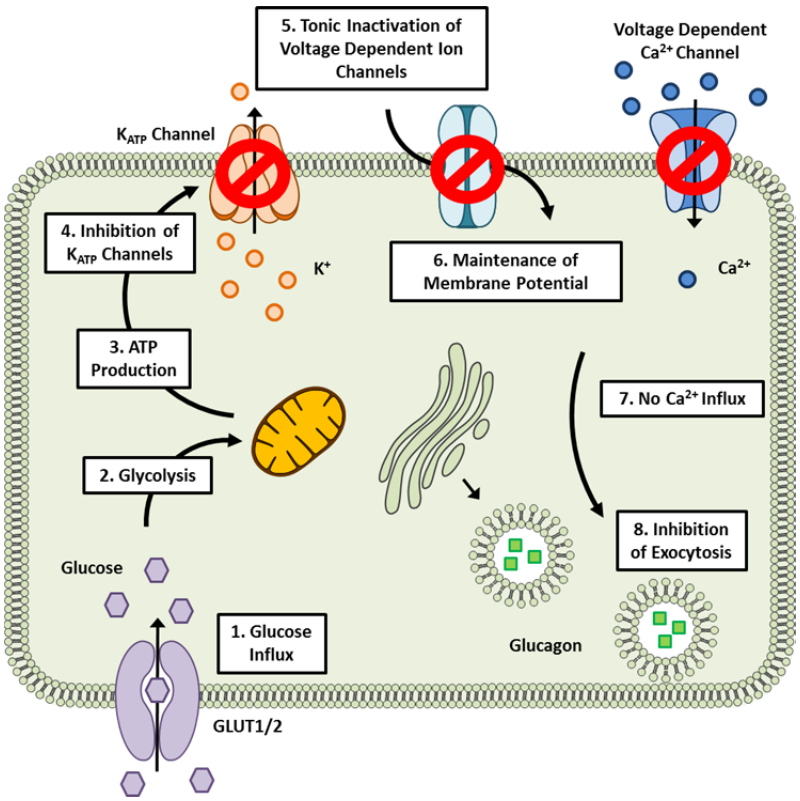


**Figure 1-11 Model of α-cell intrinsic glucose-inhibition of glucagon secretion.** (1) Glucose influx through GLUT1/2 drives (2) glycolysis. Glycolysis end-products are further metabolized in the mitochondria to (3) produce additional ATP. An increase in the ATP/ADP ratio (4) inhibits $K_{ATP}$ channels, causing extended depolarization resulting in the (5) tonic inactivation of voltage dependent ion channels. (6) This prevents membrane depolarizations that trigger (7) $Ca^{2+}$ influx through voltage-dependent $Ca^{2+}$ channels. Without full depolarization and an increase in $[Ca^{2+}]_i$, exocytosis does not occur.

### 1.9.3 Paracrine Models of Glucose Regulation of Glucagon Secretion

In paracrine models of glucose regulation of glucagon secretion, the inhibition of glucagon secretion observed at high glucose is not intrinsic to α-cells. Rather, local signaling from neighboring islet-cells is required to inhibit glucagon secretion. In these models the α-cell response to glucose is akin to that of β-cells, resulting in increased ATP/ADP, inhibition of $K_{ATP}$ channels, membrane depolarization, $[Ca^{2+}]$ influx through voltage-dependent in $Ca^{2+}$ channels, and exocytosis of secretory granules. However, high glucose also results in the release of paracrine factors from neighboring islet-cells that act on α-cells to inhibit glucagon secretion

(Figure 1-12). The presence of paracrine inhibition that blocks glucagon secretion, despite otherwise stimulatory concentrations of glucose, explains the initially 'paradoxical' stimulation of glucagon secretion at glucose concentrations above ~11 mM [114]. Thus, paracrine inhibition can overcome the intrinsic glucose-stimulation of glucagon secretion present in α-cells up to ~11 mM of glucose, but at glucose concentrations above ~11 mM glucose-stimulation of glucagon secretion begin to overcome paracrine inhibition. A number of potential paracrine factors have been proposed to fill this role including insulin, somatostatin, $Zn^{2+}$, and γ-aminobutyric acid (GABA) [110,115–127]. All of these proposed paracrine regulators of glucagon secretion have been shown to inhibit glucagon secretion from islets [109]. Each factor has its own set of merits and shortcomings as an underlying mechanism for glucose-inhibition of glucagon secretion.

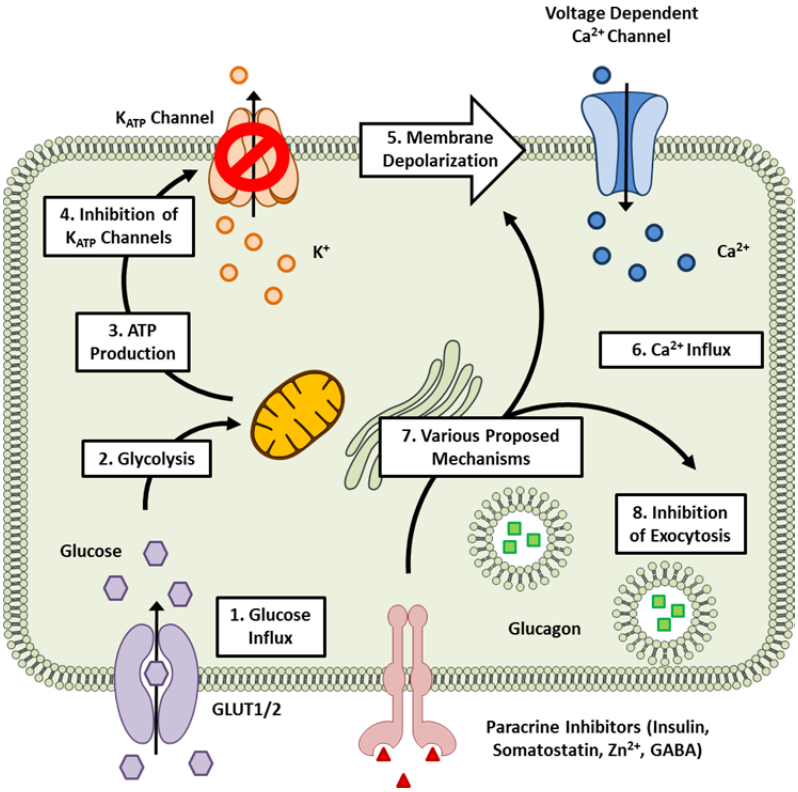


**Figure 1-12 Model of paracrine-mediated glucose-inhibition of insulin secretion from β-cells.** (1) Glucose influx through GLUT1/2 drives (2) glycolysis. Glycolysis end-products are further metabolized in the mitochondria to (3) produce additional ATP. An increase in the ATP/ADP ratio (4) inhibits $K_{ATP}$ channels, causing (5) membrane depolarization. Membrane depolarization triggers (6) $Ca^{2+}$ influx through voltage-dependent $Ca^{2+}$ channels. (7) Depending on the specific paracrine inhibition pathway the influx in $Ca^{2+}$ is either decoupled from exocytosis (insulin and somatostatin) or is prevented through preventing membrane depolarization (GABA). Regardless of the molecular pathway, paracrine signaling results in the (8) inhibition of exocytosis.

$Zn^{2+}$ is co-secreted with insulin in response to elevations in glucose. Thus, increases in zinc signaling would correspond with increased inhibition of glucagon secretion from α-cells. Additionally, $Zn^{2+}$ has been shown to open $K_{ATP}$ channels and inhibit the electrical activity of α-cells, thus preventing exocytosis [121–123]. However, β-cell specific knockout of the $Zn^{2+}$ transporter ($Znt8^{-/-}$), which severely decreases islet zinc content and secretion, results in no apparent defect in glucagon secretion [128]. GABA is also secreted from neighboring β-cells. GABA is proposed to inhibit glucagon secretion through the activation of α-cell $GABA_A$-receptor chloride channels and hyperpolarization of the α-cell membrane, thus preventing

depolarization and exocytosis [120]. However, the potential of GABA to mediate glucose-inhibition of glucagon secretion is limited by its constitutive secretion from β-cells with only minor fluctuations in secretion in response to glucose [129]. The expression of $GABA_A$-receptors has been shown to be glucose sensitive (increased expression with increased glucose), which may contribute to some glucose inhibition of glucagon secretion in the long term (days/hours), but does not explain the minute-scale dynamics of glucose-inhibition of glucagon secretion [130]. Insulin and somatostatin are secreted from β- and δ-cells, respectively, in response to elevations in glucose, corresponding with inhibition of glucagon secretion. Additionally, at elevated glucose, oscillations in insulin and somatostatin from isolated mouse islets have been shown to be antisynchronous with oscillations in glucagon secretion [39]. Further, both α-cell-specific insulin receptor null mice ($\alpha IR^{-/-}$) and islets from somatostatin null ($SST^{-/-}$) and somatostatin receptor 2 null ($SSTR2^{-/-}$) mice display defects in glucose-inhibition of glucagon secretion [116,124,125]. Insulin and somatostatin have been shown to cooperatively inhibit glucagon secretion through a reduction in intracellular cAMP in α-cells. Insulin activates phosphodiesterase 3B to degrade cAMP and somatostatin inhibits adenylyl cyclase to inhibit the production of cAMP [126]. This insulin and somatostatin cooperative model is the first model of glucose regulation of glucagon secretion (α-cell-intrinsic or paracrine) that does not depend on inhibition of $[Ca^{2+}]_i$ to mediate an inhibition of exocytosis. This is important because recent studies using genetically labeled α-cells revealed that glucose induces an increase in $[Ca^{2+}]_i$ while at the same time inhibiting glucagon secretion, suggesting that glucose-inhibition of glucagon secretion is not dependent on an inhibition of $Ca^{2+}$ activity [109]. This recent study represents an improvement on previous studies that identified the opposite effect of glucose

on $[Ca^{2+}]_i$ activity. Previous electrophysiology studies identified α-cells not by a fluorescent genetic label, but by specific electrophysiological profiles that might have unintentionally selected for a small subset of α-cells.

Fluorescent genetic labeling of α-cells allows for the separation of a pure population of individual α-cells through fluorescence-activated cell sorting (FACS). In support of paracrine models of glucagon secretion over α-cell-intrinsic models, populations of α-cells separated from their islet cell neighbors do not exhibit typical glucose-inhibition of glucagon secretion. Rather, sorted α-cells display an increase in basal glucagon secretion as compared to islets and glucose-stimulation of glucagon secretion rather than a glucose-inhibition of glucagon secretion (Figure 1-13 and [109]). Additionally, individual paracrine factors that have been shown to inhibit glucagon secretion from islets, including insulin and somatostatin, are unable to inhibit glucagon secretion from sorted α-cells [109]. However, when applied together, insulin and somatostatin inhibit glucagon secretion from sorted α-cells, highlighting the importance of multiple concurrent signaling pathways in the regulation of glucagon secretion [126].

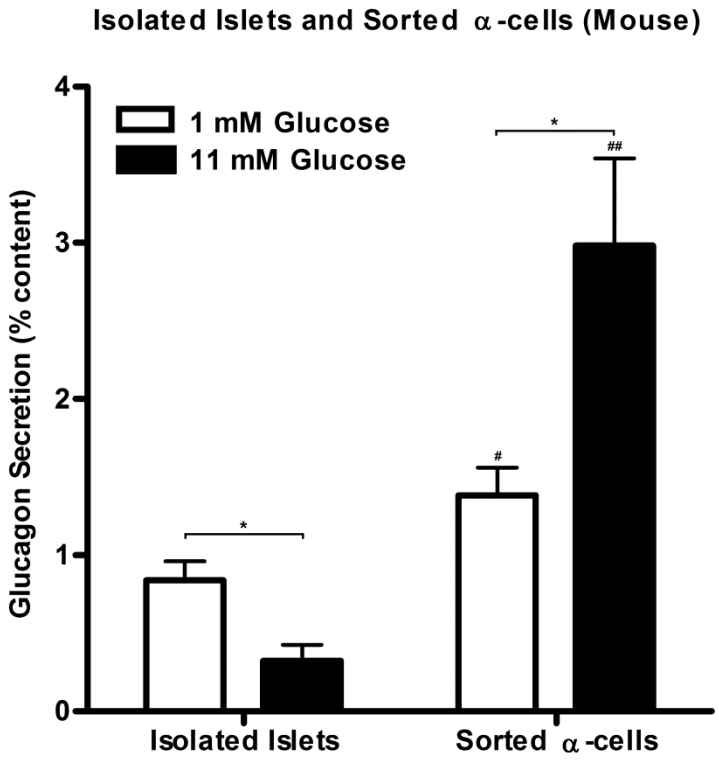


**Figure 1-13 Sorted α-cells have increase glucagon secretion at low glucose and defective glucose-inhibition of glucagon secretion as compared to islets.** Average glucagon secretion from isolated mouse islets (n = 8 mice) and sorted α-cells (n = 8 mice) at low (1 mM; open, white bars) and high (11 mM; closed, black bars) glucose. Data are shown as means (+SEM). Asterisks above brackets represent significant differences between low and high glucose within the same sample type as determined by Student's *t*-test [* $P < 0.05$]. Hash marks (#) directly above columns represent statistical differences between sorted α-cells and isolated islets at the same glucose concentration as determined by Student's *t*-test [# $P < 0.05$; ## $P < 0.01$].

## 1.10 Additional Modulators of Glucagon Secretion

Unlike β-cells, which largely self-regulate insulin secretion, α-cells require outside feedback for appropriate regulation of glucagon secretion. This outside feedback is largely provided within the islet microenvironment; as intact islets replicate the glucose-inhibition response observed *in vivo*, whereas sorted α-cells do not [109]. However, glucagon secretion has also been found to be regulated by signaling pathways that originate outside of the islet microenvironment, including both hormonal and neuronal input.

### 1.10.1 Non-paracrine Intra-islet Modulators of Glucagon Secretion

In addition to paracrine regulation, which is thought to play a large role in glucose-inhibition of glucagon secretion, glucagon secretion from α-cells plays a positive autocrine feedback role, acting to stimulate and sustain glucagon secretion. Similar to the action of glucagon in β-cells, glucagon binds to α-cell glucagon receptors resulting in an stimulation of glucagon secretion through an increase in intracellular cAMP [131].

Intracellular communication through gap junctions is responsible for the coordinated $Ca^{2+}$ oscillations and pulsatile glucose-stimulated insulin secretion response observed in β-cells. The presence and possible physiologic role of intracellular communication between α-cells and neighboring islet-cells is less well understood. Freeze-fracture electron microscopy has provided morphological evidence for gap junctions between α- and β-cells [132]. Additionally, early experiments showed that fluorescent dye was transmittable between neighboring α- and β-cell, indicating a cytoplasmic connection, indicating functional connections between the two different cell types [133,134]. However, more recent studies have failed to detect functional connections between α-cells with other α-cells or α-cells with neighboring β-cells. In electrophysiological studies using whole-cell patch clamping, the current oscillations from β-cells were not observed when recording from α-cells [135]. Additionally, glucose-induced oscillations in α-cell $[Ca^{2+}]_i$ and cAMP are asynchronous with respect to those of other α- and β-cells [136,137].

The role of known juxtacrine signaling pathways in the regulation of glucagon secretion is limited. In addition to its regulation of insulin secretion, NCAM has also been shown to regulate glucagon secretion. $NCAM^{-/-}$ islets display a defect in glucagon secretion that is attributed to an inability to reorganize the submembrane F-actin network in a manner that

facilitates exocytosis [80]. However, the fact that sorted α-cells display an increase in glucagon secretion as compared to islets at basal glucose concentrations that do not stimulate the release of paracrine inhibitors of glucagon secretion suggests that cell-cell contacts, rather than decreased exposure to paracrine factors, mediates the increase in glucagon secretion [138]. In Chapter 2, I discuss the newly emerging role that EphA/ephrin-A juxtacrine signaling plays in the regulation of glucagon secretion through similar modulation of the F-actin network.

### 1.10.2 Extra-islet Modulators of Glucagon Secretion

In addition to possible direct glucose regulation and glucose-dependent paracrine regulation, glucagon secretion is also regulated through available macronutrients, hormones, and neuronal input to reflect specific physiologic needs [139]. The amino acid arginine is a potent stimulator of glucagon secretion. Arginine-stimulation of glucagon secretion likely occurs through mechanisms that mirror arginine-stimulation of insulin secretion, where transport of the cation into the cell results in depolarization, $Ca^{2+}$ influx, and exocytosis [99,100]. Fatty acids have also been shown to induce glucagon secretion directly thought their metabolism [140].

A number of circulating hormones have been shown to directly and indirectly inhibit glucagon secretion. Epinephrine, secreted by the adrenal glands, acts directly on α-cell $\alpha_1$- and β-adrenergic receptors (primarily $\beta_2$) to stimulate glucagon secretion through the production of cAMP [94]. This ensures a steady blood glucose supply during times of sympathetic autonomic activation, including stress and exercise. The incretin hormone GLP-1 results in an inhibition of glucagon secretion. This inhibitory effect is likely mediated through an indirect stimulation of paracrine inhibitors of glucagon secretion rather than direct action on α-cells. Definitive GLP-1

receptor (GLP-1R) expression is lacking among the various islet-cell types. Some studies have found that α-, β-, and δ-cells all express GLP-1R [141], while others have found GLP-1R expression to be restricted to β-cells [142]. In support of indirect glucagon secretion through and increase in somatostatin secretion, GLP-1-induced inhibition of glucagon secretion is reduced or abolished following antibody blockade of somatostatin or SSTR2 antagonism, respectively [143]. Regardless of the mechanism, the ability of GLP-1 to potentiate insulin secretion and inhibit glucagon secretion has made GLP-1 and GLP-1 analogs an attractive option for the pharmacologic treatment of type-2 diabetes. Interestingly, GIP, another incretin, results in the stimulation of glucagon secretion [143–145]. GIP acts directly on α-cells, binding to GIP receptors and triggering an increase in intracellular cAMP and stimulating glucagon secretion [145].

The CNS plays an important role in augmenting glucagon secretion through autonomic input. Glucose sensing neurons within the hypothalamus and brainstem are believe to control the activation/inhibition of sympathetic and parasympathetic stimulation of pancreatic islets [92]. Autonomic control of glucagon secretion is largely controlled by sympathetic stimulation of glucagon secretion. At low glucose and during exercise, sympathetic stimulation via norepinephrine leads to activation of α-cell $\alpha_1$- and β-adrenergic receptors (primarily $\beta_2$), an increase in intracellular cAMP, and an increase in glucagon secretion [92,138]. Interestingly, parasympathetic stimulation also results in a stimulation of glucagon secretion. This is supported by studies indicating that stimulation of the vagus nerve induces glucagon secretion [146–148]. Additionally, cholinergic stimulation of α-cell muscarinic receptors results in an increase in $[Ca^{2+}]_i$ and glucagon secretion [139,149].

## 1.11 Diabetes Mellitus

Diabetes mellitus describes a group of etiologically diverse metabolic disorders that are all characterized by chronic hyperglycemia. In the short-term, untreated hyperglycemia can lead to ketoacidosis and non-ketotic hyperosmolarity, resulting in mental dysfunction, coma, and death. In the long term, chronic hyperglycemia associated with diabetes leads to a number of complications including the damage and dysfunction of a number of organ systems including the heart, kidneys, eyes, peripheral nerves, and blood vessels. Diabetes has traditionally been defined in terms of insulin and β-cell dysfunctions [12]. Regardless of specific etiology the hyperglycemia of diabetes is largely attributed to a defect in insulin secretion, action, or both. In recent years however, defects in glucagon secretion leading to hyperglucagonemia have been shown to contribute to the hyperglycemia of diabetes [150–152].

Clinically, diabetes often presents with a characteristic set of symptoms including polydipsia, polyuria, and polyphagia. Presentation of advanced diabetes can include weight loss, blurry vision, and paresthesia [153]. In patients displaying the classical symptoms of hyperglycemia, the clinical diagnosis of diabetes can be confirmed by abnormalities in one of four different tests of glucose homeostasis: elevated glycation of hemoglobin (A1C), elevated fasting plasma glucose (FPG), sustained glucose elevations following an oral glucose tolerance test (OGTT), or a very elevated random plasma glucose (RPG) [154]. In asymptomatic patients, only abnormalities in A1C, FPG, and OGTT can be used to establish a diagnosis of diabetes.

As of data from 2012, the Centers for Disease Control and Prevention estimates that 29.1 million people (9.3% of the U.S. population) have diabetes [155]. The prevalence of diabetes will likely continue to rise as the incidence of diagnosed diabetes has been predicted to nearly double from 2008 to 2050 (0.8% to 1.5%) [156]. This large and ever-increasing presence of

diabetes represents an enormous societal burden due to increased morbidity and mortality along with financial costs, as the health care costs of a person with diagnosed diabetes are approximately 2.3 times that of a person without [155,157,158]. Diabetes results in an estimated 176 billion dollars in direct medial costs and an additional 69 billion dollars in indirect costs due to disability, work loss, and premature death [155].

Diabetes is classified into four clinical categories: type 1, type 2, gestational, and other specific types [153]. Type 1 diabetes results from the destruction of β-cells which leads to absolute insulin deficiency. Type 2 diabetes results from acquired insulin resistance and a relative insulin deficiency. Gestational diabetes occurs during pregnancy due to a form of insulin resistance. Other specific types of diabetes are caused by a number of factors including genetic defects in β-cell function (mature onset diabetes of the young), genetic defects in insulin action (type A insulin resistance), and destruction or removal of the pancreases (cystic fibrosis, infection, neoplasia, pancreatectomy) [12]. Here, I will discuss type 1 and type 2 diabetes, as they are most relevant to the work presented.

### 1.11.1 Type 1 Diabetes

Type 1 diabetes accounts for ~5% of diagnosed cased of diabetes and is characterized by β-cell destruction that leads to an absolute insulin deficiency [155] (Figure 1-14). These individuals require exogenous insulin for survival, which led to the earlier classification of type 1 diabetes as "insulin-dependent diabetes." Type 1 diabetes has also previously been referred to as "juvenile-onset diabetes" as the peak age of onset is in the mid-teens [155]. Although rare after the age of 40, the onset of type 1 diabetes can occur at any age. Type 1 diabetes is

subclassified into immune-mediated type 1 diabetes (type 1A) and idiopathic type 1 diabetes (type 1B). The destruction of β-cells in diabetes type 1A is thought to be mediated by an autoimmune process and is characterized by the presence of autoantibodies, such as those to insulin, islet-specific glucose-6-phosphatase catalytic-subunit-related protein, insulinoma-associated protein 2, zinc-transporter 8, and glutamic acid decarboxylase [154]. Autoimmune destruction of β-cells is thought to be triggered in genetically susceptible individuals following exposure to one or more unknown environmental factors [159]. Individuals with type 1A diabetes also have an increased risk for developing other autoimmune disorders including Graves disease, Hashimoto thyroiditis, Addison disease, vitiligo, and pernicious anemia [12]. Type 1 diabetes that occurs in the absence of autoantibodies is classified as type 1B [160]. Diabetes type 1A is more common among white individuals while diabetes type 1B is more common in individuals of African or Asian heritage [12].

Independent of etiology and subclassification, type 1 diabetes is characterized by an absolute insulin deficiency. Without insulin, individuals with type 1 diabetes are unable to adequately take-up and store glucose, resulting in persistent hyperglycemia. Prior to the isolation of insulin for exogenous administration, type 1 diabetes was a terminal disease with only few years of life-expectancy [161]. Insulin was first isolated, purified, and administered to a patient in 1922 and insulin replacement therapy has since become the cornerstone of type 1 diabetes care [162]. Tight control of blood glucose through intensive insulin therapy drastically reduces the long-term sequelae of diabetes [163,164]. However, the administration of exogenous insulin holds inherent risks, including the loss of consciousness and death from insulin-induced hypoglycemia. Thus, blood glucose management using insulin replacement therapy is a balance

between the risks of long-term complications of hyperglycemia and the short-term complications of hypoglycemia.

### 1.11.2 Type 2 Diabetes

Type 2 diabetes is by far the most common form of diabetes, representing ~90-95% of all forms of diabetes [155]. It is characterized by insulin resistance and a relative insulin deficiency. However, disorders in insulin secretion are also prominent in type 2 diabetes [12]. Type 2 diabetes typically develops later in life. The median age for the diagnosis of diabetes is ~54 years [165]. The specific etiology of type 2 diabetes is unknown, however it is generally accepted that both progressive insulin resistance and β-cell death with corresponding defects in insulin secretion play a major role in the development of type 2 diabetes [166]. Patients with type 2 diabetes often present with increased plasma insulin as compensation for the increased demand caused by peripheral insulin resistance. In these patients, increased insulin secretion is supported by an expansion of β-cell mass and increased secretory function [167] (Figure 1-14). This increased demand on β-cells is thought to contribute to β-cell failure and apoptosis through a number of possible molecular pathways including mitochondrial dysfunction and the production of reactive oxygen species, impaired anaplerosis and cataplerosis, dysregulation of lipid metabolism and cycling, gluco- and lipotoxicity, endoplasmic reticulum stress, inflammation, and amyloid deposition [167,168].

A number of genetic and environmental risk factors have been implicated in the development of type 2 diabetes. A large genetic component to the pathogenesis of type 2 diabetes is demonstrated by an increased risk of developing the disease in first-degree relatives

of patients with type 2 diabetes [169], the coincidence of type 2 diabetes in monozygotic twins [170], and the disparities between different ethnic groups [171,172]. Additionally, genome-wide association analysis has identified a number of loci within genes involved with pancreatic development and insulin synthesis, secretion, and action that are associated with an increased risk of developing type 2 diabetes [173]. The largest environmental factors that contribute to the development of type 2 diabetes are obesity and physical inactivity [174]. Although these two factors are closely related, they have each been shown to independently be associated with type 2 diabetes and its comorbidities. Obesity and physical inactivity are thought to induce insulin resistance. However, the mechanism by which this occurs is not well understood. One leading hypothesis is that inflammation mediates the effects of insulin resistance [175].

Initially, glycemic control in patients with type 2 diabetes is often managed through lifestyle changes in diet and exercise and pharmaceutically with metformin [153]. Metformin primarily acts to suppress hepatic glucose production, and is often used in combination with other oral antidiabetic drugs that act to increase insulin secretion [176]. Many patients do not initially require exogenous insulin, which led to type 2 diabetes previously being referred to as "noninsulin-dependent diabetes". However, many type 2 diabetic patients are managed using insulin.

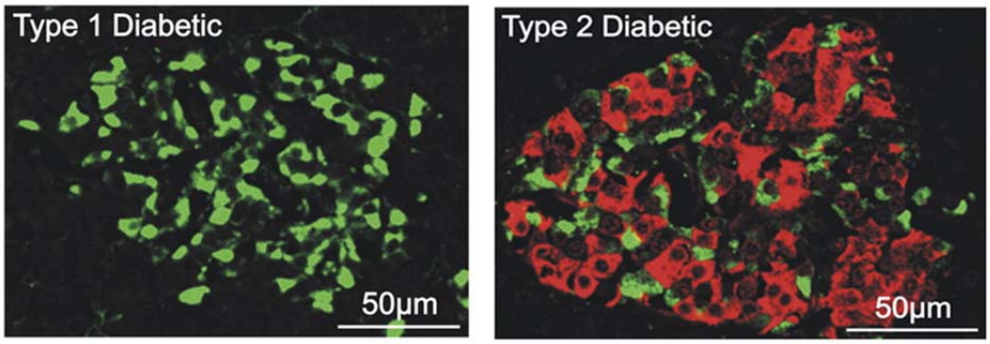


**Figure 1-14 Morphological differences between islets from type 1 and type 2 diabetic patients.** Confocal sections of a representative islet from a type 1 diabetic patient (left) and a type 2 diabetic patient (right). Glucagon containing α-cells are shown in green and insulin containing β-cells are shown in red. (Figure adapted with permission from [127])

## 1.12 Glucagon Dysfunction and Diabetes

Diabetes has traditionally been defined by the dysfunctional secretion and action of a single hormone, insulin. However, multiple metabolic and hormone dysfunctions contribute to the pathophysiology of type 1 and type 2 diabetes [177], including dysfunctional glucagon secretion [178,179] (Figure 1-15). Increased fasting glucagon and decreased glucose-inhibition of glucagon secretion, or over glucose-stimulation of glucagon secretion, have been observed in both type 1 and type 2 diabetic patients [127,180]. These defects in glucagon secretion result in hyperglucagonemia and exacerbate hyperglycemia [150–152]. The bihormonal-abnormality hypothesis suggests that an absolute or relative insulin deficiency is responsible for the lack of glucose utilization in diabetes and that an absolute or relative excess of glucagon drives the over-production of glucose in diabetes [181]. Thus, defects in insulin and glucagon signaling act together to produce the hyperglycemia of diabetes. Despite the critical role that dysfunctional glucagon secretion plays in the pathophysiology of diabetes, the regulatory mechanisms underlying this defect in glucagon secretion remain poorly understood.

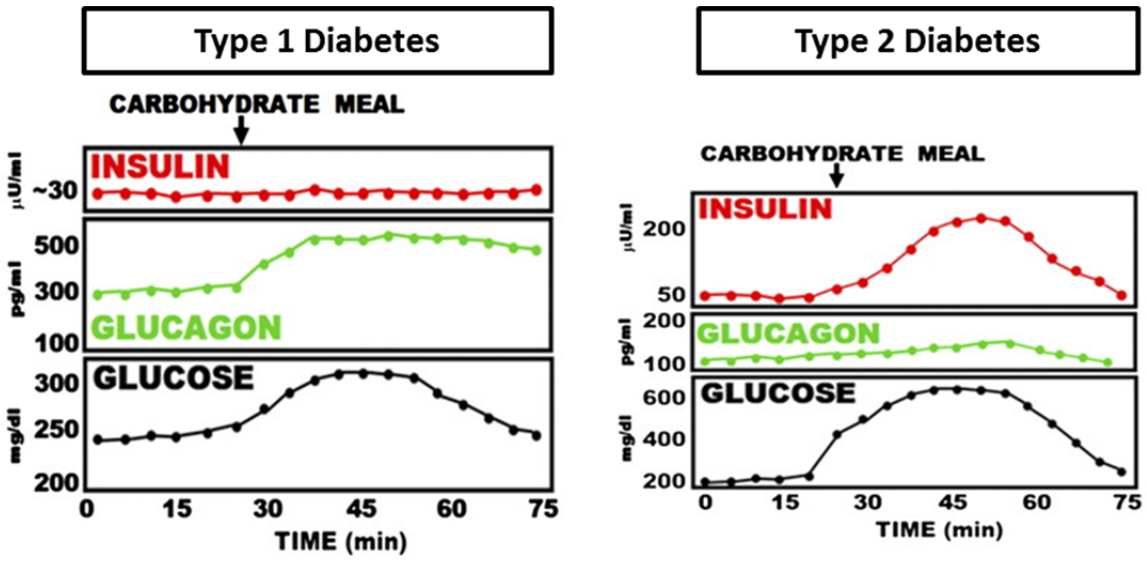


**Figure 1-15 Dysfunctional regulation of glucagon secretion in type 1 and type 2 diabetes.** Glucose and hormone response to ingestion of a carbohydrate meal in a type 1 diabetic patient (left) and a type 2 diabetic patient (right). The type 1 diabetic patient displays basal hyperglucagonemia prior to ingestion of the carbohydrate meal and further stimulation of glucagon secretion and a rise in blood glucose following the carbohydrate meal. The type 2 diabetic patient displays milder hyperglucagonemia prior to ingestion of the carbohydrate meal and a lack of glucose-inhibition of glucagon secretion following ingestion of the carbohydrate meal despite robust insulin secretion. (Figure adapted with permission from [127])

The increase in basal glucagon secretion and loss of glucose-inhibition of glucagon secretion observed in diabetes as compared to unaffected individuals is the same glucagon secretion phenotype that is observed in sorted α-cells as compared to intact islets. This suggests that the same process or processes may be responsible for the dysfunctional glucagon secretion observed in both diabetes and in sorted α-cells. Applied to a diabetic model, the paracrine hypothesis of glucose-inhibition of glucagon secretion explains the hyperglucagonemia and the lack of inhibition of glucagon secretion through absolute and relative insulin insufficiency [127,182,183]. In Chapter 2, I present data in support of novel EphA/ephrin-A-mediated regulation of glucagon secretion that complements current models of paracrine-mediated regulation of glucagon secretion in both unaffected and diabetic states.

In rodent models, the inhibition of glucagon secretion or suppression of glucagon action in diabetes leads to the restoration of euglycemia, even in the absence of insulin, demonstrating the major role that glucagon plays in the pathophysiology of diabetes. Blocking glucagon action through knockout of the glucagon receptor prevents mice from developing the clinical manifestations of diabetes associated with destruction of β-cells [184]. In multiple models of type 1 diabetes in both mice and rats, increased leptin expression corrects hyperglycemia and ketosis. These results are thought to be mediated through the suppression of hyperglucagonemia [185]. Treatment with exogenous leptin has also been shown to produce similar results [186]. Additionally, transplantation of embryonic brown adipose tissue has been shown to reverse type 1 diabetes in a mouse model. Brown adipose tissue transplantation restores euglycemia and normalizes glucose tolerance [187]. New data suggests that these effects may be mediated through the correction of hyperglucagonemia resulting from direct inhibition of glucagon secretion by a brown adipose tissue secreted factor (discussed in Chapter 3). Together, these data suggest the possibility of a new strategy to normalize blood glucose through the modulation of glucagon secretion and action. Unfortunately, agents targeting glucagon action (glucagon receptor antagonists) cause hyperlipidemia and hypertension, two outcomes that are particularly deleterious for diabetics [188]. Targeting glucagon secretion represents a more efficient method of addressing hyperglucagonemia. Thus, understanding the mechanisms underlying α-cell function and glucagon secretion is highly significant and essential for the identification of novel therapeutic α-cell targets for the inhibition of glucagon secretion. Combined with current treatment strategies, therapeutics based on α-cell targets will benefit diabetic patients by addressing multiple causes of hyperglycemia.

# CHAPTER 2
# EPHA/EPHRIN-A REGULATION OF GLUCAGON SECRETION

## 2.1 Introduction

Eph receptors were first discovered in 1987 in a search for RTKs involved in cancer. They were named for the **e**rythropoietin-**p**roducing **h**epatocellular carcinoma cell line in which they were initially identified [189]. Eph receptors are the largest subfamily of RTKs. Prototypical of RTKs, Eph receptors contain a multidomain extracellular region (including a ligand-binding domain), a single transmembrane segment, and a cytoplasmic kinase domain [190] (Figure 2-1). Like other RTKs, Eph receptors transduce extracellular stimuli into an intracellular signaling response. However, unlike other RTKs that bind soluble ligands, Eph receptors bind membrane-bound ephrin ligands. Thus, direct cell-cell contact is required to initiate signal transduction. Eph receptors and ephrin ligands are separated into two subclasses, A and B, based on sequence homology and their relative affinity for each other. There are 9 EphA (A1-A8, A10) and 5 EphB receptors (B1-B4, B6) that interact with 5 ephrin-A (A1-A5) and 3 ephrin-B (B1-B3) ligands. In general, intra-class interactions are very common while inter-class interactions are very rare. However, there are exceptions. For example, EphA4 binds eprhin-Bs and EphB2 binds ephrin-A5 [191]. Eph/ephrin signaling has been shown to play a role in diverse developmental [192], physiological [193], and pathological [191] processes. Due to the complex nature of Eph/ephrin signaling, evaluating and understanding these processes represents a significant challenge.

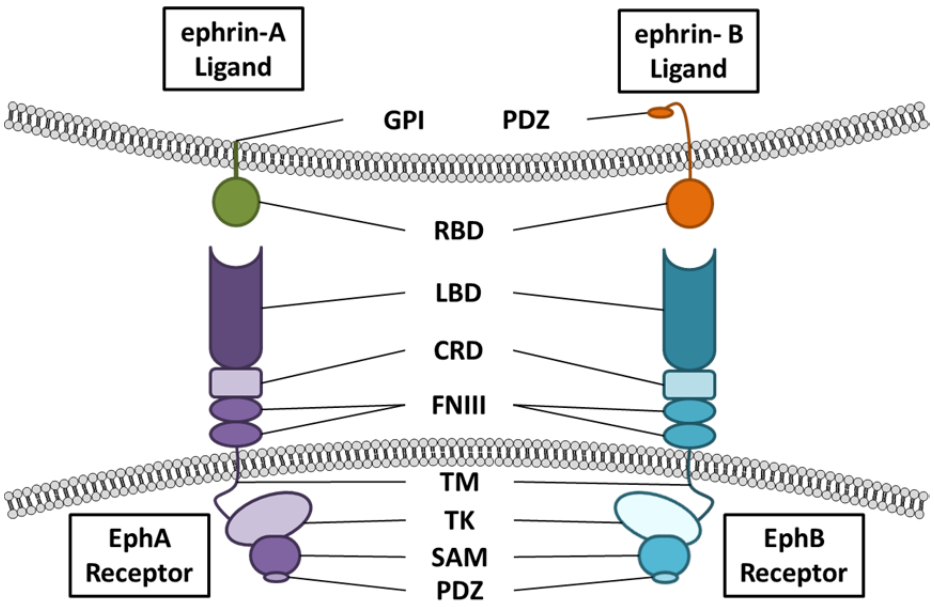


**Figure 2-1 Domain structure of Eph receptors and ephrin ligands.** The domain structure is conserved between EphA and EphB receptors. The extracellular domain of EphA and EphB receptors consists of an N-terminal ligand binding domain (LBD), a cytosine-rich domain (CRD), and 2 fibronectin type-III (FNIII) repeats. The extracellular domains are linked to the intracellular domains by a single-pass transmembrane (TM) domain. The intracellular domains consist of a tyrosine kinase domain (TK), a sterile α motif (SAM), and a post synaptic density protein/drosophila disc large tumor suppressor/zonula occludens-1 protein domain (PDZ). The ephrin ligands share a conserved extracellular receptor binding domain (RBD). Ephrin-A ligands are attached to the membrane through a glycosylphosphatidylinositol (GPI)-anchor. Ephrin-B ligands contain a transmembrane domain and a PDZ domain.

### 2.1.1 Eph/ephrin Signaling Mechanics

EphA/ephrin-A signaling is unique from other RTK signaling systems, in that EphA/ephrin-A signaling is bidirectional. This means that EphA receptors also act as ligands and ephrin-A ligands also act as receptors. In bidirectional signaling, traditional ligand-stimulated signaling to the Eph expressing cell is termed "forward signaling" and receptor-stimulated signaling to the ephrin expressing cell is termed "reverse signaling" (Figure 2-2). Upon Eph/ephrin binding, both forward and reverse signaling can occur simultaneously. In addition to traditional *trans* signaling, where a signaling occurs between two different cells, Eph receptors have also been reported to interact with ephrin ligands and other Eph receptors within the same cell, in *cis* [194].

*Cis* binding of Eph receptors and ligands does not activate kinase activity and signaling, but instead has been reported to inhibit *trans* Eph/ephrin signaling, possibly through the inhibition of *trans* interaction between Eph receptors and ephrin ligands [195]. Additionally, ligand-independent activity of EphA2 receptors has been reported in numerous cancer cell lines. The ligand-mediated and ligand-independent actions of EphA2 typically regulate opposing biological processes [86]. Further, 2 Eph receptors, EphA10 and EphB6, are involved in a number of biological functions despite their lack of kinase activity, suggesting a ligand-independent function for Eph receptors [190]. However, the extent of this phenomenon in other Eph receptors and its role in physiologic processes has yet to be determined.

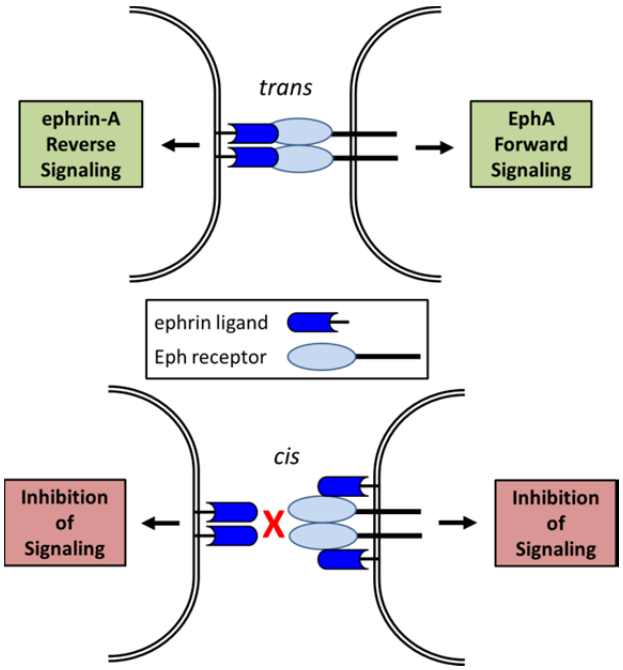


**Figure 2-2 Variations in Eph/ephrin Signaling.** (upper) With *trans* interactions between Eph receptors and ephrin ligands on separate cells, Eph/ephrin signaling is bidirectional. Signaling into the cell expressing the Eph receptor is termed forward signaling and signaling into the cell expressing the ephrin ligand is termed reverse signaling. (lower) *Cis* interactions between Eph receptors and ephrin ligands within the same cell have been shown to block *trans* interactions, inhibiting both forward and reverse signaling.

Prior to ligand binding, inactive Eph receptors are evenly dispersed across the cell membrane and exhibit little kinase activity and downstream signaling. Upon ligand binding, interacting Eph receptors and ephrin ligands oligomerize together to form efficient signaling complexes where trans-phosphorylation leads to the activation of Eph tyrosine kinase activity. Unlike other RTKs, which bind to their ligands with a 2:1 (receptor to ligand) ratio and exhibit efficient signaling upon dimerization, Eph receptors bind ephrin ligands with a 1:1 (receptor to ligand) ratio and clusters of Eph/ephrin interactions are required to establish efficient down-stream Eph/ephrin signaling [196]. Eph/ephrin clusters can be composed of heterogeneous populations of Eph receptors and ephrin ligands, the composition of which modulates downstream signaling [197]. Additionally, cross-activation between EphA and EphB receptors interacting with different ligands has been observed [198]. The clustering of Eph/ephrin complexes has also been shown to expand laterally within a single cell through ligand independent Eph/Eph receptor interactions in *cis* [199]. This represents a possible method for the amplification of a small initial ephrin-initiated signal. Adding further complexity, Eph/ephrin signaling regulates and is regulated by a number of other signaling pathways, including cell surface receptors, adhesion molecules, ion channels/pores, and cell surface proteases [195].

### 2.1.2 Eph/ephrin Signaling Pathways

Historically, Eph/ephrin signaling has largely been studied within the fields of developmental and cancer biology. Nearly all developing tissues express Eph receptors and ephrin ligands. Eph/ephrin signaling has been shown to play a key role in a diverse range of developmental processes including cardiovascular, skeletal, and neuronal development, as well as tissue

patterning [195]. The role of Eph/ephrin signaling in the development and progression of cancer is well documented. Eph/ephrin signaling has been shown to play a role in tumor growth, invasiveness and metastasis [191]. A number of features influence the complexity of Eph/ephrin signaling including bidirectional signaling, *cis*/*trans* signaling, the promiscuity of multiple receptors and ligand interactions, multiple Eph/ephrin signaling microdomains within a single cell, and crosstalk with other signaling pathways, leading to a diverse Eph/ephrin signaling network that is highly context dependent. However, many of the biological effects induced by Eph/ephrin signaling are attributed to a balance between cell adhesion and migration. Thus, the most well documented outcome of Eph/ephrin signaling is cytoskeletal rearrangement and the regulation of cell-matrix interactions. In general, activation of Eph forward signaling leads to cell rounding and migration while activation of ephrin reverse signaling leads to cell adhesion. However, it should be noted that Eph/ephrin signaling is highly context specific. Interactions of the same two Eph/ephrin receptor/ligand pairs have been shown to result in diametrically opposed outcomes in different settings [190]. In addition to adhesion and migration, Eph/ephrin regulation of cytoskeletal elements has been shown to be involved in more 'static' physiological processes. Eph/ephrin signaling has been linked to the regulation of actin polymerization within pre- and postsynaptic terminals and through this action is thought to contribute to the processes of neural plasticity, long-term potentiation, memory, and learning [200]. Eph/ephrin signaling mediated actin rearrangement is also thought to play a role in the glucose-dependent regulation of hormone secretion from pancreatic islets (discussed in 2.1.3 and 2.3) [85].

### 2.1.3 EphA/ephrin-A Regulation of Insulin Secretion

Juxtacrine signaling through EphA/ephrin-A has been shown to contribute to the regulation of insulin secretion in islets [85]. Konstantinova et al. observed that islets treated with soluble EphA receptors (EphA5-Fc) or ephrin-A ligands (ephrin-A5-Fc) exhibit opposite effects on insulin secretion. Treatment with EphA5-Fc stimulates insulin secretion at 2 and 25 mM glucose, while treatment with ephrinA5-Fc inhibits insulin secretion at 25 mM glucose (Figure 2-3).

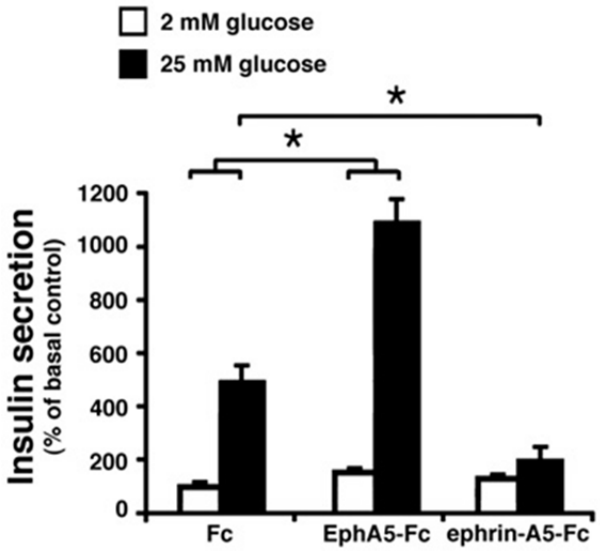


**Figure 2-3 EphA/ephrin-A signaling regulates insulin secretion from islets.** Insulin secretion from pancreatic islets treated with Fc control, EphA5-Fc, or ephrin-A5-Fc at 2 mM glucose (white bars) and 25 mM glucose (black bars). Insulin secretion is normalized to insulin content and total protein content. *$p < 0.05$. Data are shown as means ±SD (n = 3 experiments). Figure adapted with permission from [85].

Additionally, ephrin-$A5^{-/-}$ mice were found to have impaired glucose clearance and a defect in glucose stimulated insulin secretion was observed from ephrin-$A5^{-/-}$ islets. The authors attributed the EphA/ephrin-A-induced changes in insulin secretion to Rac1-mediated rearrangements in F-actin. Further, glucose-dependent decreases in EphA receptor phosphorylation was observed and reversed with inhibition of protein tyrosine phosphatase

(PTP) activity. Together, these data was used to create a model of glucose-dependent EphA/ephrin-A mediated insulin regulation where glucose mediates the balance between forward and reverse signaling and thus mediates the suppression or facilitation of insulin secretion. At low glucose, it was proposed that low PTP activity results in sustained phosphorylation of activated EphA receptors in β-cells, thus promoting forward signaling over reverse signaling. EphA forward signaling would then lead to the inhibition of Rac1 and an increase in cortical F-actin density that would physically inhibit the exocytosis of insulin granules. At high glucose, it was hypothesized that a glucose-sensitive PTP would have increased activity leading to the inactivation of EphA receptors and the promotion of ephrin-A reverse signaling over EphA forward signaling. In this model, ephrin-A reverse signaling leads to the activation of Rac1 and the depolymerization of F-actin, thus enhancing insulin secretion (Figure 2-4).

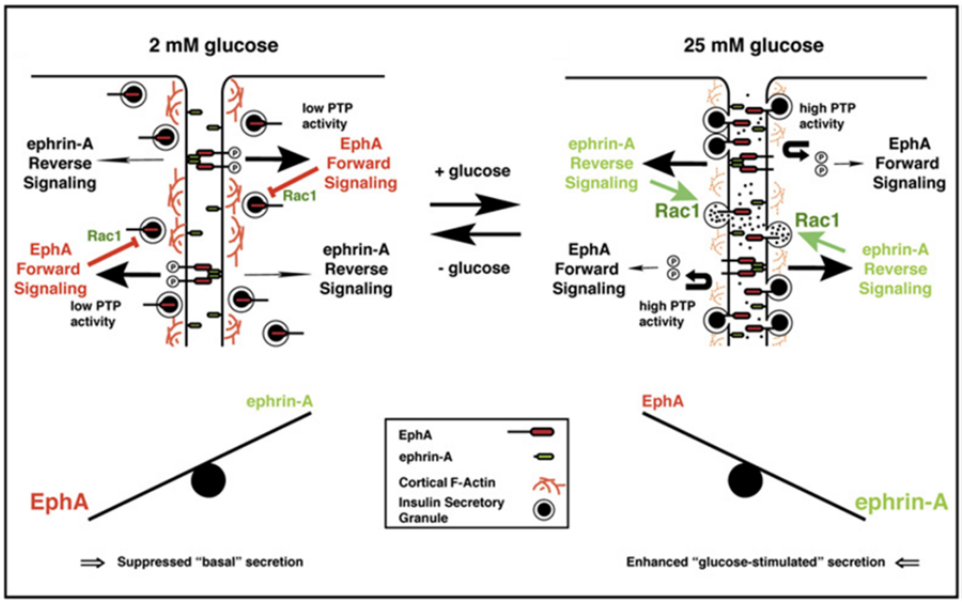


**Figure 2-4 Model of depicting the role of EphA/ephrin-A singling in the glucose-regulation of glucagon secretion.** At low glucose forward singling dominates the EphA/ephrin-A interactions between neighboring β-cells, suppressing insulin secretion. At high glucose, reverse signaling dominates the EphA/ephrin-A interactions between neighboring β-cells, enhancing insulin secretion.

Given the similarities between α- and β-cells, we hypothesized that EphA/ephrin-A signaling plays a similar role in the regulation of glucagon secretion. In order to further develop a model for the normal regulation of glucagon secretion and the dysregulation of glucagon secretion observed in diabetes, we investigated the role that EphA/ephrin-A signaling plays in the glucose-regulation of glucagon secretion. Our data support a juxtacrine signaling model of the inhibition of glucagon secretion from intact islets where ephrin-A ligands on neighboring islet cells signal to EphA receptors on α-cells, resulting in the tonic and glucose-dependent inhibition of glucagon secretion.

## 2.2 Methods

### 2.2.1 Experimental Animals

All mouse work was performed using 10-16 week old male mice in compliance with the Vanderbilt University Institutional Animal Care and Use Committee. Ephrin-A5$^{-/-}$ mice have been previously described [85]. Mice expressing red fluorescent protein in α-cells (αRFP mice) have been previously described [109]. α-cell-specific EphA4$^{-/-}$ (αEphA4$^{-/-}$) mice were generated by crossing floxed-EphA4 mice (The Jackson Laboratory) with αRFP mice. The truncated glucagon promotor in αRFP and αEphA4$^{-/-}$ mice results in Cre-recombinase expression specific to α-cells (not preset in other islet cells or L-cells) with ~76% penetrance [201]. Transgenic mice were identified by PCR. Mice without Cre-recombinase expression were used as wild-type controls.

### 2.2.2 Isolation and Culture of Mouse and Human Islets

Mouse islet isolation and culture was performed as previously described [67,109]. Mouse islets were cultured overnight prior to experiments. Human islets were obtained from the Integrated Islet Distribution Program in collaboration with Alvin C. Powers, M.D. (Vanderbilt University, Department of Medicine) and cultured in RPMI 1640 (Invitrogen) with 10% FBS (Life Technologies) and 11 mM glucose (Sigma) overnight before use. Islet donor information is available in Table 2-1.

| Donor | Age | Sex | BMI |
|---|---|---|---|
| **1** | 30 | M | 43.7 |
| **2** | 61 | F | 31.1 |
| **3** | 28 | M | 32.8 |
| **4** | 51 | M | 35.8 |
| **Average** | 42.5 ± 7.0 | | 35.9 ± 2.4 |

**Table 2-1 Human islet donor information.** This table provides the age, sex, and body mass index (BMI) for each donor of human islets utilized in this study.

### 2.2.3 α-cell Sorting

Islets with red fluorescent α-cells were dissociated in Accutase (Life Technologies) at 37°C by repeated trituration for ~3 minutes. Dissociated islet cells were pelleted and suspended in BMHH buffer (125 mM NaCl, 5.7 mM KCl, 2.5 mM $CaCl_2$, 1.2 mM $MgCl_2$, and 10 mM HEPES; pH 7.4) (all Sigma) with 0.1% BSA (EMD Millipore); pH 7.4) and 11 mM glucose. A FACSAria (BD Biosciences) was used to sort RFP positive α-cells with high viability and purity [109].

### 2.2.4 Static Hormone Secretion Assays

Islets were equilibrated in KRBH buffer (128.8 mM NaCl, 4.8 mM KCl, 1.2 mM $KH_2PO_4$, 1.2 mM $MgSO_4 \cdot 7H_2O$, 2.5 mM $CaCl_2$, 20 mM HEPES, and 5 mM $NaHCO_3$; pH 7.4) (all Sigma) with 0.1% BSA and 2.8 mM glucose for 45 minutes at 37°C. Twenty islets per sample were incubated in 250 µL of KRBH at low (1 mM) glucose in 1.5 ml microcentrifuge tubes and treated as indicated with 4 µg/mL rodent or human ephrin-A5-Fc, EphA5-Fc, Fc (all R&D Systems), 1 µM S961 (Novo Nordisk), 200 nM CYN154806 (CYN) (Tocris Bioscience), 12.5 µM 4-(2,5-dimethyl- pyrrol-1-yl)-2-hydroxy-benzoic acid (DPHBA) (Santa Cruz Biotechnology) and/or vehicle (DMSO) (0.05%) for 45 minutes at 37°C. Islets were transferred to high (11 mM) glucose containing the same drug/treatment and incubated for an additional 45 minutes at 37°C. Insulin and glucagon were

measured in duplicate by Mouse UltraSensitive Insulin ELISA (Alpco), Human Insulin ELISA (Alpco), or Glucagon ELISA (RayBiotech). Secretion assays using sorted α-cells were performed using ~200 α-cells per sample directly following sorting. Hormone secretion is expressed as percent of total hormone content, as obtained by acid/ethanol extraction (0.2 M HCL (Mallinckrodt) in 80% ethanol (Pharmco-AAPER)).

### 2.2.5 Perifusion Hormone Secretion Assay

The perifusion of islets and assessment of hormone secretion was performed in collaboration with the Islet Procurement and Analysis Core (Vanderbilt University). Islets from wild-type and ephrin-A5$^{-/-}$ (~150-200 islets) were perifused with low glucose (1 mM) for 15 minutes, high glucose (11 mM) for 30 min, and then low glucose (1 mM) again for 30 minutes. Fractions of the flow through were collected every 3 minutes. Hormone content was assessed by radio-immunoassay by the Vanderbilt Hormone Assay Core. Hormone content per islet equivalents was normalized to average hormone secretion from the first 7 fractions.

### 2.2.6 RNA Extraction and Quantitative Real-Time PCR (qRT-PCR)

Total RNA from sorted α-cells and control tissue was extracted using an RNeasy Micro Kit (Qiagen). Unique primers were designed for the detection of EphA1, EphA2, EphA3, EphA4, EphA5, EphA6, EphA7, EphA8, EphA10, and 5 housekeeping genes (Hsp90ab1, Tfrc, Ppia, Sdha, and Pgk1). Primers were validated on RNA extracted from 15 different mouse tissues. qRT-PCR was performed with SuperScript III Platinum SYBR Green One-Step qRT-PCR Kit (Life Technologies) on a CFX96 Real-Time PCR Detection System (Bio-Rad).

### 2.2.7 Glucose/Insulin Tolerance Tests and Plasma Hormones

Intraperitoneal glucose tolerance tests (IPGTTs) were performed following a 16-hour fast and intraperitoneal insulin tolerance tests (IPGTTs) were performed following a 5-hour fast. Mice under isofluorane (Henry Schein)/oxygen anesthesia received an injection of sterile glucose (Sigma) (1 g/kg) or insulin (Novo Nordisk) (0.5 U/kg). Anesthesia exposure was minimized during the IPGTT (less than 5 minutes per time point) to minimize confounding insulin resistance and hyperglycemia [202]. Blood glucose was measured by tail snip using a glucose meter (Accu-Chek) at 0, 15, 30, 60, and 90 or 120 minutes after glucose/insulin injection. An additional ~60 µL of blood was collected at 0 and 30 minutes during the IPGTT for hormone analysis of plasma insulin and glucagon using the Luminex 100 System (Luminex Corporation).

### 2.2.8 Immunofluorescence and Live-cell Imaging

Islets were treated at 1 mM glucose with or without ephrin-A5-Fc, EphA5-Fc, or Fc and incubated at 37°C for 45 minutes. Islets were immediately placed on ice and fixed/permeabilized with 4% paraformaldehyde (Electron Microscopy Sciences) and 0.1% Triton X-100 (Sigma) in PBS (Sigma). Islets were incubated with a primary mouse anti-glucagon antibody (1:50) and Alexa Fluor 594 phalloidin (1:40) or Alexa Fluor 660 phalloidin (1:40) for 72 hours followed by incubation with a secondary goat anti-mouse antibody Alexa-Fluor 488 conjugate (1:1000) for 72 hours (all Life Technologies). Live-cell imaging was performed on an environmentally controlled stage (37°C and 5% $CO_2$). Prior the imaging protocol islets were loaded with Fluo 4-AM (Life Technologies) in BMHH buffer with 2.8 mM glucose for 30 minutes at room temperature. Islets were then treated with ephrin-A5-Fc, Fc control, DPHBA, or vehicle (DMSO) and Fluo-4 and RFP fluorescence intensity were taken every 2 seconds for 10 minutes.

The $Ca^{2+}$ data represents α-cells that display $Ca^{2+}$ activity as a percentage of total α-cells within a 10 minute period. α-cell $Ca^{2+}$ activity was defined by an increase in Fluo-4 intensity that was 4 standard deviations above baseline. NAD(P)H autofluorescence was assessed in islets treated with ephrin-A5-Fc, Fc control, DPHBA, or vehicle (DMSO) following two-photon excitation in α-cells. NAD(P)H data are normalized to maximal NAD(P)H autofluorescence produced by treatment with 3mM NaCN (Sigma) following the outlined imaging protocol. All fluorescence microscopy imaging was performed using confocal and/or two-photon microscopy with appropriate excitation and spectral emission windows (LSM780; Carl Zeiss).

#### 2.2.9 Data Analysis and Statistics

Data were analyzed with Microsoft Excel, GraphPad Prism, or ImageJ software. Raw images were used for quantification of mean fluorescence intensity in specified regions of interest following background subtraction. Image brightness and contrast were adjusted linearly over the entire image only for presentation. Data are reported as mean values (+SEM), with p-values less than 0.05 considered statistically significant as determined by a Student's *t*-test between a small number of distinct planned comparisons.

## 2.3 Results

#### 2.3.1 Ephrin-A5 is required for appropriate insulin, but not glucagon secretion

Ephrin-$A5^{-/-}$ mice have previously been described to have impaired glucose tolerance due to a defect in insulin secretion [85]. Initial studies were aimed at confirming this insulin secretion phenotype and evaluating the glucagon secretion phenotype in these mice. Perifusion of wild-

type and ephrin-A5$^{-/-}$ islets confirmed the previously observed defect in insulin secretion. As compared to wild-type islets, ephrin-A5$^{-/-}$ islets display a decrease in the first and second phase of insulin secretion (Figure 2-5). However, glucagon secretion is unchanged between wild-type and ephrin-A5$^{-/-}$ islets (Figure 2-6).

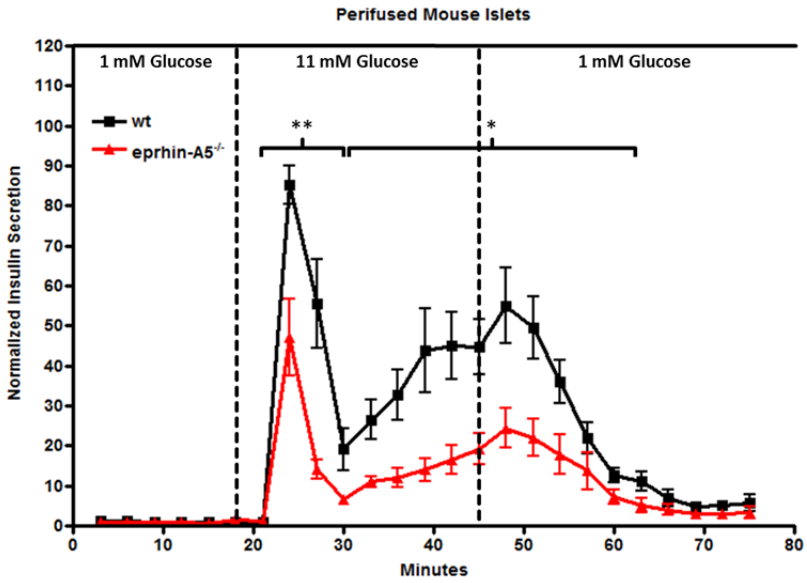


**Figure 2-5 Ephrin-A5 is required for appropriate insulin secretion.** Ephrin-A5$^{-/-}$ islets (red, n = 4 mice) have a decrease in the first and second phase of glucose-stimulated insulin secretion as compared to wild-type (wt) (black, n = 4 mice) islets. Insulin secretion is normalized to the average secretion observed in fractions 1-7. Data are shown as means (±SEM).

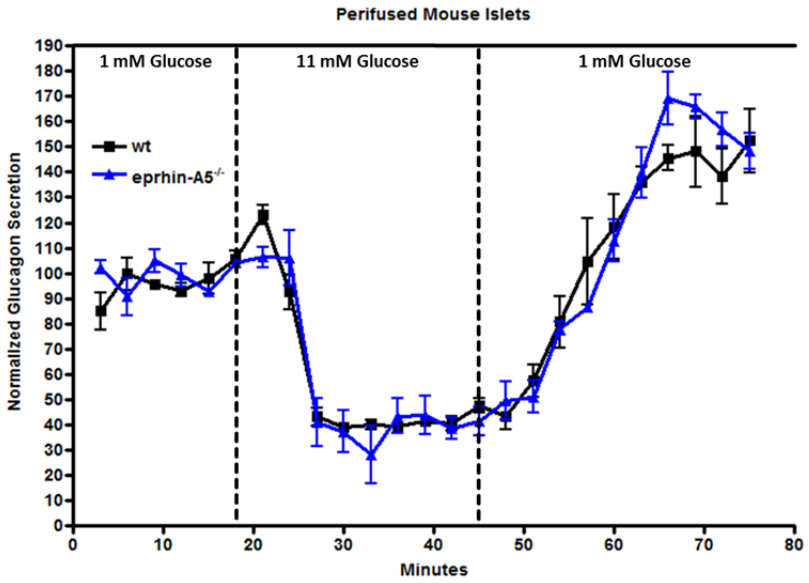


**Figure 2-6 Ephrin-A5 is not required for appropriate glucagon secretion.** No changes in the glucose-inhibition of glucagon secretion are observed between ephrin-A5$^{-/-}$ islets (blue, n = 3 mice) and wild-type (wt) islets (black, n = 4 mice). Glucagon secretion is normalized to the average secretion observed in fractions 1-7. Data are shown as means (±SEM).

### 2.3.2 Stimulation and Inhibition of EphA/ephrin-A Signaling Modulates Insulin and Glucagon Secretion in Mouse Islets

To study the effects of EphA/ephrin-A signaling on glucagon secretion, soluble disulfide-linked homodimers of ephrin-A-Fc and EphA-Fc (fusions of ligand/receptor and the crystallizable fragment of IgG) were used to manipulate EphA forward and ephrin-A reverse signaling in islets. Homodimerization results in the clustering of the ligand/receptor and is required for the initiation of EphA/ephrin-A signaling. Ephrin-A5-Fc and EphA5-Fc were chosen for their ability to bind virtually all EphA and ephrin-A family members, respectively [192]. Treatment with ephrin-A5-Fc stimulates pan-EphA forward signaling through direct stimulation of EphA receptors and inhibits endogenous pan-ephrin-A reverse signaling through the binding and blockade of endogenous EphA receptors. In contrast, application of EphA5-Fc stimulates pan-ephrin-A reverse signaling through direct stimulation of ephrin-A ligands and inhibits

endogenous pan-EphA forward signaling through the binding and blockade of endogenous ephrin-A ligands. An unconjugated Fc fragment was used as a control for both treatments. At high glucose, ephrin-A5-Fc treatment inhibited insulin secretion and EphA5-Fc treatment enhanced insulin secretion as compared to Fc control (Figure 2-7A). This is consistent with previously described experiments [85]. At low glucose, ephrin-A5-Fc treatment inhibits glucagon secretion and EphA5-Fc treatment enhances glucagon secretion as compared to Fc control (Figure 2-7B). However, different effects are observed at high glucose. At high glucose, ephrin-A5-Fc treatment enhances glucagon secretion and EphA5-Fc treatment has no effect on glucagon secretion as compared to Fc control (Figure 2-7B). These EphA/ephrin-A mediated effects on glucagon secretion at high glucose correspond with reciprocal changes in insulin secretion at high glucose.

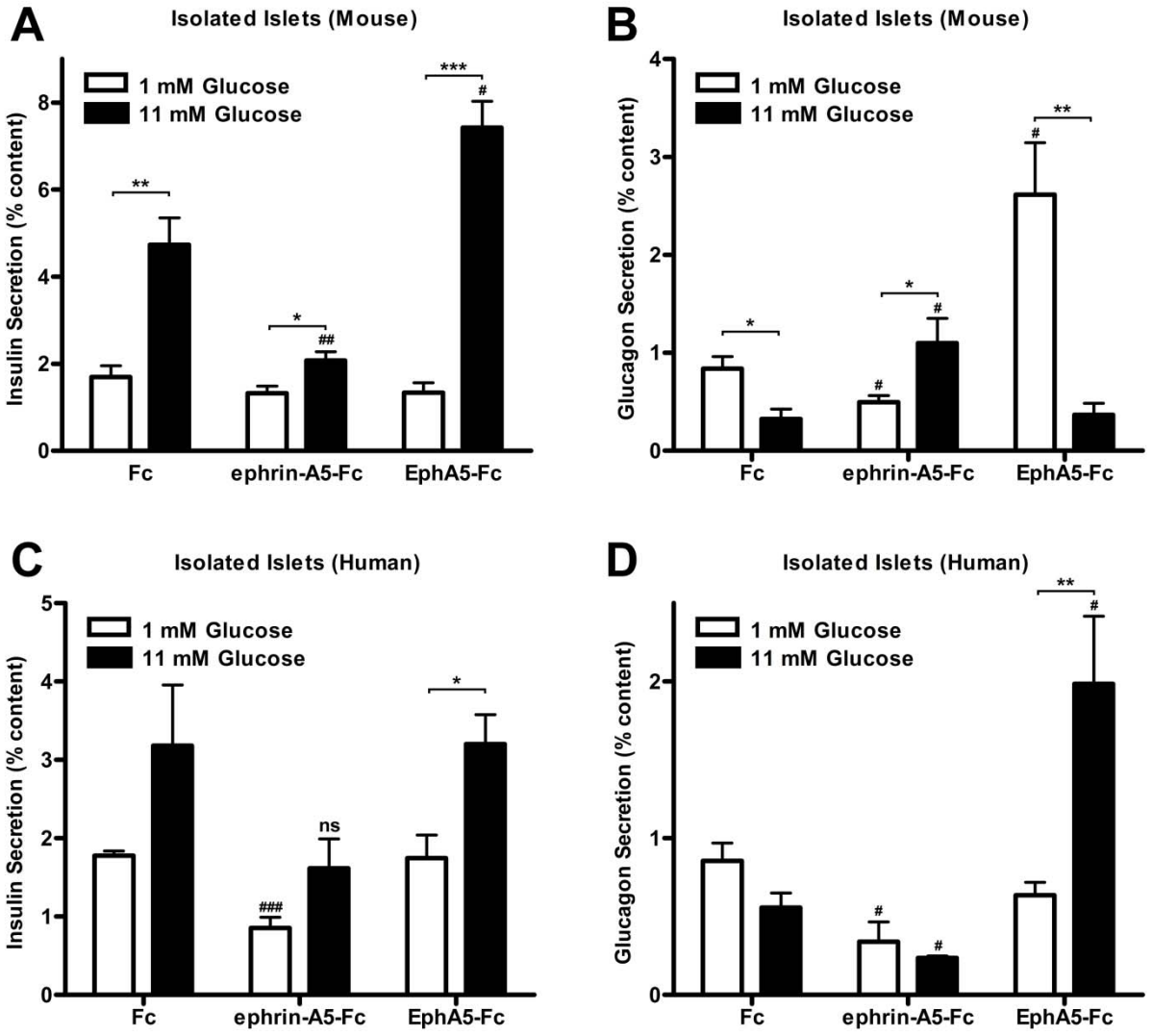


**Figure 2-7 Modulation of EphA signaling affects hormone secretion from mouse and human islets.** (A-D) Open white bars represent data from low glucose (1 mM) and closed black bars represent data from high glucose (11 mM). Data are shown as means (+SEM). Asterisks (*) above brackets represent significant differences between the same condition/control at low and high glucose as determined by Student's t-tests [* $P < 0.05$; ** $P < 0.01$; *** $P < 0.001$]. Hash marks (#) directly above columns represent statistical differences between condition and control at the same glucose concentration as determined by Student's t-tests [# $P < 0.05$; ## $P < 0.01$; ### $P < 0.001$]. (A) Average insulin secretion from isolated mouse islets (n = 8 mice) treated with Fc control, ephrin-A5-Fc, or EphA5-Fc. (B) Average glucagon secretion from isolated mouse islets (n = 9 mice) treated with Fc control, ephrin-A5-Fc, or EphA5-Fc. (C) Average insulin secretion from isolated human islets (n = 4 human donors) treated with Fc control, ephrin-A5-Fc, or EphA5-Fc. (D) Average glucagon secretion from isolated human islets (n = 4 human donors) treated with Fc control, ephrin-A5-Fc, or EphA5-Fc.

### 2.3.3 Stimulation and Inhibition of EphA/ephrin-A Signaling Modulates Insulin and Glucagon Secretion in Human Islets

To assess the role of EphA/ephrin-A-mediated regulation of hormone secretion in humans, donor islets were treated with ephrin-A5-Fc, EphA5-Fc, or Fc control. In human islets, ephrin-A5-Fc treatment at low glucose results in the inhibition of insulin secretion as compared to Fc control (Figure 2-7C). Treatment with ephrin-A5-Fc also results in an inhibition of glucagon secretion at both low and high glucose as compared to Fc control (Figure 2-7D). In human islets, treatment with EphA5-Fc has no effect on insulin secretion as compared to Fc control (Figure 2-7C), but results in an increase in glucagon secretion at high glucose (Figure 2-7D).

### 2.3.4 EphA/ephrin-A Induced Changes in Glucagon Secretion are Not Mediated through Changes in Paracrine Secretion

Insulin and somatostatin are potent paracrine inhibitors or glucagon secretion [115,116,124,125]. Given that insulin secretion is affected by EphA/ephrin-A modulation, it was necessary to assess whether EphA/ephrin-A induced changes in glucagon secretion were mediated through changes in paracrine secretion. Islets were treated with ephrin-A5-Fc, EphA5-Fc, or Fc control in the presence of the insulin receptor antagonist S961 (Figure 2-8A and B) or the somatostatin receptor type 2 (SSTR2) antagonist CYN (Figure 2-8C and D). Treatment with S961 resulted in a moderate increase in insulin secretion at low glucose, but otherwise did not affect EphA/ephrin-A modulation of insulin secretion (Figure 2-8A compared to Figure 2-7A). Inhibition of the insulin receptor disrupted glucose-inhibition of glucagon secretion in Fc control treated islets. At low glucose, concurrent treatment with S961 did not affect EphA/ephrin-A modulation of glucagon secretion (Figure 2-8B compared to Figure 2-7B). At high glucose,

glucagon secretion was unaffected by eprhin-A5-Fc or EphA5-Fc in the presence of S961 as compared to Fc control (Figure 2-8B). Treatment with CYN did not affect control or EphA/ephrin-A modulation of insulin secretion (Figure 2-8C compared to Figure 2-7A). CYN treatment resulted in a moderate increase in glucagon secretion in Fc control treated islets but did not affect EphA/ephrin-A modulation of insulin secretion at low or high glucose (Figure 2-8D compared to Figure 2-7B).

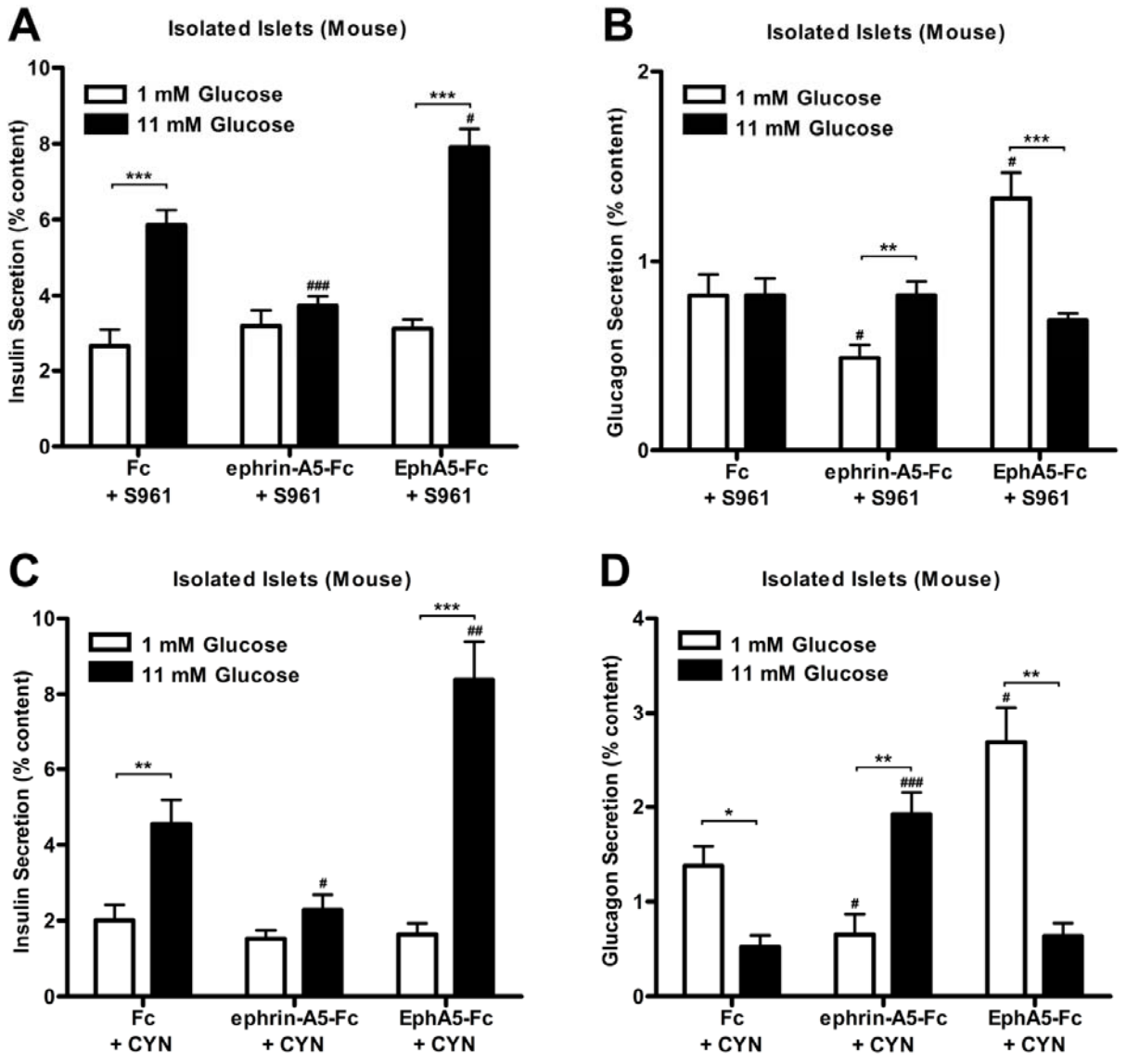


**Figure 2-8 Antagonism of insulin and somatostatin receptors does not affect EphA/ephrin-A regulation of glucagon secretion.** (A-D) Open white bars represent data from low glucose (1 mM) and closed black bars represent data from high glucose (11 mM). Data are shown as means (+SEM). Asterisks (*) above brackets represent significant differences between the same condition/control at low and high glucose as determined by Student's t-tests [* $P < 0.05$; ** $P < 0.01$; *** $P < 0.001$]. Hash marks (#) directly above columns represent statistical differences between condition and control at the same glucose concentration as determined by Student's t-tests [# $P < 0.05$; ### $P < 0.001$]. (A) Average insulin secretion from isolated mouse islets (n = 8 mice) treated with insulin receptor antagonist S961 and Fc control, ephrin-A5-Fc, or EphA5-Fc. (B) Average glucagon secretion from isolated mouse islets (n = 8-12 mice) treated with insulin receptor antagonist S961 and Fc control, ephrin-A5-Fc, or EphA5-Fc. (C) Average insulin secretion from isolated mouse islets (n = 8 mice) treated with SSTR2 receptor antagonist CYN and Fc control, ephrin-A5-Fc, or EphA5-Fc. (D) Average glucagon secretion from isolated mouse islets (n = 8 mice) treated with SSTR2 antagonist CYN and Fc control, ephrin-A5-Fc, or EphA5-Fc.

### 2.3.5 EphA4 Forward Signaling is Required for Appropriate Glucagon Secretion in Mouse Islets

To better assess the direct role of EphA/ephrin-A signaling in α-cells, alternative experimental approaches were used to selectively manipulate EphA/ephrin-A signaling in α-cells independent of EphA/ephrin-A signaling in β-cells. Islets have been shown to express numerous EphA receptors and ephrin-A ligands [85]. In both humans and mice, EphA4 is much more highly expressed in α-cells than in β-cells [203–205]. By targeting EphA4, EphA/ephrin-A signaling in α-cells can be assessed with minimal interference from concurrent changes in insulin secretion. DPHBA has been shown to selectively inhibit EphA2/4 forward signaling through the competitive inhibition of the ligand binding pocket [206]. Corresponding to relative levels of EphA4 expression in α and β-cells, DPHBA treatment does not significantly change insulin secretion as compared to vehicle control in islets (Figure 2-9A). However, DPHBA treatment enhances glucagon secretion at both high and low glucose as compared to vehicle control (Figure 2-9B). Data from mice containing an α-cell-specific knockout of the EphA4 receptor ($\alpha EphA4^{-/-}$) confirm the effect of EphA4 forward signaling on the inhibition of glucagon secretion independent of possible off-target effects. Insulin secretion is equivalent from $\alpha EphA4^{-/-}$ islets and wild-type littermate controls (Figure 2-9C), whereas glucagon secretion from $\alpha Epha4^{-/-}$ islets is enhanced as compared to wild-type islets at both low and high glucose (Figure 2-9D). No changes in total hormone content were observed between wild-type (40.3 ± 1.5 ng insulin and 3.7 ± 0.4 pg glucagon per islet) and $\alpha Epha4^{-/-}$ islets (41.8 ± 3.1 pg insulin and 3.8 ± 0.8 pg glucagon per islet).

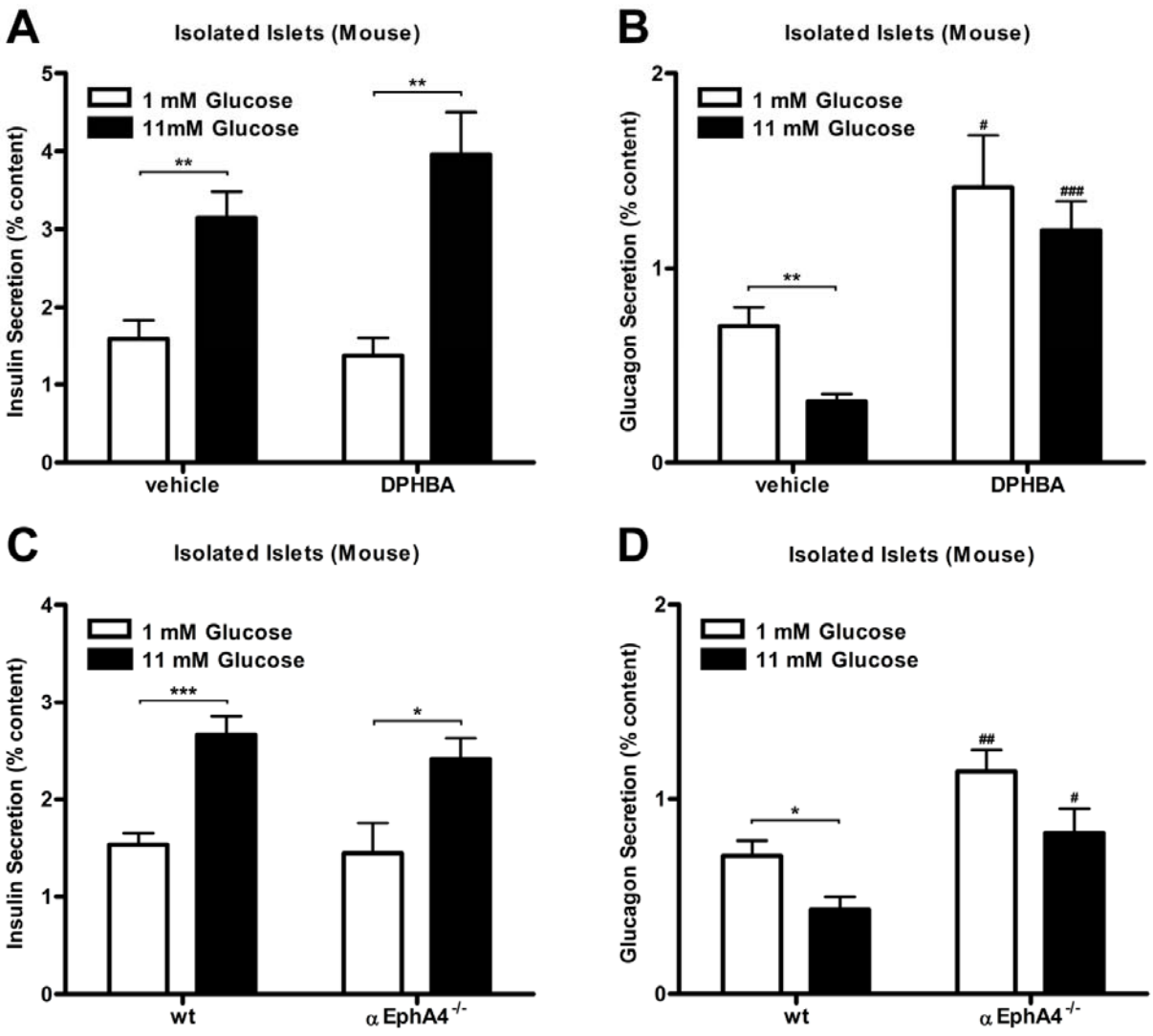


**Figure 2-9 EphA4 forward signaling is required for inhibition of glucagon secretion in mouse islets.** (A-D) Open white bars represent data from low glucose (1 mM) and closed black bars represent data from high glucose (11 mM). Data are shown as means (+SEM). Asterisks (*) above brackets represent significant differences between the same condition/control at low and high glucose as determined by Student's t-tests [* $P < 0.05$; ** $P < 0.01$; *** $P < 0.001$]. Hash marks (#) directly above columns represent statistical differences between condition and control at the same glucose concentration as determined by Student's t-tests [# $P < 0.05$; ## $P < 0.01$; ### $P < 0.001$]. (A) Average insulin secretion from isolated mouse islets (n = 8 mice) treated with vehicle control (DMSO) or EphA2/4 inhibitor DPHBA. (B) Average glucagon secretion from isolated mouse islets (n = 8 mice) treated with vehicle control (DMSO) or EphA2/4 inhibitor DPHBA. (C) Average insulin secretion from isolated mouse islets from $\alpha EphA4^{-/-}$ mice and wild-type (wt) littermate controls. (D) Average glucagon secretion from isolated mouse islets from $\alpha EphA4^{-/-}$ mice and wild-type (wt) littermate controls.

### 2.3.6 Restoration of EphA Forward Signaling Corrects Glucagon Hypersecretion and Reestablishes Glucose-inhibition of Glucagon Secretion in Sorted Mouse α-cells

Ephrin-A5-Fc and EphA5-Fc treatments affect both EphA forward and ephrin-A reverse signaling in opposite manners. Using islet studies alone, it is not possible to separate changes due to altered EphA forward signaling, ephrin-A reverse signaling, or a combination of both. For example, at low glucose, treatment with EphA5-Fc results in an enhancement of glucagon secretion (Figure 2-7B), which could be mediated directly by stimulation of ephrin-A reverse signaling in α-cells, or indirectly through binding endogenous ephrin-A receptors on neighboring islet cells thus inhibiting EphA forward signaling in α-cells. Sorted α-cells were used to isolate the direct stimulation effects (both forward and reverse) of ephrin-A5-Fc and EphA5-Fc from their indirect effects on the inhibition of endogenous EphA/ephrin-A interactions. In sorted α-cells, EphA5-Fc is only capable of stimulating reverse signaling since endogenous EphA/ephrin-A interactions have been removed through dispersion and sorting. Although α-cells express the required ephrin-A ligands [203,205], α-to-α-cell EphA/ephrin-A interactions are not expected in sorted α-cells as pure populations do not cluster, but remain as dispersed single cells in culture (Figure 2-10).

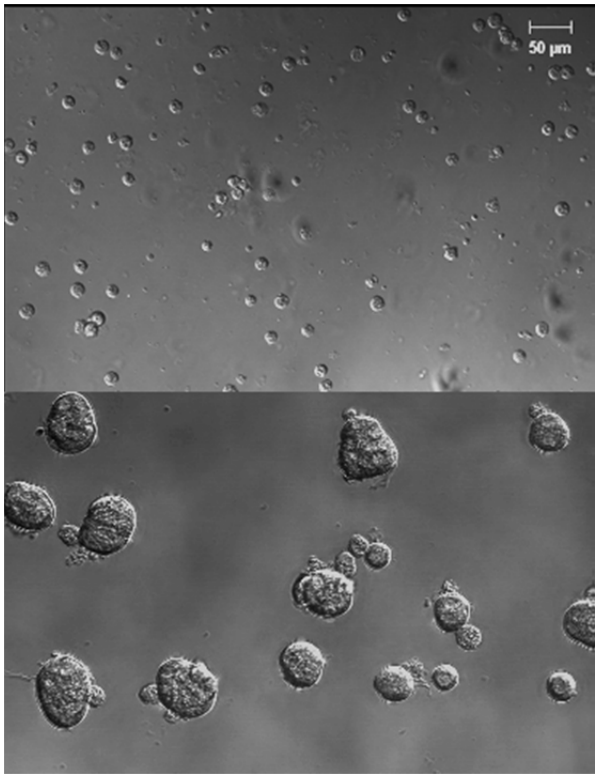


**Figure 2-10 Sorted α-cells do not cluster in culture.** (Top panel – sorted α-cells) Plated flow sorted α-cells remain as a dispersion of single cells that persists for up to 72 hours, with no evidence of glucose-inhibition of glucagon secretion. (Bottom panel – mixed islet-cell population) Plated dispersed islet cells or flow sorted α-, β-, and δ-cell populations yield islet-like cell clusters immediately upon plating. These islet-like cell clusters exhibit glucose-inhibition of glucagon secretion within 24 hours, and by 72 hours after plating, these clusters recapitulate all normal isolated islet behaviors.

In addition to disrupting existing juxtacrine signaling, sorting α-cells removes paracrine signals that are present in the islet environment. The combined lack of juxtacrine and paracrine signaling is thought to underlie the increased glucagon secretion observed from sorted α-cells as compared to islets and the observed glucose-stimulation rather than glucose-inhibition of glucagon secretion (Figure 1-13) [109]. Thus, sorted α-cells enable the direct study of EphA/ephrin-A signaling, independent of paracrine and other juxtacrine signaling. Glucagon secretion from sorted α-cells treated with ephrin-A5-Fc is reduced at both low and high glucose as compared to the Fc control (Figure 2-11A). Further, ephrin-A5-Fc stimulation leads to islet-like glucose-inhibition of glucagon secretion (Figure 2-11A). Treatment with EphA5-Fc or

DPHBA does not change glucagon secretion from sorted α-cells at either low or high glucose as compared to the Fc control (Figure 2-11A).

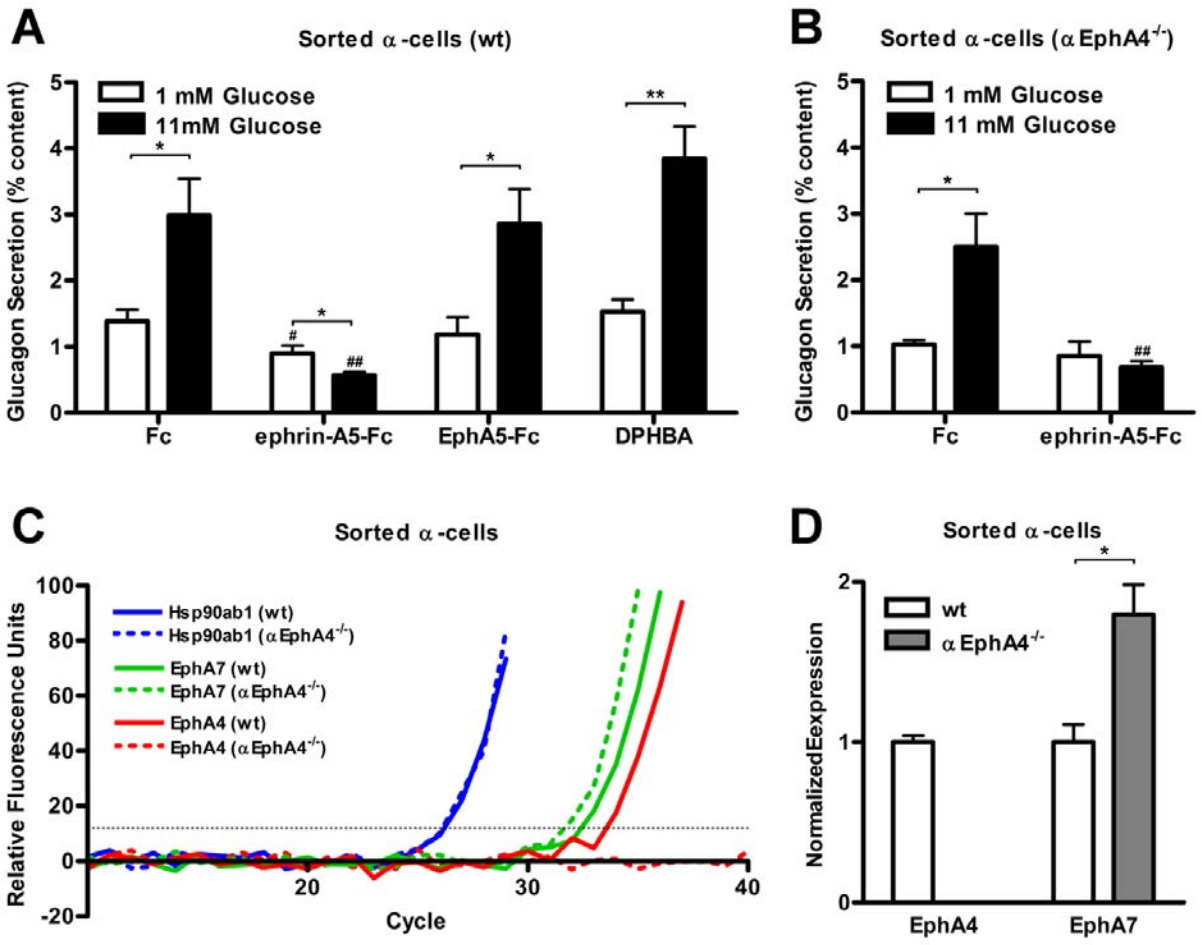


**Figure 2-11 Restoration of EphA forward signaling in sorted α-cells inhibits glucagon secretion and restores glucose-inhibition of glucagon secretion.** (A-B) Open white bars represent data from low glucose (1 mM) and closed black bars represent data from high glucose (11 mM). Data are shown as means (+SEM). Asterisks (*) above brackets represent significant differences between the same condition/control at low and high glucose as determined by Student's t-tests [* $P < 0.05$; ** $P < 0.01$]. Hash marks (#) directly above columns represent statistical differences between condition and control at the same glucose concentration as determined by Student's t-tests [# $P < 0.05$; ## $P < 0.01$]. (A) Average glucagon secretion from sorted wild-type (wt) α-cells (n = 8 mice) treated with Fc control, ephrin-A5-Fc, EphA5-Fc, or EphA2/4 inhibitor DPHBA. (B) Average glucagon secretion from sorted EphA4$^{-/-}$ α-cells (n = 8 mice) treated with Fc control or ephrin-A5-Fc (C) Representative plot of SYBR Green fluorescence as a function of cycle number from a single qRT-PCR experiment with wild-type (wt) and EphA4$^{-/-}$ α-cell RNA. Only data from EphA4, EphA7, and a single housekeeping control gene (Hsp90ab1) are shown. (D) Normalized expression of EphA4 and EphA7 transcripts in wild-type (wt) and αEphA4$^{-/-}$ α-cells. Data are shown as means (+SEM) and represents the average of 3 independent experiments. P-value was determined by Student's t-test [*$P < 0.05$].

### 2.3.7 EphA7 Contributes to EphA Forward Signaling-mediated Inhibition of Glucagon Secretion and is Upregulated in αEphA4$^{-/-}$ Mice

We aimed to determine whether EphA4 acts alone or in combination with other EphA receptors in regulating glucagon secretion. αEphA4$^{-/-}$ mice were engineered to contain an RFP reporter driven by the same truncated glucagon promoter, enabling us to generate a pure population of EphA4$^{-/-}$ α-cells by FACS. Similar to wild-type, sorted EphA4$^{-/-}$ α-cells display glucose-stimulation of glucagon secretion (Figure 2-11B). Stimulation of EphA forward signaling with ephrin-A5-Fc fails to inhibit glucagon secretion in sorted EphA4$^{-/-}$ α-cells at low glucose, consistent with a major role for EphA4 in the observed EphA forward signaling-mediated inhibition of glucagon secretion in sorted wild-type α-cells (Figure 2-11A and B). However, ephrin-A5-Fc treatment of EphA4$^{-/-}$ α-cells still inhibits glucagon secretion at high glucose, indicating that other EphA receptors likely play a role in inhibiting glucagon secretion. Unlike wild-type α-cells, ephrin-A5-Fc treatment of EphA4$^{-/-}$ α-cells does not inhibit glucagon secretion at low glucose, nor does it restore glucose-inhibition of glucagon secretion (Figure 2-11A and B). To better understand which members of the EphA receptor class are involved in the inhibition of glucagon secretion in α-cells, mRNA expression of all EphA receptors (A1-8,10) was quantified by qRT-PCR in sorted wild-type and EphA4$^{-/-}$ α-cells. Wild-type α-cells express EphA4 and EphA7, whereas EphA4$^{-/-}$ α-cells only express EphA7 (Figure 2-11C). Normalizing transcript expression to housekeeping genes, EphA7 was found to be upregulated in EphA4$^{-/-}$ α-cells as compared to wild-type α-cells (Figure 2-11D).

### 2.3.8 αEphA4$^{-/-}$ Mice Are Insulin Resistant and Require Increased Insulin Secretion to Maintain Euglycemia

Isolated islets largely recapitulate the physiological glucose-dependent changes in hormone secretion observed *in vivo* [39,40]. Still, glucose homeostasis is a complex process that is maintained by numerous interdependent organ systems [7–10]. To assess the gene deletion's effect on glucose homeostasis, αEphA4$^{-/-}$ mice were characterized by IPGTT and IPITT. Additionally, plasma insulin and glucagon were assessed at fasting and following glucose stimulation. No appreciable differences in glucose clearance following a glucose challenge are observed between αEphA4$^{-/-}$ mice and wild-type littermate controls (Figure 2-12A). However, αEphA4$^{-/-}$ mice display insulin resistance as compared to wild-type littermate controls (Figure 2-12B). Consistent with insulin resistance, fasted and glucose-stimulated plasma insulin levels are elevated in αEphA4$^{-/-}$ mice as compared to wild-type littermate controls, despite equivalent glucose control (Figure 2-12B). Additionally, plasma glucagon in αEphA4$^{-/-}$ mice is decreased at fasting, as compared to wild-type littermate controls (Figure 2-12D). The level of plasma glucagon observed in fasted αEphA4$^{-/-}$ mice represents the lower limit of detection.

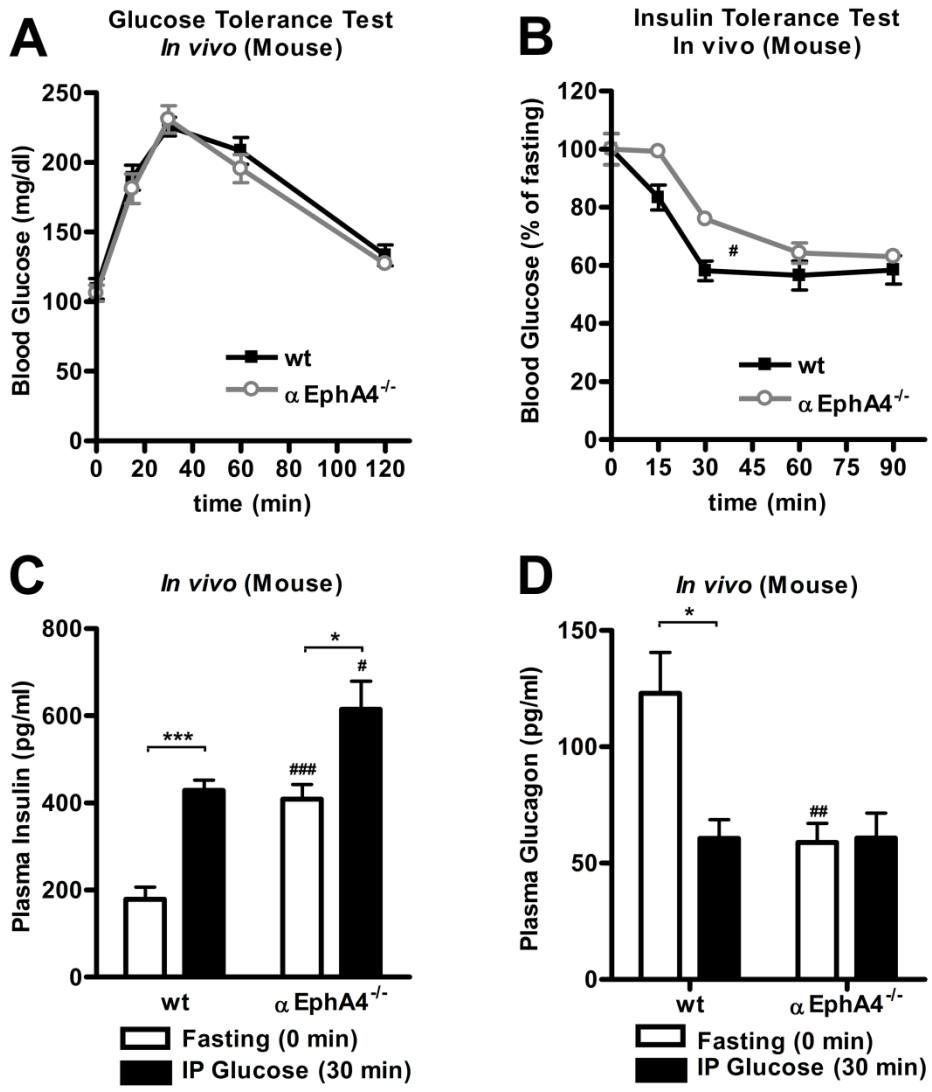


**Figure 2-12 αEphA4$^{-/-}$ mice are euglycemic and insulin resistance.** (A) IPGTTs of wild-type (wt) (n = 8 mice) and αEphA4$^{-/-}$ mice (n = 8 mice). Mice were fasted for 16 hours prior to intraperitoneal injection of sterile glucose (1 g/kg) at 0 minutes. (B) IPITTs of wild-type (wt) (n = 6 mice) and αEphA4$^{-/-}$ mice (n = 6 mice). Mice were fasted for 5 hours prior to intraperitoneal injection of insulin (0.5 U/kg) at 0 minutes. Blood glucose is presented as a percentage of fasting glucose (0 minutes). The asterisk (*) represents a significant differences between wt and αEphA4$^{-/-}$ mice as determined by a Student's t-test [P < 0.05] of area under curve analyses. (C-D) Open white bars represent data from fasting (0 minutes) and closed black bars represent data from glucose stimulation (30 minutes). Data are shown as means (+SEM). Asterisks (*) above brackets represent significant differences between the same genotype at 0 minutes (fasting) and 30 minutes (glucose stimulation) as determined by Student's t-tests [* P < 0.05; *** P < 0.001]. Hash marks (#) directly above columns represent statistical differences between αEphA4$^{-/-}$ mice and wild-type (wt) littermate controls at the same time point (before or after glucose stimulation) as determined by Student's t-tests [# P < 0.05; ## P < 0.01; ### P < 0.001]. (C) Plasma insulin in wild-type (wt) (n = 8 mice) and αEphA4$^{-/-}$ mice (n = 8 mice) before (0 minutes; Fasting) and after (30 minutes; IP Glucose) intraperitoneal glucose injection. (D) Plasma glucagon in wild-type (wt) (n = 8 mice) and αEphA4$^{-/-}$ mice (n = 8 mice) before (0 minutes; Fasting) and after (30 minutes; IP Glucose) intraperitoneal glucose injection.

### 2.3.9 pan-EphA and EphA4 Induced Changes in Glucagon Secretion are Associated with Altered F-Actin Density

In β-cells, disruption of the F-actin network results in increased insulin secretion and stabilization of the F-actin network results in decreased insulin secretion [80,207,208]. Stimulation of EphA forward signaling in β-cells increases F-actin density and decreases insulin secretion, while its inhibition decreases F-actin density and increases insulin secretion [85]. We hypothesize that similar changes in the α-cell F-actin network mediate EphA regulation of glucagon secretion. Islets were treated with ephrin-A5-Fc, EphA5, or Fc control in the presence of low glucose, and then fixed, stained, and visualized. Ephrin-A5-Fc treatment induces a moderate increase in F-actin density within islets and α-cells, as compared to Fc control (compare Figure 2-13C and D to Figure 2-13A and B). This moderate increase in α-cell F-actin density is consistent with the degree of glucagon inhibition observed with ephrin-A5-Fc treatment at 1 mM glucose. EphA5-Fc treatment induces a decrease in F-actin density within islets and α-cells, as compared to Fc control (compare Figure 2-13E and F to Figure 2-13A and B). Again, this decrease in α-cell F-actin density correlates with the degree of enhanced glucagon secretion observed with EphA5-Fc treatment at 1 mM glucose. Quantification of F-actin density in α-cells following ephrinA5-Fc, EphA5-Fc, or Fc treatment is shown in Figure 2-13G. Differences in F-actin density were also assessed in EphA4$^{-/-}$ and wild-type α-cells. Within αEphA4$^{-/-}$ islets, RFP-positive EphA4$^{-/-}$ α-cells have less dense F-actin than RFP-negative wild-type α-cells (compare Figure 2-13K to Figure 2-13H). This reduced F-actin density is consistent with the enhanced glucagon secretion observed in αEphA4$^{-/-}$ islets (Figure 2-9D). The density of the F-actin network in EphA4$^{-/-}$ and wild-type α-cells is quantified in Figure 2-13N.

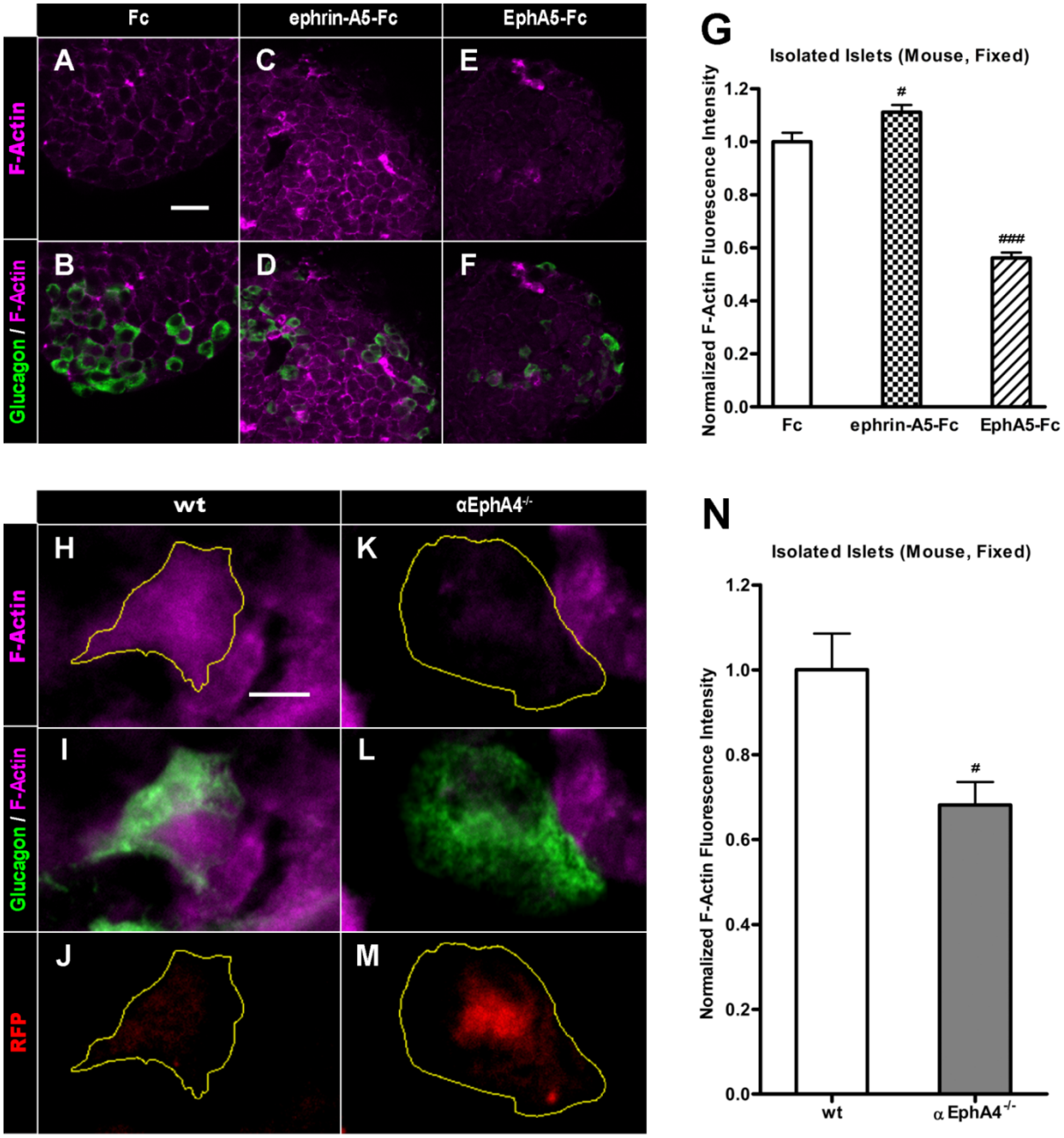


**Figure 2-13 EphA(4) forward signaling activity is associated with F-actin density.** (A-F) Scale bar represents 20 µM. F-actin (magenta) and glucagon (green) staining of isolated mouse islets at 1 mM glucose treated with (A-B) Fc control, (C-D) ephrin-A5-Fc, or (E-F) EphA5-Fc. (G) Quantification of mean F-actin intensity in raw images represented by A-F in regions of interest determined by glucagon fluorescence intensity threshold. Data are normalized to Fc control and represents islets from 6 mice and 100-200 α-cells. Hash marks (#) represent statistical differences between treatment and control as determined by Student's t-test [# $P < 0.05$; ### $P < 0.001$]. (H-M) Scale bar represents 5 µM. F-actin (magenta) and glucagon (green) staining of isolated islets from αEphA4$^{-/-}$ mice. α-cells from αEphA4$^{-/-}$ islets are comprised of (H-J) RFP (red) negative wild-type α-cells (~14%) and (K-M) RFP positive EphA4$^{-/-}$ α-cells (~76%). (N) Quantification of mean F-actin intensity in raw images represented by H-M in regions of interest determined by glucagon fluorescence intensity threshold. Wild-type (wt) and EphA4$^{-/-}$ α-cells were identified by RFP intensity within the same region of interest and stratified into two distinct populations; RFP negative (wt) α-cells and RFP positive EphA4$^{-/-}$ α-cells. Data are normalized to wild-type (wt) α-cells and represents islets from 4 mice and 20-50 α-cells. Hash mark (#) represents a statistical differences between wild-type (wt) and EphA4$^{-/-}$ α-cells as determined by Student's t-test [# $P < 0.05$].

2.3.10 Glucose Induces Moderate Dephosphorylation and Deactivation of EphA4 in α-cells

EphA/ephrin-A-mediated insulin secretion has previously been reported to be glucose sensitive. In the current β-cell model, glucose levels determine the balance between EphA forward signaling-mediated inhibition of glucagon secretion at low glucose and ephin-A reverse signaling mediated facilitation of insulin secretion at high glucose. This model is based on the glucose dependent dephosphorylation of EphA receptors by a glucose sensitive protein tyrosine phosphatase [85]. The phosphorylation state of EphA4 was determined in α-cells at both low and high glucose to assess whether dephosphorylation plays a role in the potential glucose regulation of EphA4-mediated inhibition of glucagon secretion. Elevated glucose results in a moderate decrease in EphA4 receptor phosphorylation (Figure 2-14).

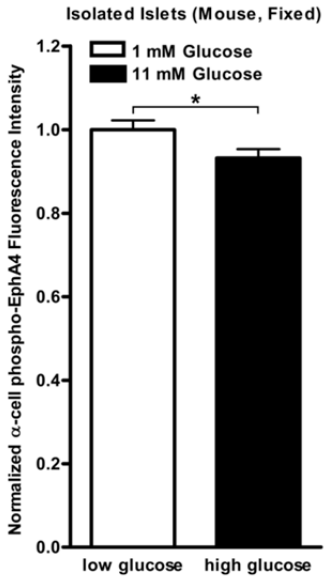


**Figure 2-14 EpA4 is dephosphorylated and deactivated upon glucose stimulation in α-cells.** Quantification of phospho-specific EphA4 in α-cells from fixed islets. Data represents the quantification of mean fluorescence intensity in regions of interest determined by glucagon fluorescence intensity threshold in raw images. Data are normalized to 1 mM glucose and represents islets from 4 mice and 350-400 α-cells. Asterisk (*) represents a statistical differences between low and high glucose as determined by Student's *t*-test [* $P < 0.05$].

### 2.3.11 Modulation of EphA/ephrin-A Signaling does not Affect α-cell $Ca^{2+}$ activity or metabolism

$Ca^{2+}$ activity and metabolism are key regulators of hormone secretion from islet cells. The percentage of α-cells displaying $Ca^{2+}$ activity and α-cell NAD(P)H autofluorescence, a marker for α-cell metabolism, were measured to determine whether EphA/ephrin-A mediated regulation of glucagon secretion was facilitated through changes in α-cell $Ca^{2+}$ activity or metabolism. The role of α-cell $Ca^{2+}$ activity in response to elevations in glucose is disputed. A number of conflicting results on various measures of $Ca^{2+}$ activity have been reported including a an initial decease in intracellular [$Ca^{2+}$] (~4 minutes) followed by an increase in intracellular [$Ca^{2+}$] [209], a decrease in $Ca^{2+}$ oscillations [136,210,211], an increase in intracellular [$Ca^{2+}$] and oscillation frequency with minimal change in the percentage of active cells [109], and a minimal change in intracellular [$Ca^{2+}$] levels, with no change the percentage of active cells [126]. Here, we present new findings where elevations in glucose recruit a larger percentage of α-cells that display $Ca^{2+}$ activity over a 10 minute time period (Figure 2-15A). The imaging and analysis protocol was defined to capture as many potential changes as possible, as most other studies have been done over shorter periods of time and have given inconsistent results. This measure of α-cell $Ca^{2+}$ activity does not account for oscillation number/frequency/amplitude or net changes in intracellular calcium. These α-cell $Ca^{2+}$ findings are not central to EphA/ephrin-A regulation of glucagon secretion, but represent a unique addition that is consistent with the complexity of the α-cell $Ca^{2+}$ response. Treatment of isolated islets with ephin-A5-Fc or DPHBA does not affect α-cell $Ca^{2+}$ activity or NAD(P)H as compared to Fc and vehicle controls (Figure 2-15).

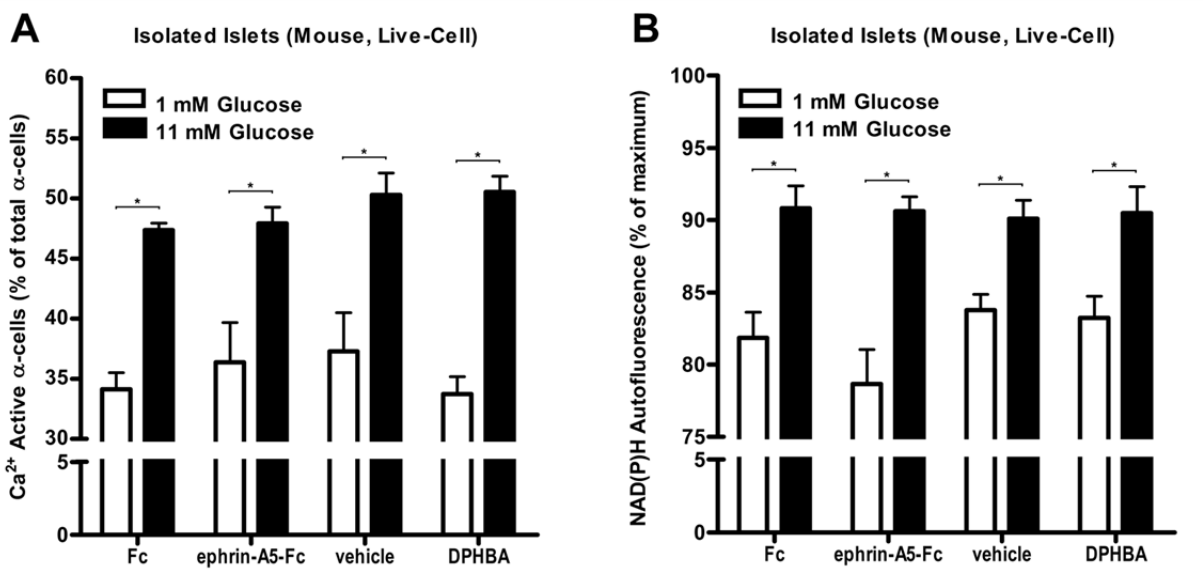


**Figure 2-15 α-cell $Ca^{2+}$ activity and metabolism are not affected by stimulation of EphA forward signaling or inhibition of EphA4 forward signaling.** Asterisks above brackets represent significant differences between the same condition/control at low and high glucose as determined by Student's *t*-test [*P < 0.05]. (A) α-cell $Ca^{2+}$ activity expressed as the percentage of α-cells displaying $Ca^{2+}$ activity during the experimental period in islets treated with Fc control, eprhin-A5-Fc, vehicle (DMSO), or DPHBA. (B) α-cell NAD(P)H autofluorescence in islets treated with Fc control, eprhin-A5-Fc, vehicle (DMSO), or DPHBA.

## 2.4 Discussion

We examined the role of EphA/ephrin-A signaling in the regulation of glucagon secretion. Stimulation or inhibition of EphA forward signaling results in a reduction or enhancement, respectively, of insulin secretion at high glucose (Figure 2-7A and [85]) and glucagon secretion at low glucose from mouse islets (Figure 2-7B). Additionally, our findings indicate that EphA forward signaling in human islets shows some similarities to mouse islets in that stimulation of EphA forward signaling inhibits hormone secretion and inhibition of EphA forward signaling enhances hormone secretion (Figure 2-7A-D). A number of discrepancies exist between the mouse and human data, but a complete comparison of mouse and human EphA/ephrin-A signaling is currently restricted by the limited availability of human islets.

### 2.4.1 EphA Forward and ephrin-A Reverse Signaling in α-cells

In β-cells, glucose alters the balance between EphA forward and ephrin-A reverse signaling through activation of a glucose-dependent protein tyrosine phosphatase which leads to dephosphorylation and inactivation of EphA receptors [85]. This glucose-inactivation of EphA receptors biases bidirectional EphA/ephrin-A signaling that normally favors EphA forward signaling and the inhibition of insulin secretion to favor ephrin-A reverse signaling and the facilitation of insulin secretion. This same glucose dependent balance in EphA forward and ephrin-A reverse signaling is not observed in α-cells. Rather in α-cells, EphA/ephrin-A mediated changes in glucagon secretion are facilitated primarily through EphA forward signaling with a minor if any role for ephrin-A reverse signaling. These conclusions are based on data that show that EphA5-Fc treatment, which is only capable of stimulating reverse signaling in sorted α-cells, has no effect on glucagon secretion (Figure 2-11A). Thus, we attribute the observed islet effect to an inhibition of endogenous EphA forward signaling rather than direct stimulation of reverse signaling or a combination of the two.

### 2.4.2 Glucose-dependent Changes in EphA/ephrin-A-mediated Regulation of Glucagon Secretion

Our data suggest that EphA forward signaling similarly regulates hormone secretion from α-cells at low glucose and β-cells at high glucose, in that a stimulation of EphA forward signaling inhibits hormone secretion and an inhibition of EphA forward signaling facilitates hormone secretion. However, EphA/ephrin-A-mediated changes in glucagon secretion at high glucose differ based on the experimental approach. In islets at high glucose, stimulation of EphA forward signaling with ephrin-A5-Fc results in an increase in glucagon secretion while inhibition

of EphA forward signaling with EphA5-Fc has no effect (Figure 2-7B). In other ex vivo experiments (sorted α-cells, DPHBA treated islets, and αEphA4$^{-/-}$ islets), EphA forward signaling regulation of glucagon secretion is consistent across low and high glucose, suggesting that stimulation or inhibition of EphA forward signaling results in an inhibition or facilitation of glucagon secretion, respectively (Figure 2-9 and Figure 2-11). Perturbations in paracrine factors present in islets treated with ephrin-A5-Fc and EphA5-Fc but not in sorted α-cells, DPHBA treated islets, or αEphA4$^{-/-}$ islets represent a possible mechanism underlying the differences in EphA/ephrin-A-mediated changes in glucagon secretion observed at high glucose between these sets of experiments. However, receptor antagonism of two prominent paracrine inhibitors of glucagon secretion revealed that changes insulin and somatostatin signaling are not responsible for the differing changes in glucagon secretion observed at high glucose with ephrin-A5-Fc and EphA5-Fc treatment (Figure 2-8). Currently, the cause of the discrepancies in EphA/ephrin-A mediated glucagon secretion at high glucose between the two sets of experimental approaches remains unknown, but suggests important differences in these approaches for studying EphA/ephrin-A signaling.

### 2.4.3 Role of EphA Forward Signaling-mediated Inhibition of Glucagon Secretion in Normal Physiology and Diabetes

We have shown that tonic Eph4A forward signaling is required for appropriate inhibition of glucagon secretion from α-cells at low and high glucose. However, it remains unclear whether EphA forward signaling-mediated inhibition of glucagon secretion plays a role in physiologic glucose-inhibition of glucagon secretion. The loss of EphA4 forward signaling leads to increased glucagon secretion at both low and high glucose as compared to control, but also disrupts

glucose-inhibition of glucagon secretion (Figure 2-9B and D). In sorted α-cells, elevated glucose potentiates the inhibitory effects of EphA forward signaling on glucagon secretion, resulting in a further inhibition of glucagon secretion at high glucose, as compared to low glucose (Figure 2-11A). These data support a glucose-dependent increase in EphA forward signaling-mediated inhibition of glucagon secretion and a potential role for EphA/ephrin-A signaling in physiologic glucose-inhibition of glucagon secretion. However, we have yet to identify a molecular mechanism underlying glucose-dependent changes in EphA forward signaling. Neither glucose-dependent EphA4 receptor dephosphorylation in α-cells (Figure 2-14), nor glucose-dependent increases in α-cell metabolism and $Ca^{2+}$ activity (Figure 2-15) are consistent with a glucose-dependent increase in EphA forward signaling. This suggests that any potential glucose-dependent changes are further downstream in the EphA forward signaling pathway. Glucose dependence of EphA/ephrin-A-mediated regulation of glucagon secretion could explain the observed glucose-inhibition of glucagon secretion at glucose concentrations (less than 5 mM) that do not stimulate putative paracrine mediators of glucagon secretion [212]. However, inhibition of F-actin polymerization has previously been shown to enhance glucagon secretion at low glucose but not affect glucagon secretion at high glucose [80]. This is consistent with the effects that EphA5-Fc treatment has on glucagon secretion and F-actin reorganization, and suggests that actin-mediated regulation of glucagon secretion may only affect glucagon secretion at low glucose.

Our findings are consistent with an increase in glucagon secretion triggered by the loss of cell-cell contacts, as observed in sorted α-cells as compared to islets [109]. In support of this hypothesis, the aberrantly high and dysregulated glucagon secretion from sorted α-cells is

corrected by restoring EphA forward signaling independent of other islet cell interactions including paracrine factors (Figure 2-10A). Similar to sorted α-cells, islets from type 1 (and type 2, following β-cell death) diabetes patients have a deficiency of β-cells and thus a likely deficiency in available ephrin-A ligands capable of stimulating EphA forward signaling in α-cells. Thus, the loss of β-cells may result in a decrease in EphA forward signaling in α-cells, and may contribute to the lack of inhibition of glucagon secretion and hyperglucagonemia associated with diabetes (Figure 2-16).

### 2.4.4 EphA/ephrin-A-mediated Glucagon Secretion *in vivo* and *ex vivo*

Islets isolated from αEphA4$^{-/-}$ mice exhibit normal insulin secretion and elevated glucagon secretion at low and high glucose (Figure 2-9C and D). However, *in vivo*, these mice display an increase in fasting and glucose-stimulated plasma insulin and a decrease in fasting plasma glucagon. αEphA4$^{-/-}$ mice are insulin resistant, explaining the increase in plasma insulin required to maintain euglycemia. It remains unknown, though, how αEphA4$^{-/-}$ mice develop insulin resistance. Prolonged hyperglucagonemia is associated with an impairment in insulin-mediated glucose disposal [213]. Thus, one possible cause for this insulin resistance could be persistent elevation in glucagon secretion, such as that observed in isolated αEphA4$^{-/-}$ islets. In this case, however, it is unclear why the increased glucagon secretion observed *ex* vivo does not translate to observed hyperglucagonemia *in vivo,* although increased insulin in the islet milieu could act to inhibit glucagon secretion.

### 2.4.5 Summary

Our data suggest a new model of juxtacrine-mediated tonic inhibition of glucagon secretion, where ephrin-A ligands on neighboring islet cells stimulate EphA receptors on α-cells to inhibit glucagon secretion (Figure 2-16). Disruption of EphA4 receptors and EphA forward signaling results in enhanced glucagon secretion and a corresponding decrease in F-actin density, while stimulation of EphA forward signaling results in further inhibition of glucagon secretion and a corresponding increase in F-actin density. Sorted α-cells that lack cell-cell contacts display glucagon hypersecretion and lack glucose-inhibition of glucagon secretion. Consistent with our juxtacrine model, restoring EphA forward signaling to sorted α-cells inhibits glucagon secretion down to levels observed in islets and reestablishes glucose-inhibition of glucagon secretion. Through specific pharmacological manipulation and αEphA4$^{-/-}$ mice we have shown that EphA4 plays a prominent role in juxtacrine-mediated inhibition of glucagon secretion and is required for appropriate inhibition of glucagon secretion at both low and high glucose. This new juxtacrine-mediated model of glucagon secretion suggests that selective stimulation of α-cell EphA forward signaling through EphA4 represents a potential therapeutic target against glucagon hypersecretion associated with diabetes.

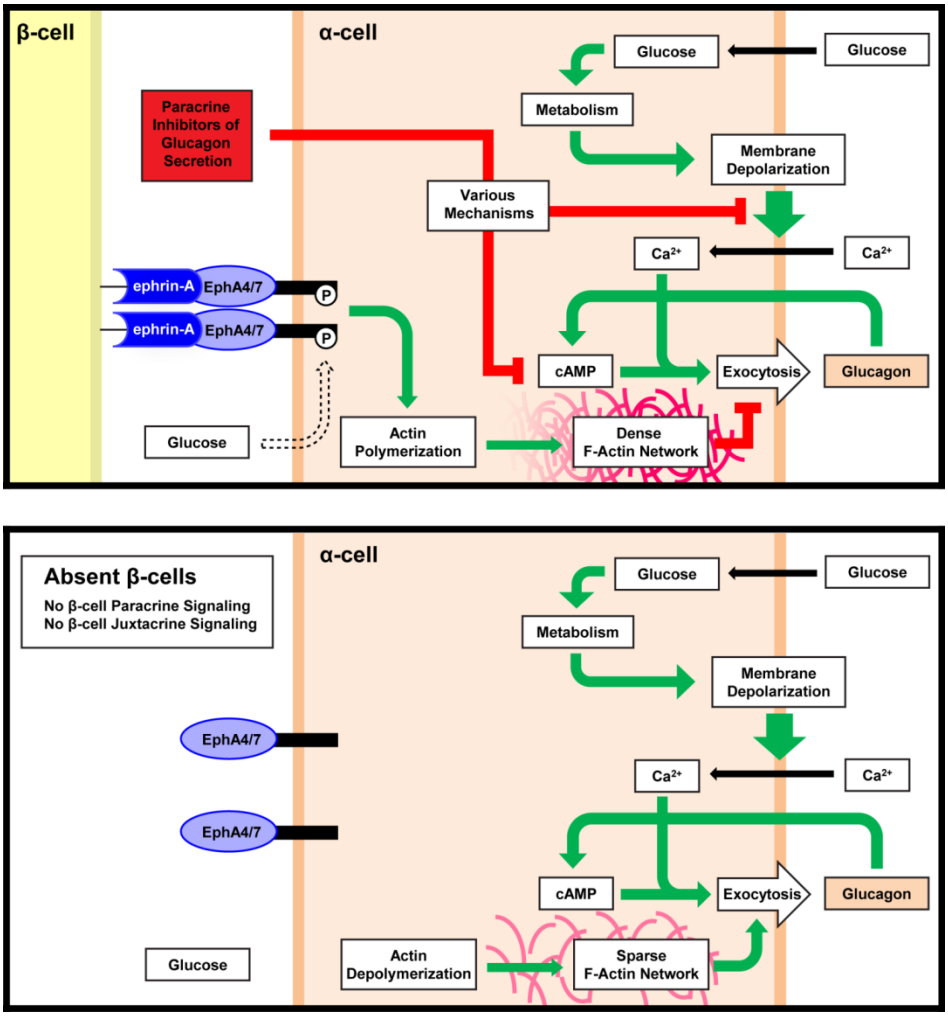


**Figure 2-16 Model of juxtacrine-mediated inhibition of glucagon secretion.** (Top panel – Islets) This is a model of EphA forward signaling in α-cells within intact islets. β-cells express a number of ephrin-A ligands capable of stimulating EphA4 and EphA7 receptors on α-cells. Constant EphA forward signaling stimulates actin polymerization and maintains a dense F-actin network. A dense F-actin network inhibits the exocytosis of glucagon downstream of glucose-stimulated metabolism and Ca2+ influx. Tonic juxtacrine-mediated inhibition of glucagon secretion functions in parallel with paracrine-mediated inhibition of glucagon secretion present at high glucose. Our data indicates that EphA forward signaling-mediated inhibition of glucagon secretion may be potentiated by glucose, however the mechanism by which this occurs is unknown. Glucose-dependent dephosphorylation of EphA receptors represents potential negative-feedback regulation of glucose-dependent increases in EphA forward signaling-mediated inhibition of glucagon secretion (dashed arrow outline). (Bottom panel – α-cells without β-cells) This is a model of EphA forward signaling in sorted α-cells and α-cells in type 1 diabetes and type 2 diabetes following β-cell loss. Without neighboring β-cells, ephrin-A ligands do not stimulate α-cell EphA receptors and do not induce EphA forward signaling within α-cells. This lack of EphA forward signaling permits actin depolymerization and results in a sparse F-actin network that facilitates the exocytosis of glucagon. Additionally, the loss of β-cells results in the loss of a number of reported β-cell derived paracrine inhibitors of glucagon secretion.

# CHAPTER 3
# SECRETED BROWN ADIPOSE TISSUE FACTOR INHIBITS GLUCAGON SECRETION

## 3.1 Introduction

White adipose tissue (WAT) and brown adipose tissue (BAT) serve different physiological functions. WAT is the site for long term storage of lipids in the form of triglycerides. While WAT is relatively metabolically inactive, it contributes to energy homeostasis through the uptake and release of lipid energy sources. WAT has also been shown to have an endocrine function, releasing metabolically active hormones such as leptin and adiponectin. BAT is very metabolically active and contributes to energy homeostasis through non-shivering thermogenesis [214]. Morphologically, white adipocytes contain a single large lipid droplet whereas brown adipocytes contain multilocular lipid droplets (Figure 3-1). WAT and BAT were named for their macroscopic appearance. While they both contain stores of lipids, the high density of mitochondria within BAT contributes to its darker appearance [215]. Unique to BAT, uncoupling protein 1 (UPC1) is expressed on inner mitochondria membrane. UPC1 mediates the ATP synthase-independent transport of protons across the proton electrochemical gradient present between the intermembrane space and mitochondrial matrix. Thus, the energy produced via the electron transport chain is uncoupled from ATP production, and instead dissipates as heat. The heat produced by BAT is quickly dispersed due to its high vascularization [216].

Metabolically active BAT has been identified within the adult population of a number of different species of small mammals [217]. In humans, on the other hand, BAT was originally

thought to be present within newborns but regress with age, resulting in little to no active BAT in adult humans [218]. However in 2007, unexpected results in a nuclear medicine study suggested the possible existence of BAT in adult humans. During fluorodeoxyglucose positron emission tomography for the surveillance of tumor metastases, confounding symmetrical tracer uptake that did not correspond with cancer was observed in the neck and shoulder areas of patients [219]. These areas were hypothesized to be metabolically active BAT. Within a few years, the presence of metabolically active BAT in adult humans was independently confirmed through histologic morphology and UPC1 messenger RNA transcription/protein expression [220,221]. The discovery of metabolically active BAT within adult humans spurred research into the field of BAT regulation and its potential therapeutic benefit in diseases such as obesity and metabolic syndrome.

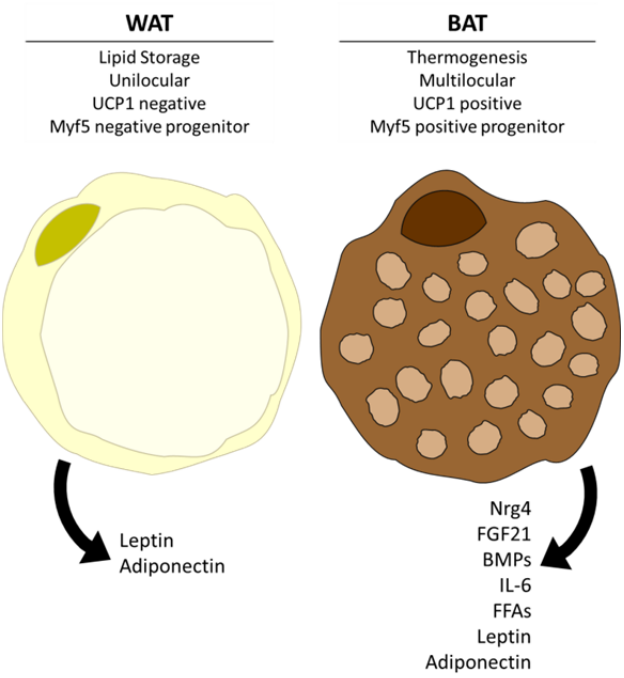


**Figure 3-1 Comparison of white adipose tissue (WAT) and brown adipose tissue (BAT).** White adipocytes are derived from Myf5 negative precursors, are UCP1 negative, and primarily play a role in the storage of lipids within a single lipid droplet. Brown adipocytes primarily play a role in non-shivering thermogenesis, are multilocular, UCP1 positive, and are derived from Myf5 positive progenitors. Both WAT and BAT have been shown to have an endocrine function in the regulation of metabolism. Major secretory products of WAT and BAT are shown.

### 3.1.1 Regulation of Brown Adipose Tissue Thermogenesis

In mammalians, information on body temperature, feeding status, and energy reserves is centrally coordinated within the ventromedial hypothalamic nucleus (VMN). Working through the VTM, these stimuli coordinate the metabolic activity of BAT through direct sympathetic innervation and norepinephrine release. Thus, a decrease in body temperature, a recent meal, or an abundance of energy reserves will result in an increase in BAT metabolism [214]. In humans, cold-induced non-shivering thermogenesis of BAT is well established [222]. Nutritional activation of BAT has been observed but is still debated [223,224]. Regardless of specific stimuli, BAT activation is largely controlled by the activation of β-adrenergic stimulation, primarily through $\beta_3$-adrenoceptors. β-adrenergic receptors couple to $G_s$ subtype GPCRs and promote an

increase in cAMP through the stimulation of adenylyl cyclase. cAMP activates PKA and triggers the release of free fatty acids from stored triglycerides which drives thermogenesis in the presence of UPC1 [214]. Prolonged stimuli, such as long-term exposure to cold, has been shown to increase the thermogenic capacity of BAT through hyperplasia, increased UPC1 transcription, and mitochondrial biogenesis [225]. These effects are believed to be mediated through PKA-dependent phosphorylation of the transcription factor cAMP response element-binding protein (CREB) [214].

### 3.1.2 Beige/Brite Adipocytes

In addition to brown and white adipocytes, an additional type of adipocyte known as "beige" or "brite" adipocytes have recently been identified. Beige/brite adipocytes share a number of features with brown adipocytes, and are thought by some to represent a distinct cell type with some overlapping function [226]. Beige/brite adipocytes are found in small numbers within WAT. They are also known as inducible brown adipocytes as several "brown-like" features can be induced by prolonged exposure to cold or increased intracellular ATP, including multilocular lipid droplets, increased mitochondrial biogenesis, and high UCP1 expression. However, brown and beige/brite adipocytes have distinct developmental origins and gene expression profiles [226,227]. Brown adipocytes are derived from a myf-5 positive muscle-like cell lineage, whereas beige/brite adipocytes are derived from a myf-5 negative cell lineage similar to traditional white adipocytes [227,228]. Prior to cold adaptation beige/brite adipocytes are found in very small numbers within WAT, but upon prolonged exposure to cold, their numbers are dramatically increased. There are two prevailing models for the origin of beige/brite adipocytes prior to

induction of cold adaptation. The first is that beige/brite adipocytes are derived from pre-beige/brite adipocytes that are morphologically similar to white adipocytes at normothermia, but represent a distinct cell type that undergoes temperature induced changes. The second model is that beige/brite adipocytes are derived from white adipocytes and that transdifferentiation occurs between white and beige/brite adipocytes based on temperature adaptation [227]. Both of these models indicate the plasticity of adipose tissue in regulating energy storage vs utilization. The induction or activation of beige/brite adipocytes is of therapeutic interest as a possible treatment for the comorbidities associated with obesity, such as type 2 diabetes, through an increase in energy expenditure.

### 3.1.3 Brown Adipose Tissue Secretome

Since its discovery in humans, stimulating BAT and browning of WAT/inducing beige adipocytes, have been therapeutic targets for treating obesity and diabetes by increasing energy expenditure. Further, BAT has been shown to regulate metabolism independent of its non-productive energy expenditure through the release of hormones (Figure 3-1). While WAT has been shown to have a significant endocrine function; notably secreting leptin and adiponectin to regulate energy balance and glucose homeostasis/fatty acid catabolism, respectively [229]. The endocrine function of BAT is less established. Yet, BAT has been noted to secrete a number of biologically active molecules that act in an autocrine, paracrine, and endocrine fashion to regulate metabolism and energy expenditure independent of thermogenesis. Here, I will focus primarily on the endocrine function of BAT. Neuregulin-4 (Nrg4) is a ligand of the epidermal growth factor (EGF) family of receptors and is secreted by BAT in response to acute cold

exposure and sympathetic stimulation [230]. In addition to stimulating local neurite outgrowth, Nrg4 has also been shown to regulate hepatic lipogenesis through the stimulation of ErbB3 and ErbB4 [231]. Acute cold exposure also stimulates the secretion of the widely active endocrine factor fibroblast growth factor-21 (FGF21) [232]. Among its other actions, FGF21 acts to stimulate hepatic fatty acid β-oxidation, gluconeogenesis, and sympathetic outflow to BAT [233,234]. In addition to being an important secretory product of BAT, bone morphogenetic proteins (BMPs) have been shown to regulate adipocyte differentiation and energy expenditure by upregulating the expression of several key BAT genes including UCP1 [235,236]. BMPs are also associated with the induction and development of beige adipocytes [237]. BMPs have been shown to regulate energy expenditure through centrally mediated action in the hypothalamus [236]. BAT has also been shown to secrete interleukin-6 (IL-6). Independent of its role in the inflammatory response, IL-6 has been implicated to play a role in glucose metabolism and energy balance through the repression of genes associated with hepatic gluconeogenesis and glucose output [231]. IL-6 is thought to mediate the metabolic benefit of exercise and induce the browning of white adipocytes leading to the development of beige adipocytes [231,238]. Supporting its role in glucose metabolism, mice lacking IL-6 are predisposed to obesity and diabetes [239]. Another secretory product of BAT includes free fatty acids (FFAs), which are released upon cold exposure-stimulated lipolysis [231]. In addition to being a fuel source, biologically active branched fatty acid esters of hydroxyl fatty acids act on free fatty acid receptors to improve glucose tolerance and reduce adipose tissue inflammation associated with obesity [240]. Both leptin and adiponectin are also secreted by BAT, but compared to their secretion from WAT, BAT-originating leptin and adiponectin only comprise a small fraction of the circulating hormones

[214,231]. BAT also secretes a number of other locally acting factors including basement membrane proteins, adipsin, basic fibroblast growth factor, insulin-like growth factor, prostaglandins, angiotensinogen, triiodothyronine, nerve growth factor, vascular endothelial growth factor, lactate, retinaldehyde, retinoic acid, nitric oxide, and adenosine [214,231].

### 3.1.4 Brown Adipose Tissue Transplantation

The endocrine function of BAT has been further demonstrated in recent studies that observe a number of metabolic effects following BAT transplantation. The effects observed in these studies cannot be explained solely through increased energy utilization within the transplanted tissue, suggesting that secreted factors from the BAT transplants are responsible for the observed changes in whole body metabolism. In one study, transplantation of BAT was shown to increase glucose tolerance and insulin sensitivity within 8 weeks and to be protective against high fat diet induced obesity and insulin resistance [241]. The increased insulin sensitivity in animals receiving a BAT transplant was shown to be mediated by increased glucose uptake in endogenous BAT, WAT, and cardiac muscle, but not skeletal muscle. Mice receiving the BAT also displayed a dramatic increase in serum FGF21 and IL-6. Further, the effects of BAT transplantation were lost when the BAT transplants were harvested from IL-$6^{-/-}$ mice, suggesting that IL-6 plays a key role in mediating the effect of the transplanted BAT or BAT development/competency prior to harvest [241]. Another study has found that BAT transplantation is capable of correcting the clinical manifestations associated with diabetes in a streptozotocin-treated (STZ) mouse model of diabetes [187]. STZ is a β-cell specific toxin that emulates type-1 diabetes through the loss of β-cells and a deficiency of insulin. In this study,

transplantation of BAT improved glucose tolerance and restored euglycemia independent of insulin (Figure 3-2). Additionally, BAT transplantation resulted in an increase in plasma adiponectin, leptin, and IGF-1. Another interesting result of BAT transplantation was the correction of hyperglucagonemia that is observed in diabetes. Within 5 weeks of transplantation, plasma glucagon was reduced to below normal levels (Figure 3-3)[187]. The loss of glucagon signaling has previously been shown to be protective against STZ-induced diabetes [184,242]. Thus, the inhibition of glucagon secretion may mediate the correction of the diabetic phenotype observed with BAT transplantation. Here, I present evidence for a new BAT secreted factor that inhibits glucagon secretion from α-cells. This currently unidentified factor may offer a significant therapeutic benefit in the treatment of diabetes and management of blood glucose through the reduction of hyperglucagonemia.

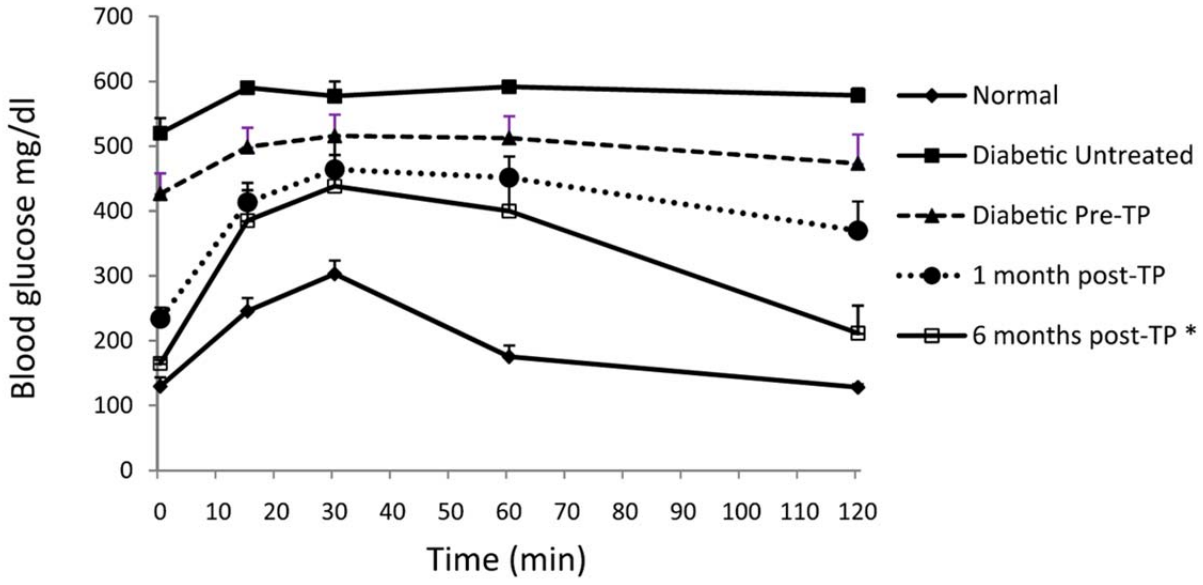


**Figure 3-2 Subcutaneous transplantation of embryonic BAT improves glucose tolerance.** Intraperitoneal glucose tolerance tests on mice, untreated diabetic, and BAT transplant receiving diabetic mice. $P < 0.05$ when comparing 6-months post-transplant with untreated diabetic controls or diabetic pretransplant condition. (Figure adapted with permission from [187])

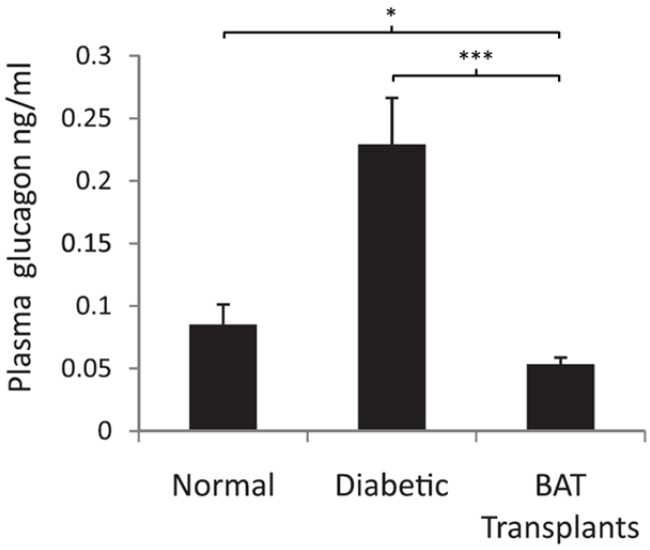


**Figure 3-3 Subcutaneous transplantation of embryonic BAT corrects hyperglucagonemia and lowers plasma glucagon below normal.** Plasma glucagon from normal, diabetic, and mice receiving BAT transplant at 5 months post-transplant. [* $P < 0.05$; *** $P < 0.0005$] (Figure adapted with permission from [187])

## 3.2 Methods

### 3.2.1 Experimental Animals

In compliance with the Vanderbilt University Institutional Animal Care and Use Committee, 10-14 week old male wild-type C57Bl/6 (Harlan Sprague Dawley, Inc) mice were used for these experiments.

### 3.2.2 Isolation and Culture of Mouse and Human Islets

Mouse islet isolation and culture was performed as previously described (2.2.2) [67,109]. Human islets (donor information: age, 28; sex, M; BMI, 32.8) were obtained from the Integrated Islet Distribution Program in collaboration with Alvin C. Powers, M.D. (Vanderbilt University, Department of Medicine) and cultured as described in 2.2.2.

### 3.2.3 Conditioning KRBH buffer

BAT was isolated from embryonic mice at E15-17 as previously described [187]. BAT was then incubated in KRBH buffer (50 µL per 1 interscapular section of BAT) with 15 mM glucose for 4 hours at 37°C with occasional shaking. N13 and nbat9 cells were provided by Bruce M. Spiegelman, Ph.D. (Harvard Medical School, Department of Cell Biology) and differentiated in vitro as previously described [226]. To condition buffer, differentiated N13 and nbat9 cells were incubated with KRBH (1 mM glucose, 100 µL/cm$^2$ of cell culture surface area) at 37°C. Cell-line conditioned buffer was transferred to a fresh set of differentiated cells after 1 hour for a total of 6 x 1-hour incubations. All conditioned buffer was passed through a 0.2 µM syringe filter (Fisher).

### 3.2.4 Size Fractionation and Dialysis of Conditioned Buffer

Conditioned buffer was size fractionated using an Amicon Ultra centrifugal filter unit (Millipore) with a molecular weight cutoff (MWCO) of 3 kDa. Two filtrations (filtration of the filtrate) were performed in series to ensure efficient removal of factors less than 3 kDa from the unfiltered fraction containing factors greater than 3 kDa. The fraction containing factors less than 3 kDa was further dialyzed using a Micro Float-A-Lyzer Dialysis Device (Spectrum Labs) with a MWCO of 500-100 and 100-500.

### 3.2.5 Hormone Secretion Assays

Static hormone secretion assays on islets were performed as described in Chapter 2, with different treatment conditions. In these experiments, islets were treated with a 1:15 dilution of BAT, N13, nbat9, or fractionated conditioned buffer at low (1 mM) and high (11 mM) glucose.

Treatment with unconditioned buffer was used as a control. Insulin secretion is normalized to insulin secretion observed from unconditioned buffer at low glucose. For the assessment of leptin secretion from adipocyte cell lines, media was collected from differentiated adipocyte cells following 24 hour incubation. Media conditioned in a cell-free environment was used as control. Media was size fractionated as described in (3.2.4). Leptin content was assessed using a Mouse Leptin ELIDA Kit (Sigma).

### 3.2.6 Data Analysis and Statistics

Data were analyzed with Microsoft Excel or GraphPad Prism. Data are reported as mean values (+SEM), with p-values of less than 0.05 considered statistically significant as determined by Student's *t*-test of a small number of distinct planned comparisons.

## 3.3 Results

### 3.3.1 A Secreted Factor from Brown Adipose Tissue Inhibits Glucagon Secretion from Mouse Islets

I hypothesize that a factor secreted by BAT is directly responsible for the inhibition of glucagon secretion observed following BAT transplantation in diabetic mice. To test this hypothesis, glucagon secretion was assessed from isolated mouse islets treated with buffer conditioned with embryonic BAT. Islets exposed to BAT-conditioned buffer display a potent inhibition of glucagon secretion at both low and high glucose as compared to islets exposed to unconditioned buffer (Figure 3-4). BAT-conditioned buffer does not affect insulin secretion (Figure 3-5).

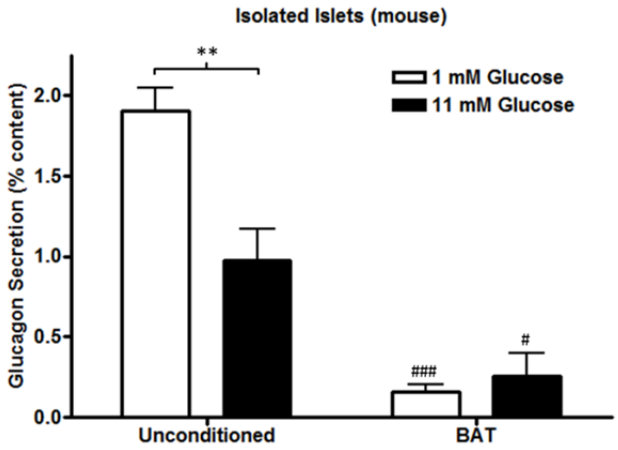


**Figure 3-4 BAT conditioned buffer inhibits glucagon secretion at low and high glucose.** Average glucagon secretion from isolated mouse islets (n = 7) treated with unconditioned or BAT conditioned buffer. Open white bars represent data from low glucose (1 mM) and closed black bars represent data from high glucose (11 mM). Data are shown as means (+SEM). Asterisks (*) above brackets represent significant differences between the same condition/control at low and high glucose as determined by Student's *t*-tests [** P < 0.01]. Hash marks (#) directly above columns represent statistical differences between condition and control at the same glucose concentration as determined by Student's *t*-tests [# P < 0.05; ### P < 0.001].

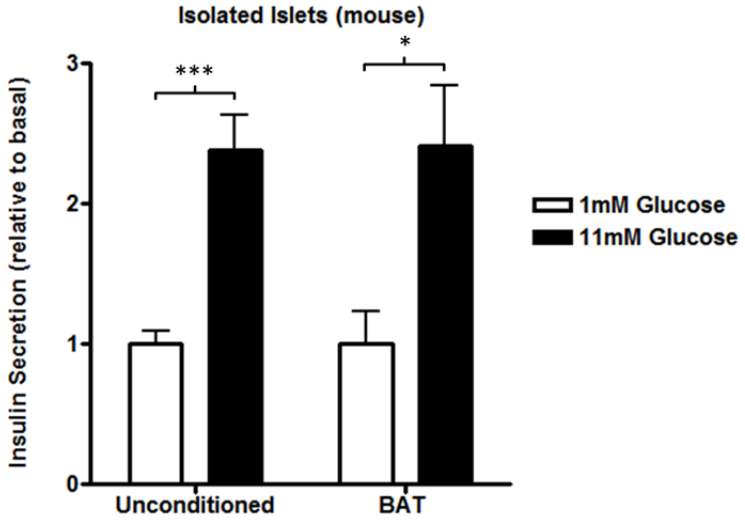


**Figure 3-5 BAT conditioned buffer has no effect on insulin secretion at low or high glucose.** Average normalized insulin secretion from isolated mouse islets (n = 7) treated with unconditioned or BAT conditioned buffer. Open white bars represent data from low glucose (1 mM) and closed black bars represent data from high glucose (11 mM). Data are shown as means (+SEM). Asterisks (*) above brackets represent significant differences between the same condition/control at low and high glucose as determined by Student's *t*-tests [* P < 0.05; *** P < 0.001].

### 3.3.2 A Secreted Factor from Brown Adipose Cell Line (nbat9) Inhibits Glucagon Secretion from Mouse Islets

Determining the identity of the glucagon-inhibiting factor secreted by BAT will require a large volume of BAT-conditioned buffer, which is currently limited by the time and energy intensive process of harvesting primary BAT from embryonic mice. Additionally, consistency between BAT-conditioned buffer samples will provide easier assessment of activity. Thus, I assessed whether the glucagon-inhibiting effect of BAT-conditioned buffer could be replicated using the brown adipose cell line, nbat9. Similar to BAT-conditioned buffer, treatment with nbat9 conditioned buffer results in an inhibition of glucagon secretion as compared to both unconditioned and white adipose cell line (N13)-conditioned buffer controls. However, the glucagon-inhibiting effect of nbat9-conditioned buffer is less potent than BAT-conditioned buffer and is only observed at low glucose when glucagon secretion is maximal (Figure 3-6). Additionally, no changes in insulin secretion are observed between unconditioned, N13-conditioned, and nbat9-conditioned buffer (Figure 3-7).

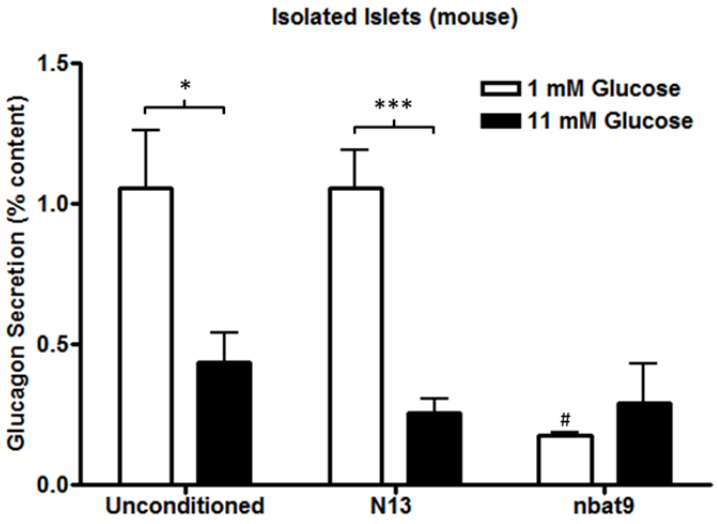


**Figure 3-6 nbat9 conditioned buffer inhibits glucagon secretion at low and high glucose.** Average glucagon secretion from isolated mouse islets (n = 8) treated with unconditioned, N13 (WAT), or nbat9 (BAT) conditioned buffer. Open white bars represent data from low glucose (1 mM) and closed black bars represent data from high glucose (11 mM). Data are shown as means (+SEM). Asterisks (*) above brackets represent significant differences between the same condition/control at low and high glucose as determined by Student's *t*-tests [* $P < 0.05$; *** $P < 0.001$]. Hash marks (#) directly above columns represent statistical differences between condition and control at the same glucose concentration as determined by Student's *t*-tests [# $P < 0.05$].

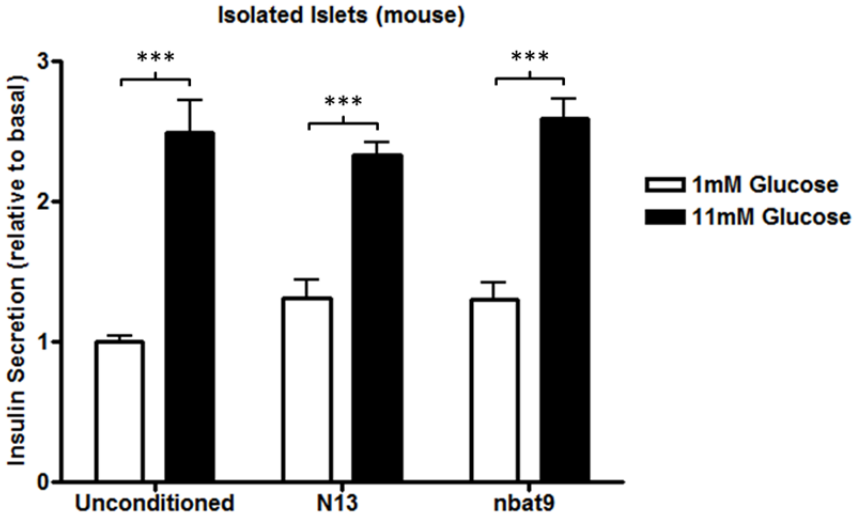


**Figure 3-7 nbat9 conditioned buffer has no effect on insulin secretion at low or high glucose.** Average normalized insulin secretion from isolated mouse islets (n = 8) treated with unconditioned, N13 (WAT), or nbat9 (BAT) conditioned buffer. Open white bars represent data from low glucose (1 mM) and closed black bars represent data from high glucose (11 mM). Data are shown as means (+SEM). Asterisks (*) above brackets represent significant differences between the same condition/control at low and high glucose as determined by Student's *t*-tests [*** $P < 0.001$].

### 3.3.3 BAT Glucagon-inhibiting Factor is Less than 3 kDa

BAT conditioned buffer was size fractionated through a combination of spin column filtration with molecular weight cutoff and dialysis. To narrow down the identity of the active glucagon-inhibiting factor, glucagon secretion was assessed in islets exposed to each fraction at low glucose. The BAT-conditioned fraction containing factors greater than 3 kDa did not have any inhibitory activity on glucagon secretion as compared to unconditioned control (Figure 3-8). All BAT-conditioned fractions containing factors less than 3 kDa retained an inhibitory effect on glucagon secretion, including the dialyzed 0.5-3 kDa and 1-3 kDa fractions (Figure 3-8). A similar effect was observed with size fractionated nbat9-conditioned buffer samples. Nbat9 conditioned buffer was size fractionated solely through a spin column filtration with molecular weight cutoff. Glucagon secretion was assayed at both high and low glucose in islets exposed to each fraction. The nbat9-conditioned buffer fraction containing factors greater than 3 kDa did not display any inhibitory effect on glucagon secretion, which was unchanged as compared to unconditioned control at low and high glucose (Figure 3-9). The nbat9-conitioned buffer fraction containing factors less than 3 kDa retained its inhibitory effect on glucagon secretion at low glucose (Figure 3-9). Together, these data are consistent with a glucagon-inhibiting factor secreted by BAT and nbat9 cells that is less than 3 kDa.

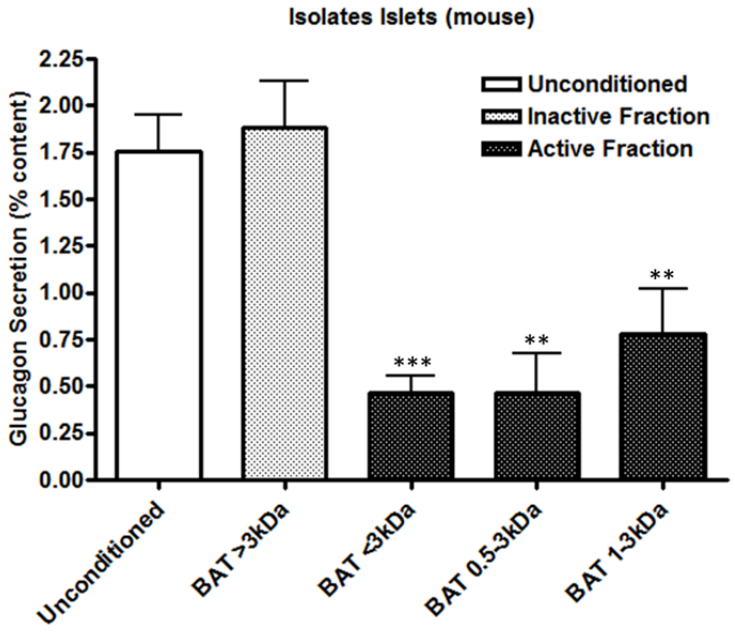


**Figure 3-8 Fractions of BAT conditioned buffer containing factors less than 3 kDa inhibit glucagon secretion at low glucose.** Average glucagon secretion from isolated mouse islets (n = 8) treated with unconditioned or size fractionated BAT conditioned buffer. Asterisks (*) above brackets represent significant differences between specific fractionation samples and unconditioned buffer as determined by Student's *t*-tests [** P < 0.01; *** P < 0.001].

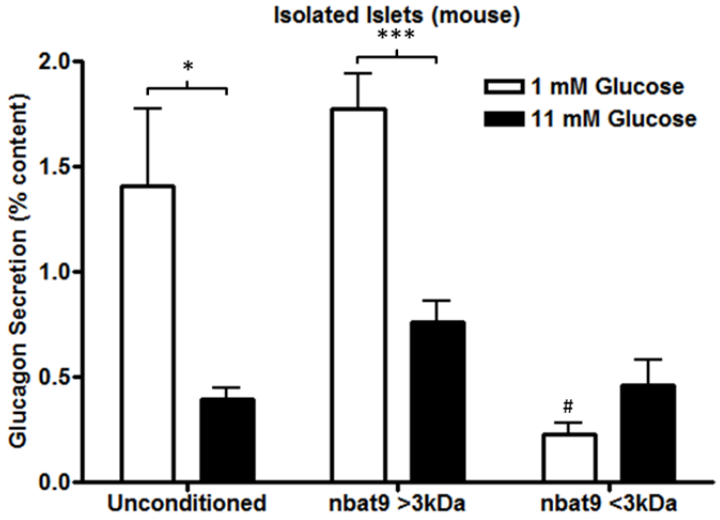


**Figure 3-9 Fractions nbat9 conditioned buffer containing factors less than 3 kDa inhibit glucagon secretion at low glucose.** Average glucagon secretion from isolated mouse islets (n = 8) treated with unconditioned or size fractionated nbat9 conditioned buffer. Open white bars represent data from low glucose (1 mM) and closed black bars represent data from high glucose (11 mM). Data are shown as means (+SEM). Asterisks (*) above brackets represent significant differences between the same condition/control at low and high glucose as determined by Student's *t*-tests [* P < 0.05; *** P < 0.001]. Hash marks (#) directly above columns represent statistical differences between condition and control at the same glucose concentration as determined by Student's *t*-tests [# P < 0.05].

### 3.3.4 Leptin is Secreted by Brown Adipocyte Cell Line (nbat9) but is Removed by less than 3 kDa Size Filtration

BAT secretes a number of factors that have diverse effects on metabolism (discussed in 3.1.3). One of these factors, leptin, has previously been shown to inhibit glucagon secretion [243]. Although leptin (18.7 kDa) is secreted by both N13 and nbat9 cell lines, it is removed by spin column filtration with a molecular weight cutoff of 3 kDa (Figure 3-10). Thus, it is unlikely that the glucagon-inhibiting effect observed with nbat9-conditioned buffer fraction containind factors less than 3 kDa is mediated by leptin.

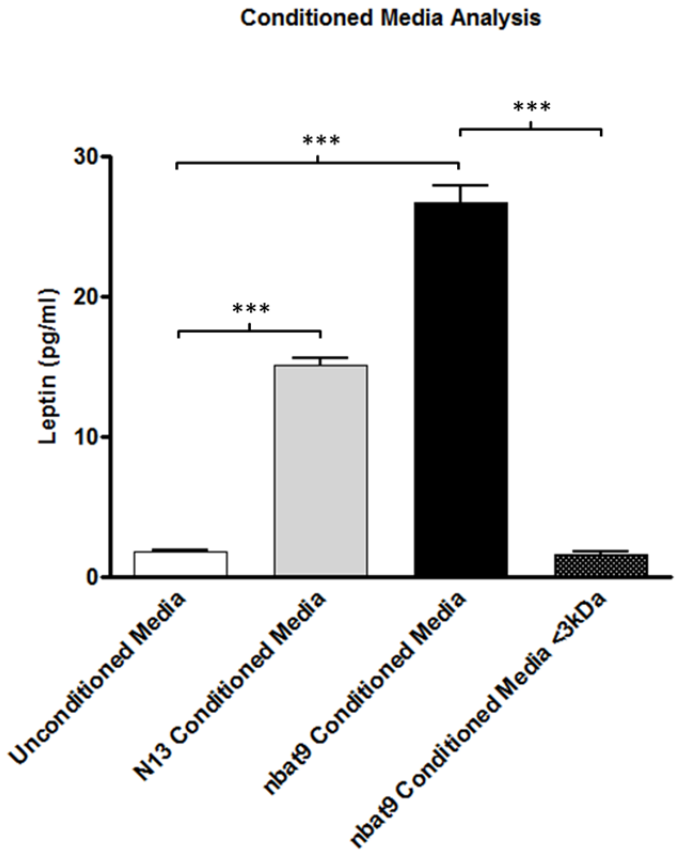


**Figure 3-10 Leptin is secreted into conditioned media by both N13 and nbat9 and is removed by spin filtration with a molecular weight cutoff of less than 3 kDa.** Average leptin content of unconditioned, N13, and nbat9 conditioned media (24 hour condition). Leptin content of nbat9 conditioned media following less than 3 kDa filtration was also assessed. [*** $P < 0.001$ as determined by Student's *t*-tests]

### 3.3.5 Secreted Factor Inhibits Glucagon Secretion from Human Islets

Given the potential therapeutic benefits of a glucagon-inhibiting BAT secreted factor, it is essential to understand if the same BAT secreted factor that inhibits glucagon secretion in mice plays a role in human physiology and the regulation of human glucagon secretion. In preliminary studies, human islets were exposed to BAT-conditioned buffer at both low and high glucose. The initial results indicate that the mouse derived BAT secreted factor also inhibits glucagon secretion from human islets (Figure 3-11). As shown here, the lack of glucose-inhibition of glucagon secretion is occasionally observed from some human islets samples. It is currently unclear whether this lack of glucose-inhibition of glucagon secretion is a result of unique biological differences between samples (a lack of glucose-inhibition of glucagon secretion is often observed in type 2 diabetes) or a confounding effect due to the isolation/preparation of the islets.

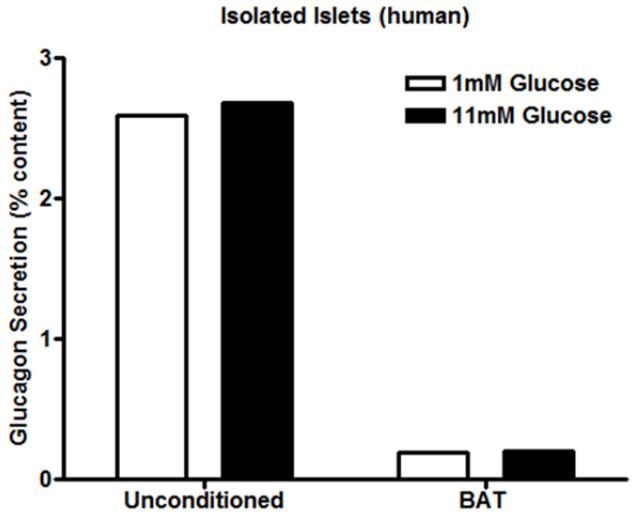


**Figure 3-11 Preliminary results suggest that mouse BAT conditioned buffer inhibits glucagon secretion at low and high glucose in human islets.** Average glucagon secretion from isolated human islets (n = 1) treated with unconditioned or BAT conditioned buffer. Open white bars represent data from low glucose (1 mM) and closed black bars represent data from high glucose (11 mM).

### 3.3.6 Towards the Identification of the Glucagon-inhibiting Brown Adipose Tissue Secreted Factor

Here, size fractionation was used to isolate the glucagon-inhibiting BAT secreted factor to a less complex fraction containing factors less than 3 kDa. Preliminary results comparing less than 3 kDa fractionated nbat9 and N13 conditioned buffer were performed using hydrophilic interaction liquid chromatography (HILIC) coupled with mass spectrometry in collaboration with John McLean, Ph.D. (Vanderbilt University, Department of Chemistry). The analysis of nbat9 conditioned buffer indicated an abundance of lipid motilities despite normal phase separation, but was still overly complex for efficient candidate identification. The less than 3 kDa fraction of nbat9 conditioned buffer has been further fractionated through a diethylaminoethyl cellulose column in collaboration with Richard Gross, M.D., Ph.D. (Washington University School of Medicine, Department of Chemistry). However, the activity of these fractions has yet to be assessed. Additionally, a two-phase liquid extraction using the Folch method was used to isolate lipid factors in conditioned nbat9 buffer. Preliminary, analysis of both the lipid and aqueous fractions has not shown any inhibitory activity of glucagon secretion.

## 3.4 Discussion

Previous experimental findings suggested that the restoration of euglycemia and the reversal of diabetes in mice receiving a BAT transplant may be due to a potent inhibition of glucagon secretion [187]. To examine the direct effects of secreted BAT factors on glucagon secretion, buffer was conditioned in the presence of BAT and a brown adipocyte cell line (nbat9) and used to treat isolated islets. Buffer containing secreted BAT factors was shown to inhibit glucagon secretion. Further, size fractionation of BAT conditioned buffer indicates that the active

factor(s) are less than 3 kDa. Thus, the data presented in this chapter support the hypothesis of a novel BAT hormone that acts directly on α-cells to inhibit glucagon secretion.

### 3.4.1 Interactions Between Brown Adipose Tissue and Glucagon

Brown adipose tissue has been shown to release a number of endocrine factors that regulate metabolism through various effects (discussed in 3.1.3). However, the direct regulation of glucagon secretion has not previously been shown to be one of these effects. Although leptin is secreted by BAT [214,231] and nbat9 cells (Figure 3-10) and leptin has been shown to inhibit glucagon secretion [243], leptin is not responsible for the effects described here. Leptin is an 18.7 kDa protein that is removed by the spin filtration technique used to fractionate conditioned BAT into an inactive greater than 3 kDa fraction and an active less than 3 kDa fraction (Figure 3-10). Additionally, the major source of circulating leptin originates from WAT and the white adipose cell line N13 was also shown to secrete leptin. Yet, N13 conditioned media did not affect glucagon secretion as compared to unconditioned media (Figure 3-6). Thus, the data presented here are consistent with a previously undescribed interaction between BAT and glucagon secretion. The glucagon-inhibiting BAT secreted factor described here may represent one arm of a negative feedback loop between BAT and α-cells.

Intraperitoneal injection of glucagon has been shown to induce thermogenesis [244]. This effect is largely attributed to the activation of BAT. Physiological relevant concentrations of hyperglucagonemia have been shown to increase BAT metabolism and BAT-mediated thermogenesis [245]. Additionally, glucagon has been shown to be essential for cold-induced BAT thermogenesis. Glucagon knockout mice display decreased cold tolerance, likely mediated

through a decrease in thermogenic BAT genes including UCP1 and an overall decrease in oxygen consumption [246]. Yet, it remains unclear whether BAT is regulated directly by glucagon or if glucagon-induced activation of BAT is mediated through an increase in catecholamines and/or sympathetic stimulation. Denervation of BAT has been shown to both partially [247] or completely [248] remove its response to glucagon stimulation, indicating that increased sympathetic stimulation plays a major, but possibly not the sole role in glucagon-stimulated BAT activation. Other studies have indicated that circulating catecholamines are required for glucagon-stimulated BAT activation [249]. Glucagon stimulation of isolated BAT has been shown to either increase BAT metabolism[250] or have no effect [248], thus possible direct activation of BAT by glucagon remains unknown. Although the specific contributions from each mechanism remain disputed, the current literature clearly establishes glucagon-stimulated activation of BAT. Together with the BAT secreted factor-induced inhibition of glucagon secretion described here, a new negative feedback model can be described between BAT and α-cells within pancreatic islets. In this model, glucagon secretion directly or indirectly stimulates BAT metabolism and possibly the secretion of the unknown BAT secreted factor that would then feedback on α-cells to negatively regulate glucagon secretion (Figure 3-12).

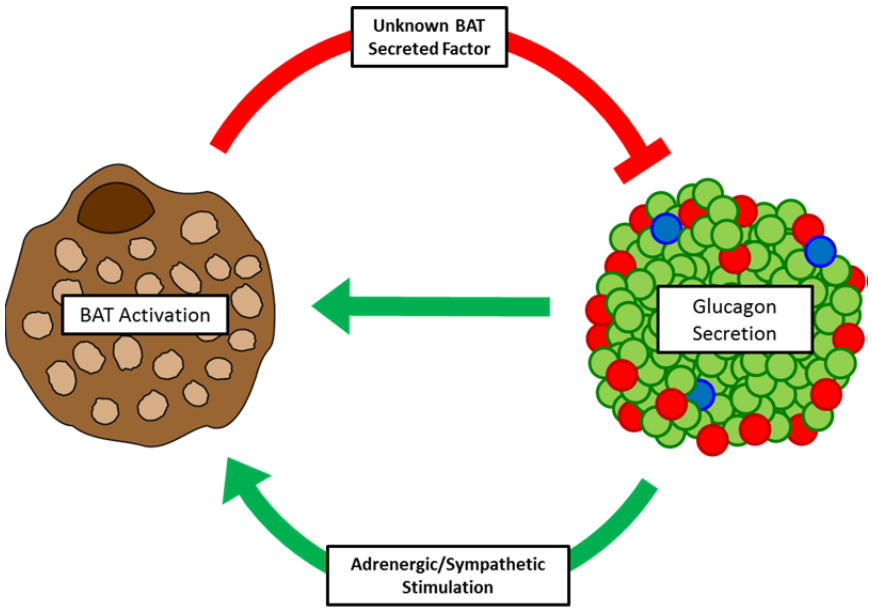


**Figure 3-12 Potential negative feedback model between brown adipose tissue and α-cells with pancreatic islets.** Glucagon secretion has been shown to activate BAT, leading to increased metabolism and thermogenesis. The secretion of the unknown BAT factor described here (a possible metabolic product) may be directly influenced by this activation, thus resulting in negative feedback through the inhibition of glucagon secretion.

### 3.4.2 Identification of the Glucagon-inhibiting Brown Adipose Tissue Secreted Factor

The identification of unknown factors within complex mixtures, such as conditioned buffer, is often accomplished through a number of complementary approaches. Fractionation of the complex mixture, such as the size fractionation described here, is often used to simplify the mixture and remove a large number of inactive factors prior to identification. In addition to size fractionation, common fractionation techniques include various types of chromatography, phase extractions, and electrophoretic fractionation. Independent of the specific technique used, each fraction must be assessed for activity, ideally in a high throughput assay. Unfortunately, the current glucagon secretion assays are time and resource intensive and there is a need for higher throughput assessment of glucagon secretion. Additionally, these fractionation techniques may be used in series to further simplify a complex mixture. Exclusion

experiments, such as heat inactivation/denaturation of proteins and protease digestion can be used to exclude classes of macromolecules and inform future identification studies.

Once the complex mixture containing the active compound is simplified through fractionation, mass spectrometry can be used to specifically identify potential candidates. Generally, a more complex mixture will generate more candidates that require more individual or pooled assessments of activity. One strategy to reduce the number of candidates is the comparison of identified factors from an active complex mixture (nbat9 conditioned buffer) with that of a similar but inactive complex mixture (N13 conditioned buffer) that may contain a similar profile of factors. In this case, since the active factor is only expected in the nbat9 conditioned buffer, only candidates that are considerably more abundant in the nbat9 conditioned buffer as compared to the N13 condition buffer need be considered for additional testing. Additional experiments are required to identify the class of macromolecule to which the glucagon-inhibiting BAT secreted factor belongs. However, our initial experiments utilizing a Folch extraction suggest that the factor is not a lipid. Peptides also represent a common class of hormones. Interestingly, few peptide hormones are less than 3 kDa; most are much larger than 3 kDa. Based on the average molecular mass of an amino acid, if the unknown glucagon-inhibiting BAT secreted factor were a peptide, it would need to be less than ~27 residues to have a molecular mass of less than 3 kDa. In comparison, glucagon and somatostatin, which are considered a short peptide hormones, are composed of 29 and 14-amino acids, respectively. Although rare, peptides as short as 3-4 residues have been shown to be biologically active and play diverse physiologic roles in the regulation of metabolism [251,252].

### 3.4.3 Potential Therapeutic Benefits of Potent Glucagon-inhibiting Brown Adipose Tissue Secreted Factor

Diabetes is characterized by the dysfunctional inhibition of glucagon secretion that causes hyperglucagonemia and contributes to hyperglycemia, particularly during fasting (discussed in 1.12). Very few diabetic therapies are directed towards inhibiting glucagon signaling or secretion. Rather, current therapies are directed at reducing blood glucose through an enhancement of insulin signaling, decreased hepatic glucose production, and increased urinary excretion of glucose. However, GLP-1 analogues have been shown to both potentiate insulin secretion and inhibit glucagon secretion. Once isolated, the glucagon-inhibiting BAT secreted factor described here could potentially be used to treat hyperglycemia of both type 1 and type 2 diabetic patients. In combination with therapies that enhance insulin secretion, the glucagon-inhibiting BAT secreted factor could be used to address both hormonal dysfunctions (lack of insulin signaling and excess glucagon signaling) that contribute to the hyperglycemia of diabetes, ultimately leading to better glycemic control.

### 3.4.4 Summary

The data presented here support the existence of a previously unreported and currently unidentified factor that is secreted by BAT and acts directly on islets to inhibit glucagon secretion. The glucagon-inhibiting action of this BAT secreted factor was evaluated through the assessment of glucagon secretion from islets following treatment with buffer previously conditioned in the presence of primary embryonic BAT or a brown adipocyte cell line (nbat9). Conditioned buffer from both of these sources produced a similar inhibition of glucagon secretion at low glucose. However, the BAT conditioned buffer produced a more potent

inhibition of glucagon secretion and was capable of further inhibiting glucagon secretion at high glucose. The glucagon-inhibiting activities of these two samples of conditioned buffer are presumed to be caused by the same factor. When size fractionated, fractions of both BAT and nbat9 conditioned buffer containing factors over 3 kDa lose their activity while fractions containing factors under 3 kDa maintain their activity. Future efforts in identifying the active factor within these conditioned buffer samples will enable a potentially new therapeutic tool in the treatment of diabetes.

# CHAPTER 4
# FLUORESCENCE-BASED IMAGING AND QUANTIFICATION

## 4.1 Introduction

Controlled stimulation and detection of fluorescence is an essential tool in the investigation and examination of biological processes. A number of these techniques have been utilized in previous chapters including confocal fluorescence microscopy and fluorescence-activated cell sorting. Here, I will describe a number of projects that involve fluorescence-based imaging and/or quantification, primarily through confocal fluorescence microscopy. The work described here is the product of collaborative projects and represents a diverse range of techniques that can be applied to variety of biological problems within and outside the field of islet biology.

## 4.2 Spatiotemporal $Ca^{2+}$ Wave Dynamics within Pancreatic Islets

### 4.2.1 Introduction

Synchronized $[Ca^{2+}]_i$ oscillations between β-cells within individual islets result in pulsatile insulin secretion (discussed in 1.7.3). Synchronized $Ca^{2+}$ activity is enabled by Cx36 gap junctions that physically and electrically couple adjacent β-cells. Although synchronized, high-speed imaging has revealed that each peak in $[Ca^{2+}]_i$ represents a $Ca^{2+}$ wave that propagates through the islet, reaching individual β-cells at different points in time [63]. Based on a computational model, the origin of the waves was predicted to be the product of β-cell heterogeneity within an islet [63]. This model suggests that $Ca^{2+}$ waves originate from an intrinsic pacemaker area of increased metabolism and $K_{ATP}$ channel inhibition. To experimentally test this model, a custom-made

microfluidic device was used to stimulate islets with a glucose gradient in a controlled and spatially defined manner.

### 4.2.2 Methods

A two-channel microfluidic device was constructed as previously described [253]. Mouse islets were isolated and cultured as previously described (2.2.2) [67,109] . Islets were stained with 4 µM Fluo4-AM (Life Technologies) for 1.5 hours at room temperature, guided into the microfluidic device within an environmentally controlled stage (37°C and 5% $CO_2$), and stimulated with the following glucose protocol; 2 mM, 2-11 mM gradient, 11 mM, 2 mM, 11-2 mM gradient (reverse of previous gradient), 11 mM glucose (Figure 4-1). Following a 15 minute incubation period, a series of images were acquired for 2 minutes for each glucose stimulation pattern. Imaging was performed using fluorescent confocal microscopy with appropriate excitation and spectral emission windows (LSM710 and LSM780; Carl Zeiss).

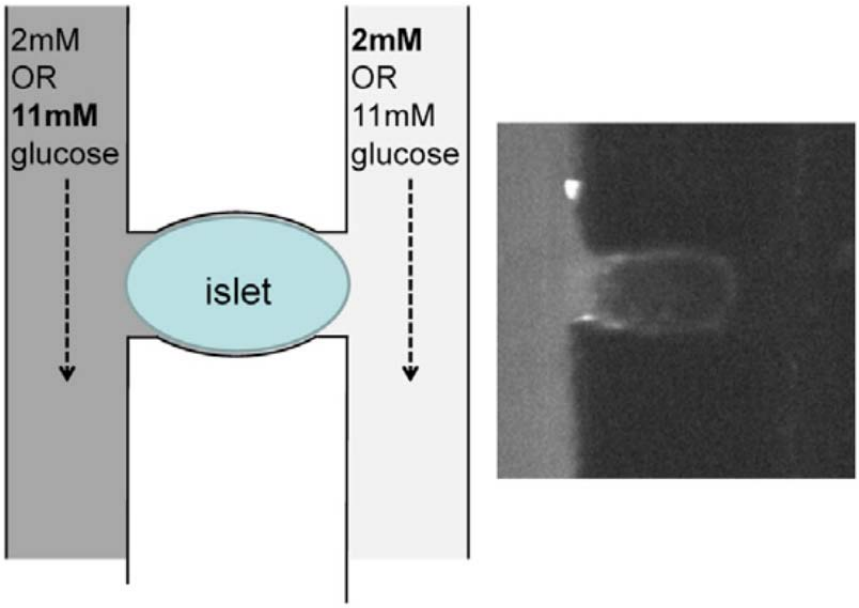


**Figure 4-1 Two-channel microfluidic device.** (left) Schematic of islet within two-channel microfluidic device. (right) Rhodamine B applied to left channel with no Rhodamine B present in the right channel. Figure adapted with permission from [254].

### 4.2.3 Results

When exposed to a glucose gradient, the $Ca^{2+}$ wave nearly always propagates from high to low glucose (Figure 4-2A). In the majority of cases (>80%), the application of a glucose gradient determines the $Ca^{2+}$ wave direction independent of whether it is applied towards or against the preferred wave direction as observed with uniform 11 mM glucose stimulation (Figure 4-2B). Thus, locally elevated glucose was found to fully determine $Ca^{2+}$ wave direction independent of the direction of the gradient. Additionally, prior gradient stimulation does not affect preferred $Ca^{2+}$ wave direction under uniform 11 mM glucose stimulation (Figure 4-2C). When a gradient is applied towards the preferred $Ca^{2+}$ wave direction observed with uniform 11 mM glucose, the preferred $Ca^{2+}$ wave direction does not change when re-stimulated with uniform 11 mM glucose in the majority of cases. When a gradient is applied against the preferred $Ca^{2+}$ wave

direction observed with uniform 11 mM glucose, the preferred $Ca^{2+}$ wave direction was only reversed in a small percentage of cases when re-stimulated with uniform 11 mM glucose (Figure 4-2D). The low level of directional switching between preferred $Ca^{2+}$ wave directions at uniform 11 mM glucose is consistent with the low number of waves that did not propagate in a consistent direction without prior stimulation with a glucose gradient.

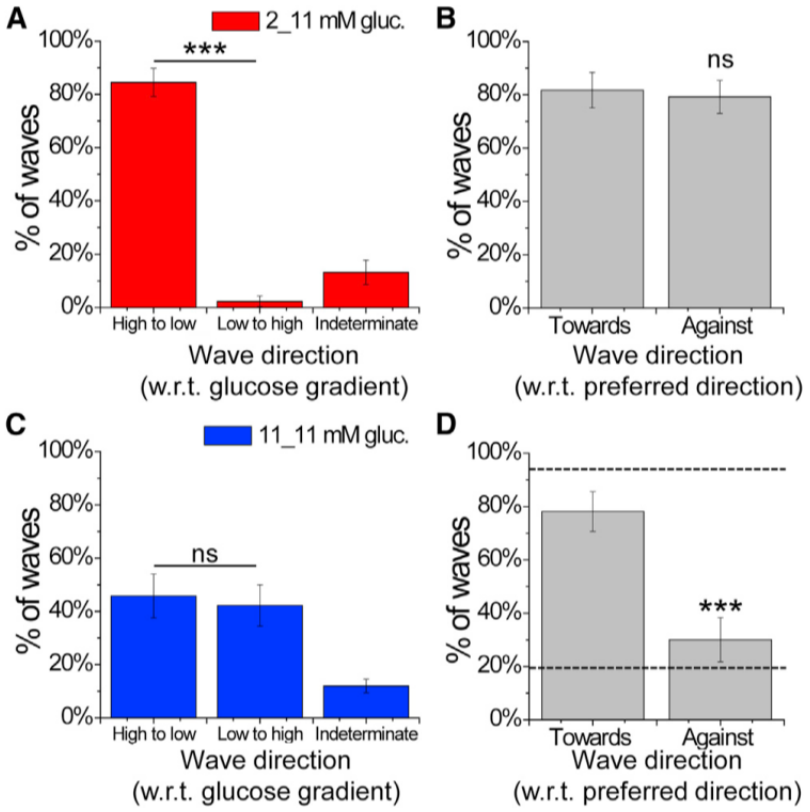


**Figure 4-2 $Ca^{2+}$ wave direction is dependent on extrinsic and intrinsic islet heterogeneity.** (A) Percentage of $Ca^{2+}$ waves that propagate with respect to an applied glucose gradient; high to low, low to high, or in an unrelated or indeterminate direction. (n = 22 islets) (B) Percentage of $Ca^{2+}$ waves that propagate with respect to the gradient when the gradient is applied towards or against the preferred $Ca^{2+}$ wave direction at uniform 11 mM glucose. (n = 22 islets) (C) Percentage of $Ca^{2+}$ waves that propagate with respect to a previously applied glucose gradient; high to low, low to high, or in an unrelated or indeterminate direction; during uniform 11 mM glucose stimulation. (n = 16 islets) (D) Percentage of $Ca^{2+}$ waves that propagate with respect to a gradient previously applied towards or against the preferred $Ca^{2+}$ wave direction at uniform 11 mM glucose, during a second uniform 11 mM glucose stimulation. (n = 16 islets) [Significance determine by Student's t-test where *** indicates $p < 0.001$ and ns indicates no significant difference ($p > 0.05$)] Figure adapted with permission from [254].

### 4.2.4 Discussion

$Ca^{2+}$ waves were previously predicted by computational models to originate from local areas of increased metabolism/excitability within islets [63]. This prediction was experimentally tested by using a microfluidic device to apply a glucose gradient across islets and determining how local areas of increased excitability affected the direction and origin of $Ca^{2+}$ waves. $Ca^{2+}$ waves were found to originate from the area of increased glucose stimulation, independent of which side they were applied to, confirming the original prediction. These experimental findings were additionally confirmed with a computational islet model with a simulated glucose gradient [254]. These data support a pacemaker region within islets that is defined by an intrinsic increased excitability. Although the cause of this increased excitability remains unknown, it may be due to random distribution of excitability among the β-cells. The experimental findings described here were fully explained by the addition of random heterogeneity in β-cell excitability to the previous coupled β-cell model.

## 4.3 Glucagon Aptamer and Biosensor

### 4.3.1 Introduction

Aptamers are short oligonucleotides (DNA or RNA) that exhibit highly sensitive and specific binding (similar to antibodies) to a number of different biologically relevant targets through unique three-dimensional structures. Aptamers are currently being developed for a number of different applications including new therapeutics, drug delivery, bio-imaging, diagnosis, and analytical reagents [255]. As compared to antibodies, aptamers possess a number of advantages such as higher thermal stability, higher throughput production, low immunogenicity/toxicity (for therapeutics), and their ability to be designed against toxic targets [255]. Aptamer-based

biosensors have been developed for a number of different targets including VEGF, thrombin, IgE, and ATP [256,257]. We are interested in developing a glucagon aptamer that can be functionalized as a glucagon biosensor. Current methods for glucagon detection (ELISA, RIA, and Luminex) are dependent on expensive glucagon antibodies and require long incubation times. Ideally, a glucagon aptamer would have increased sensitivity, allowing for a lower limit of detection. Also, depending on its functionalization, the aptamer could be developed into biosensors that offered higher throughput real-time glucagon detection and possibly even single cell spatial resolution of glucagon secretion. Here, I describe the efforts towards achieving this goal.

### 4.3.2 Methods

Aptamers are typically designed through a process known as **S**ystematic **E**volution of **L**igands by **EX**ponential enrichment process (SELEX) [8]. In this process, a random nucleic acid library is incubated with an immobilized target of interest. Unbound oligonucleotides are discarded while bound oligonucleotides are eluted and used as a PCR template for generating a new pool of enriched oligonucleotides for incubating with the target. This process is applied through multiple rounds until a final library of aptamers is cloned and sequenced. Additional negative selection steps may be added to select for specificity. After performing an initial 14 rounds of selection using a modified Flu-Mag-SELEX process, as described in [258], the enriched pool of aptamers were unable to be sequenced due to complex secondary structure. The development of a glucagon aptamer has since been passed onto Base Pair Biotechnologies Inc, an aptamer discovery company.

A glucagon spiegelmer ($K_d$ = 6.3 nM) or a mirror image aptamer (D- to L-isomer) has previously been described to bind and inhibit circulating glucagon and improve glucose tolerance when administered *in vivo* [259]. This published anti-glucagon aptamer is an unnatural L-form stereoisomer oligonucleotide that binds to natural L-form glucagon. Interestingly, due to the properties of spiegelmers, the natural D-form the aptamer should be capable of binding unnatural D-glucagon. The published spiegelmer sequence was adapted to a natural D-form aptamer (for ease of synthesis and optimization) and functionalized into a biosensor for unnatural D-glucagon. The D-form anti-glucagon aptamer was fluorescently labeled with 6-carboxy-2 ,4,4 ,5 ,7,7 -hexachlorofluorescein succinimidyl ester (HEX). The affinity of the adapted D-form anti-glucagon aptamer for D-glucagon was assessed through a standard binding assay and a competition assay. In the standard binding assay, a range of concentrations of biotinylated D-glucagon (0-1000 nM) (Bio Synthesis Inc) was bound to streptavidin coated plates (Thermo Scientific). HEX-labeled D-form anti-glucagon aptamer (100 nM) (eurofins Genomics) was incubated with immobilized biotinylated D-glucagon and washed out. The total fluorescence of the bound HEX-labeled D-form anti-glucagon aptamer was measured in a Synergy H4 microplate reader (BioTek). For the competition binding assay, a fixed concentration of biotinylated D-glucagon (100 nM) was immobilized on the streptavidin coated plates. A range of concentrations of soluble D-glucagon (0-1000 nM) was co-incubated with a fixed concentration of HEX-labeled D-form anti-glucagon aptamer (300 nM). Following washing, the total fluorescence of bound HEX-labeled D-form anti-glucagon aptamer was measured.

### 4.3.3 Results

The standard binding assay produced a functional standard curve where an increase in fluorescence intensity was measured with an increase in immobilized D-glucagon (Figure 4-3). However, no change in fluorescence was observed with increases in immobilized D-glucagon less than 100 nM. It was unclear whether the loaded amount of biotinylated D-glucagon represented the actual concentration of D-glucagon bound to the plates or if only a smaller fraction of the loaded D-glucagon was bound. A competition binding assay was used to generate a standard curve that would be representative of actual detectable concentrations of D-glucagon (Figure 4-4). In this assay, a decrease in fluorescence was observed with increasing concentrations of competing D-glucagon. Similar to the standard binding assay, no change in fluorescence was observed with increases in competing D-glucagon less than 100 nM.

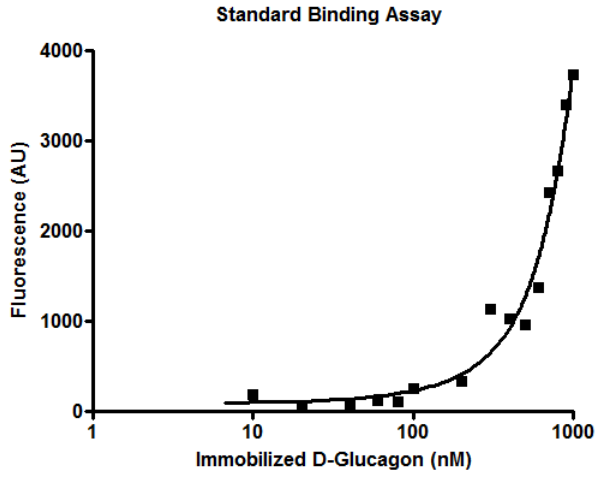


**Figure 4-3 Standard binding assay of HEX-labeled D-form aptamer for immobilized D-glucagon.** Data was fit using 4-parameter logistic regression.

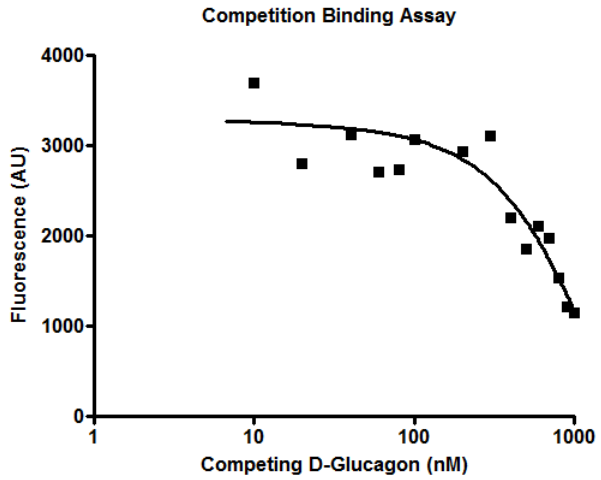


**Figure 4-4 Competition binding assay of soluble D-glucagon to competing with immobilized D-glucagon for HEX-labeled D-form aptamer.** Data was fit using 4-parameter logistic regression.

### 4.3.4 Discussion

The published spiegelmer was successfully incorporated into a quantitative assay for the detection of D-glucagon, suggesting that the original spiegelmer could similarly be used for the detection of L-glucagon. However, the limit of detection was approximately 100nM; about 2-3 magnitudes higher than expected, given the published $K_d$ of 6.3 nM. Ideally, a glucagon aptamer would have a $K_d$ in the picomolar range to be useful as a biosensor. This discrepancy in affinity may be due to the use of different stereoisomers of both the aptamers and their targets. Alternatively, the addition of a HEX fluorophore may interfere with binding. Base Pair Biotechnologies has been successful in developing a couple of glucagon aptamers with $K_d$ values of 108 and 185 nM. Current glucagon ELISA kits (RayBiotech) have a lower limit of detection around 30 fM, thus the aptamer-based quantitative assay described here and those aptamer developed by Base Pair Biotechnologies do not represent an advantage in sensitivity. However, use of the original L-form spiegelmer with an optimized fluorophore and linker may result in a

lower limit of detection in the low picomolar range for natural L-glucagon. This would enable it to be functionalized into a useful biosensor for more high throughput and real-time glucagon detection either in combination with surface plasmon resonance [260] or as a molecular aptamer beacon [261].

## 4.4 Single Molecule Detection of Epidermal Growth Factor Receptors on Exosomes

### 4.4.1 Introduction

Exosomes are small (30-100 nm) protein and nucleic acid rich vesicles comprised of a lipid bilayer that are released from a number of cell types. Originally, exosomes were thought to have little biological relevance. Recently however, exosomes have been shown to play an important role in cell-to-cell signaling and cell/stroma interactions in a number of physiologic and pathologic processes [262]. In cancer, exosomes contribute to the unique tumor microenvironment. Exosomes have been shown to promote tumor progression, metastasis, and chemoresistance through direct promotion of cell growth, stimulation of angiogenesis, activation of stromal fibroblasts to create a favorable extracellular matrix, while suppressing the host immune response [262,263]. Recently, exosomes have also been investigated as potential biomarkers [263]. Exosomal epidermal growth factor receptor (EGFR) expression as detected through ELISA was observed to be significantly higher in a number of cancer cases as compared to normal controls, indicating its possible use as a diagnostic or prognostic biomarker [264]. Additionally, exosomal EGFR signaling through Amphiregulin, an EGFR ligand, has been shown to contribute to tumor invasiveness [265]. To further study potential diagnostic/prognostic and pathologic roles that exosomal EGFR expression plays in cancer, exosomal EGFR expression was

assessed in collaboration with Robert J. Coffey, M.D. (Vanderbilt University, Department of Medicine).

### 4.4.2 Methods

Exosomes are smaller than the focal volume of a confocal microscope and are too small to be resolved. However, fluorescence intensity can still be used as a measure of the number of fluorescently labeled proteins on an exosome. For an exact quantification of the number of fluorescent molecules, this fluorescence intensity is correlated with a standard curve of fluorescence intensity of purified fluorophore of known concentrations. Exosomes were isolated from enhanced green fluorescent protein (EGFP) expressing cells, EGFP-tagged EGFR expressing cells, and unlabeled cells as previously described [265]. Exosomes were placed in PBS with 25 mM HEPES (pH 7.2) and imaged with appropriate excitation and spectral emission windows (LSM780; Carl Zeiss). A range of concentrations of purified EGFP was also imaged using the same excitation and detection settings. Maximum pixel intensity was measured for each exosome within a circular ROI. This was correlated with a standard curve of fluorescence intensity and EGFP concentration that was generated with purified EGFP to determine the concentration of EGFP per pixel and ultimately the number of EGFP-tagged EGFRs per exosome.

### 4.4.3 Results

Focal areas of increased fluorescence intensity were only visible from exosomes isolated from cells that expressed EFGP-tagged EGFR. Exosomes from cells that expressed free/untagged

EGFP and cells that did not express any fluorescent label did not produce any focal areas of increased fluorescence intensity (Figure 4-5).

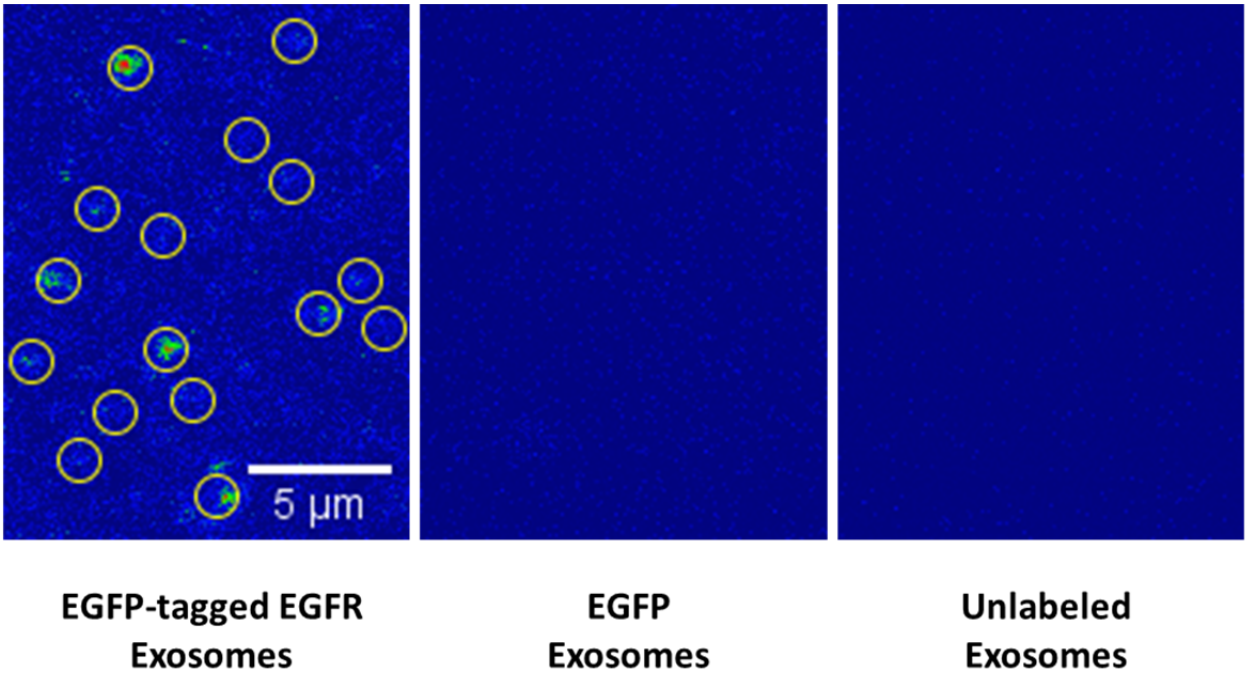


**Figure 4-5 Fluorescence intensity image of unresolved exosomes.** EGFP-tagged EGFR exosomes are highlighted by circular ROIs. Untagged EGFP and unlabeled exosomes do not produce and focal areas of increased fluorescence intensity.

After being correlated with the standard curve of fluorescence intensity of purified EGFP (Figure 4-6), the maximum pixel intensity for each exosome was compiled into a histogram of the distribution of EGFP molecules per exosome (Figure 4-7). The median number of EGFP-tagged EGFR molecules per exosome was found to be 2.7 ± 0.1.

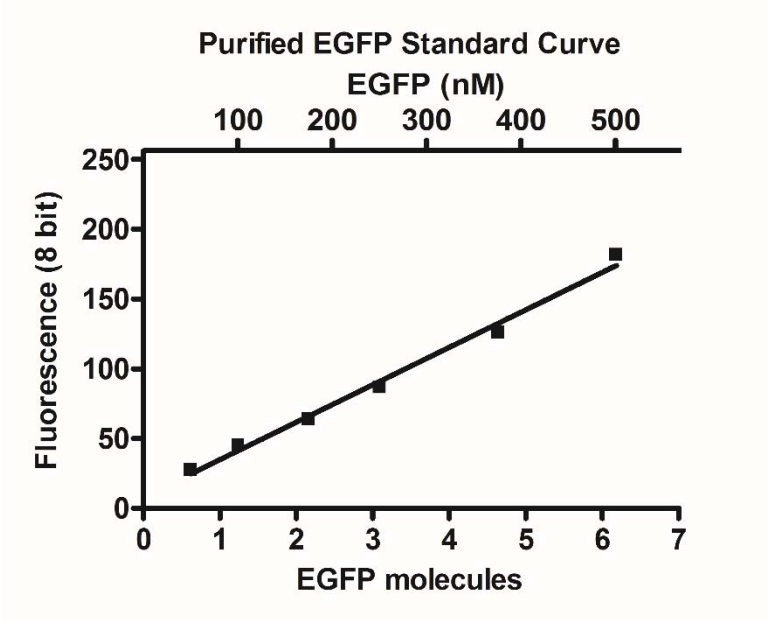


**Figure 4-6 Standard curve of fluorescence as a function of EGFP concentration and EGFP molecules per focal volume.** Linear regression was used to fit the standard curve ($R^2$ = 0.99).

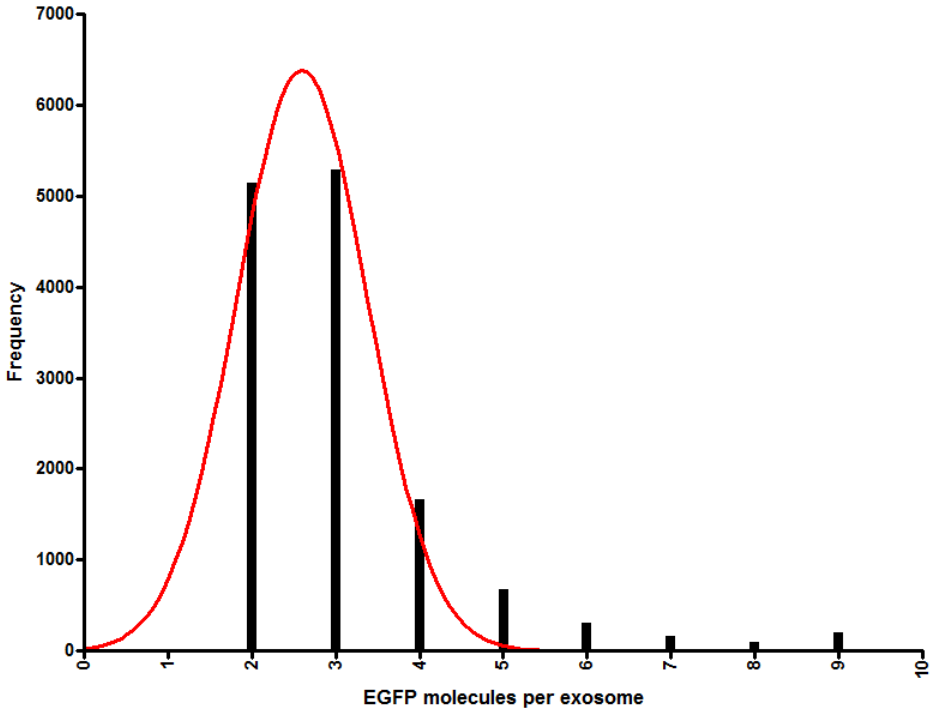


**Figure 4-7 Histogram of EGFP molecules per exosome.** The red line represents a Gaussian fit of the histogram, with a median of 2.7 ± 0.1 EGFP molecules per exosome. Data represents analysis of 13509 exosomes.

### 4.4.4 Discussion

Exosomes are below the resolution limit. However, using a fluorescently-labeled EGFR, fluorescence imaging was used to quantify the median number of EGFR molecules per exosome. Currently, the significance of this specific EGFR expression level remains unknown. As previously implicated, exosomal EGFR expression may serve as a biomarker for the diagnosis or prognosis of specific cancers [264]. Additionally, the expression of EGFR on exosomes may contribute to biologically significant EGFR signaling within the tumor microenvironment, regulating cell/stroma interactions.

## 4.5 Intravital Microscopy of C-peptide Secretion from β-cells

### 4.5.1 Introduction

C-peptide is a short 31 amino acid peptide fragment that is cleaved from pro-insulin during insulin biosynthesis. C-peptide was originally thought to be an inactive byproduct of insulin synthesis without a biological function. Due to its 1:1 stoichiometric co-secretion with insulin it has primarily been used as a biomarker for insulin secretion. Recently however, C-peptide has been shown to have a functional and beneficial role in preventing diabetic microvascular complications [266,267]. Due to its short half-life of approximately 30 minutes and lack of hepatic retention, C-peptide is a good marker for current total insulin secretion [266]. However, it cannot be used to study insulin secretion from individual islets or β-cells. Instead, intracellular $Ca^{2+}$, which is directly tied to insulin exocytosis, is often used as a surrogate for insulin secretion from islets and β-cells. Currently, direct visualization of insulin secretion is limited to viral transfection of fluorescent protein-labeled insulin. However, this method is limited by transfection efficiency and has limited utility *in vivo*. Here, I describe the work I performed

evaluating intravital secretion events from β-cells within live mice using a new EGFP-labeled C-peptide transgenic mouse in collaboration with Peter R. Arvan, M.D, Ph.D. (University of Michigan, Department of Internal Medicine).

### 4.5.2 Methods

EGFP-labeled C-peptide mice (hPro-CpepSfGFP) were provided by Dr. Arvan. Mice were anesthetized with ketamine/xylazine (80/20 mg/kg ip) prior to exteriorization of the pancreas. Mice were placed in custom plate with a coverslip insert. Pancreata were stretched across the coverslip and sandwiched under an appropriately spaced and weighted glass slide to minimize movement translated from the heart. Mice and exteriorized pancreata were maintained at 30-34°C using disposable iron oxidation heating pads. Glucose (1 g/kg) was administered via direct gastric injection and visualized islets were imaged every 2 seconds for 2 minutes. Imaging was performed using fluorescent confocal microscopy with appropriate excitation and spectral emission windows (LSM780; Carl Zeiss). Images were aligned based on cell morphology to restore a consistent field despite movement between and during frames.

### 4.5.3 Results

A small number of islets were located close enough to the surface of the pancreas to allow for visualization. A β-cell secretory event from one of these islets is shown in Figure 4-8. The secretory event is identified by a focal increase in fluorescence within the β-cell that quickly appears and disappears. This represents the trafficking of a secretory granule to the β-cell membrane, fusion with the membrane, and diffusion of the fluorescently labeled C-peptide.

The increase in local fluorescence intensity is observed between frames 12 and 13 and then fluorescence returns to baseline between frames 13 and 14.

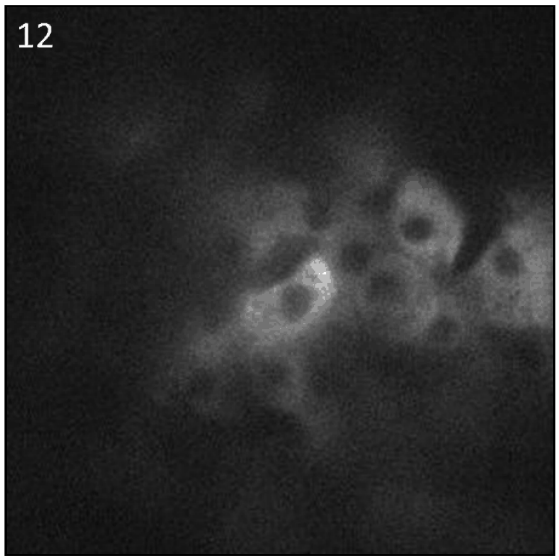


**Figure 4-8 Movie of EGFP-tagged C-peptide secretion event.** If viewing electronically, click the image above to play the movie. The secretion event is observed in frame 13. Frames 12 and 14 have been included to provide context.

A grid of ROIs was applied to the series of images to identify secretion events in an unbiased manner based on the mean fluorescence intensity of each grid box (Figure 4-9 left). Grid box 32 was identified to have a peak in fluorescence intensity at frame 13 that was 3 standard deviations above baseline. The nearby grid box 19 does not show any significant changes in fluorescence intensity.

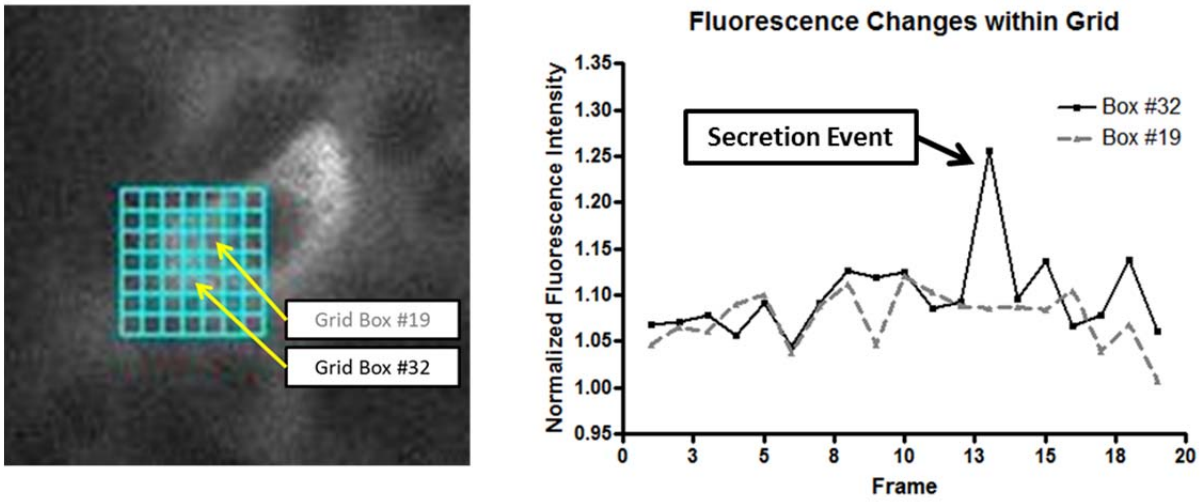


**Figure 4-9 Unbiased grid-based ROI identification of secretion event.** (Left) A grid of ROIs was placed over the aligned image series. (Right) Mean fluorescence intensity of grid boxes 19 and 32 over frames 1-19.

### 4.5.4 Discussion

A subcellularly resolved β-cell secretion event was recorded from an islet within a live mouse. Isolating the exteriorized pancreas away from the body results in improved stability, however it also results in a drop in pancreas temperature. Exocytosis from a number of different cell types has been shown to be highly temperature sensitive, with a steep drop-off of exocytosis events with a decrease in temperature [268–270]. Thus, a tighter maintenance of temperature closer to normal physiology might result in an increased number of observed secretory events. Previous attempts at fluorescently labeling C-peptide have resulted in fluorescent but non-functional secretory granules that are not secreted. Here, I validated a new EGFP-tagged C-peptide transgenic mouse through direct visualization of *in vivo* β-cell secretion. This EGFP-tagged C-peptide transgenic mouse is an important tool for the investigation of β-cell secretion that allows for the real-time analysis of individual secretory events from β-cells.

## 4.6 Temporal and Descriptive α-cell $Ca^{2+}$ Activity Dynamics in Islets

### 4.6.1 Introduction

Regulation of intracellular $Ca^{2+}$ activity is highly disputed within the α-cell field (discussed in 1.9.1 and 2.3.11). Many groups report that various measures of α-cell $Ca^{2+}$ activity are inhibited by elevated glucose and directly lead to glucose-inhibition of glucagon secretion [136,149,210,211]. However, my own data and data generated by previous members of the Piston lab show an increase in α-cell $Ca^{2+}$ activity (Figure 2-15 and [109]) or at least a lack of inhibition of α-cell $Ca^{2+}$ activity [126], suggesting that glucagon secretion is not dependent on, and can be decoupled from, intracellular $Ca^{2+}$ activity. In my own studies, only a small fraction of α-cells are active at low glucose (30-35% Figure 2-15). The underlying differences between this population of active α-cells and the population of inactive α-cells remain unknown. Further, it is unclear whether these two populations are composed of the same set of α-cells over a given period of time or if individual α-cells change between being active and inactive with a high frequency. This set of experiments was designed to assess whether or not individual α-cells remain consistently active or inactive over a long period of time and to provide insight into the heterogeneous nature of α-cell $Ca^{2+}$ activity.

### 4.6.2 Methods

RFP labeled mouse islets were isolated and cultured as previously described (2.2.2) [67,109]. Islets were stained with 4 μM Fluo4-AM (Life Technologies) for 30 minutes at room temperature. Islets were imaged within an environmentally controlled stage (37°C and 5% $CO_2$) in BMHH buffer with 1 mM glucose. Images were taken every 1 second for a 5 minute period every 30 minutes for 2 hours. Imaging was performed using fluorescent confocal microscopy with

appropriate excitation and spectral emission windows (LSM780; Carl Zeiss). α-cell $Ca^{2+}$ activity was defined by an increase in Fluo-4 intensity that was 3 standard deviations above baseline and further characterized as either a single burst or oscillation pattern.

### 4.6.3 Results

The percentage of α-cells displaying $Ca^{2+}$ activity remained constant across the 2 hour imaging period. However, the exact composition of these cells changed over the same period of time. Individual α-cells displaying $Ca^{2+}$ activity were found to have three distinct temporal $Ca^{2+}$ activity patterns. 21.4% of $Ca^{2+}$ active α-cells were found to be active throughout the entire 2 hour imaging period, 21.4% of $Ca^{2+}$ active α-cells were originally inactive but became active and stayed active for at least 1 hour until the end of the imaging period, and 57.1% of $Ca^{2+}$ active α-cells were found to switch between active and inactive states while not maintaining Ca2+ activity for longer than 30 minutes (Table 4-1).

| Always Active | Turn and Stay Active (> 1hr) | Switch Active and Inactive (< 30 min) |
|---|---|---|
| 21.4% (3 α-cells) | 21.4% (3 α-cells) | 57.1% (8 α-cells) |

**Table 4-1 α-cell temporal $Ca^{2+}$ activity patterns.** This table describes the breakdown of $Ca^{2+}$ active α-cells into three distinct temporal $Ca^{2+}$ activity patterns. Data are from a total of 14 α-cells that displayed $Ca^{2+}$ activity at any point during the imaging period.

Interestingly, the pattern of α-cell $Ca^{2+}$ activity (single bursts vs oscillations) was notably different between α-cells that were consistently active ('Always Active' and 'Turn and Stay Active' categories above) and those that switched between active and inactive states ('Switch Active and Inactive' category above). 100.0% of α-cells that fall into the 'Always Active' and

'Turn and Stay Active' categories displayed an oscillation pattern of $Ca^{2+}$ activity. Only 50% of α-cells in the 'Switch Active and Inactive' category displayed an oscillatory pattern during their time(s) of $Ca^{2+}$ activity. The rest of the α-cells within the 'Switch Active and Inactive' category displayed a single burst pattern (37.5%) or a mixed pattern (12.5%) during their time(s) of $Ca^{2+}$ activity (Table 4-2).

| | Always Active | Turn and Stay Active (> 1hr) | Switch Active and Inactive (< 30 min) |
|---|---|---|---|
| Oscillation Pattern | 100.0% (3 α-cells) | 100.0% (3 α-cells) | 50.0% (4 α-cells) |
| Single Burst Pattern | 0.0% | 0.0% | 37.5% (3 α-cells) |
| Mixed Pattern | 0.0% | 0.0% | 12.5% (1 α-cell) |

**Table 4-2 Descriptive α-cell $Ca^{2+}$ activity patterns.** This table describes the breakdown of descriptive $Ca^{2+}$ activity patterns within the temporal $Ca^{2+}$ activity categories described in Table 4-1. Data are from a total of 14 α-cells that displayed $Ca^{2+}$ activity at any point during the imaging period.

### 4.6.4 Discussion

α-cells are a heterogeneous population with regards to $Ca^{2+}$ activity. At any given time at low glucose, a portion of $Ca^{2+}$ active α-cells displays persistent $Ca^{2+}$ activity while another portion displays transient $Ca^{2+}$ activity. α-cells that display persistent $Ca^{2+}$ activity are characterized by an oscillatory pattern of $Ca^{2+}$ activity while α-cells that display transient $Ca^{2+}$ activity are characterized by oscillatory, single burst, or a mixed pattern of $Ca^{2+}$ activity. It remains unclear how these temporal or descriptive patterns of $Ca^{2+}$ activity correlate with glucagon secretion, as $Ca^{2+}$ activity is necessary for, but can be uncoupled from, glucagon secretion. Additionally, we currently lack a single-cell resolution method for the detection of glucagon secretion. The simplest explanation for the heterogeneity observed in α-cell $Ca^{2+}$ activity is a normal

distribution of α-cell excitability. In this model, α-cells (like β-cells [254]) have a distribution of excitability and thus would behave like dispersed or uncoupled β-cells [62,271] where only the most excitable cells display $Ca^{2+}$ activity at a given glucose threshold. Also in this model, transient α-cell $Ca^{2+}$ activity might be glucose independent or represent differences (cell-cell interactions) between currently active and inactive α-cells that occur on a faster time scale than protein expression regulated distribution of excitability. Despite its limited size, this set of experiments emphasizes the heterogeneous nature of α-cells and provides possible explanations for the discrepancies in α-cell $Ca^{2+}$ activity based on different definitions of activity, α-cell identification, and experimental protocols present in the literature.

# CHAPTER 5
# SIGNIFICANCE, FUTURE DIRECTIONS, AND EXPERIMENTS

## 5.1 Introduction

This chapter is a discussion of the future directions and experiments that I feel would best benefit the projects described in this dissertation. For the large part, the data presented in previous chapters represents the start of new projects rather than the continuation of previous or ongoing work. Thus, there still exist a number of unanswered questions regarding the novel regulators of glucagon secretion discussed in Chapter 2 and Chapter 3. This chapter is designed to address general directions for future investigation as well as provide specific and concrete experiments in a very candid manner.

## 5.2 Significance

The ultimate goal of the work presented here is to provide better treatment for the management of diabetes by addressing elevated and dysfunctional glucagon secretion. Numerous therapeutic strategies exist to lower blood-glucose levels; however the hyperglycemia of diabetes is largely managed by increasing available insulin. This strategy addresses the absolute or relative insulin deficiencies present in diabetes, but neglects the contribution that elevated glucagon secretion makes to the hyperglycemia of diabetes. Inhibiting glucagon secretion from α-cells directly addresses hyperglucagonemia associated hyperglycemia and provides an additional treatment strategy that can be combined with insulin-mediated strategies to better regulate blood-glucose in diabetic patients. Currently, pharmaceutical agents that inhibit glucagon secretion are limited to GLP-1 analogs. Identifying

new α-cell specific druggable targets to inhibit glucagon secretion will require a better understanding of how glucagon secretion is regulated. Presently, there is no consensus model for the regulation of glucagon secretion. Thus, increased investigation into the regulation of glucagon secretion is a high priority.

The work described here has contributed significantly to current models of regulated glucagon secretion and taken the field closer to the realization of a consensus model. Chapter 2 demonstrates the complex role that the islet environment plays in the regulation of glucagon secretion. Previous to this work, juxtacrine mediated regulation of glucagon secretion was nonexistent. The role of cell adhesion proteins in the regulation of glucagon secretion had previously been investigated, but the involvement of a robust juxtacrine signaling pathway such as the EphA/ephrin-A signaling pathway remained uninvestigated. The involvement of EphA/ephrin-A signaling has added a layer of complexity to current models of regulated glucagon secretion and serves to demonstrate the intricacy of regulating glucagon secretion. It has become increasingly apparent that the regulation of glucagon secretion cannot be explained by a single mechanism, but rather requires multiple parallel and converging signaling pathways. Continued investigation into juxtacrine and other mechanisms of regulated glucagon secretion are required for the comprehensive understanding of glucagon secretion necessary for efficient pharmaceutical targeting.

Additionally, the efforts described here have laid the groundwork for identifying two independent and novel α-cell specific targets for the inhibition of glucagon secretion. Chapter 3 demonstrates the existence of a potentially druggable signaling pathway that potently and selectively inhibits glucagon secretion without affecting insulin secretion. This is a completely

new endocrine role for BAT. BAT has never previously been shown or suggested to regulate islet hormone secretion. Discovering the identity of the unknown BAT secreted factor and mechanism by which it selectively inhibits glucagon secretion will provide a directly translatable lead compound and therapeutically targetable signaling pathway.

**5.3 Future Directions and Experiments – EphA/ephrin-A Regulation of Glucagon Secretion**

EphA/ephrin-A signaling had previously been shown to play a role in the glucose regulation of insulin secretion through EphA forward signaling-mediated inhibition of insulin secretion at low glucose and ephrin-A reverse signaling-mediated facilitation of insulin secretion at high glucose [85]. The work presented in Chapter 2 supports a similar role for EphA/ephrin-A mediated regulation of glucagon secretion. Through this work, EphA receptor forward signaling, specifically through EphA4, was shown to be essential for appropriate inhibition of glucagon secretion. However, our understanding of EphA/ephrin-A mediated glucagon secretion is far from complete. The model of EphA/ephrin-A mediated glucagon secretion stands to be improved through further understanding how EphA/ephrin-A signaling interacts with other known modulators of glucagon secretion. EphA/ephrin-A signaling has been shown to be involved in crosstalk with a number of other classes of signaling molecules that play a role in glucagon secretion including RTKs and numerous cell-adhesion and matrix associated proteins including integrins and connexins [86,195,272]. Depending on the specific experimental approach, modulation of EphA/ephrin-A signaling regulates glucagon secretion differently at high glucose. The reason for this discrepancy is currently unknown. Additionally, EphA forward signaling regulation of glucagon secretion was also shown to regulate the density of the F-actin network.

However, it is still unclear whether this is the direct mechanism of action as the data are correlative. Other intermediates involved in this pathway have yet to be identified. Discovering the answers to these unknowns would greatly bolster the EphA/ephrin-A signaling-mediated model of glucagon secretion. Additionally, this work has opened up a number of new and interesting questions not directly related to EphA/ephrin-A regulation of glucagon secretion.

### 5.3.1 Intermediate Glucose Concentrations

Stimulation of EphA receptor forward signaling has been shown to inhibit glucagon secretion at low glucose, while inhibition of EphA forward signaling has been shown to enhance glucagon secretion at low glucose. However, the role of EphA/ephrin-A signaling at high glucose is less clear. Data from certain experimental approaches (DPHBA treatment, EphA4$^{-/-}$ islets, sorted α-cells) support similar EphA receptor forward signaling mediated inhibition of glucagon secretion at both low and high glucose. However, data from other experimental approaches (EphA5-Fc and ephrin-A5-Fc treatment of islets) suggest that EphA receptor forward signaling has no effect or possibly oppositely regulates glucagon secretion at high glucose. Treating islets with ephrin-A5-Fc and EphA5-Fc (as in Figure 2-7) within a glucose dose response curve between 1 and 11 mM glucose would confirm any glucose dependent changes in EphA/ephrin-A regulation of glucagon secretion. Any potential glucose dependent change in the ephrin-A5-Fc and EphA5-Fc-induced effects on glucagon secretion might be due to either the glucose dependent nature of α-cell EphA regulation of glucagon secretion or an confounding islet effect on glucagon secretion caused by treatment with ephrin-A5-Fc and EphA5-Fc (such as perturbed insulin

secretion). The involvement of paracrine factors (insulin and somatostatin) acting to confound glucagon secretion at high glucose has been investigated, but was not found to be the cause of the change in effect on glucagon secretion observed with EphA5-Fc and ephrin-A5-Fc treatment at high glucose. Intermediate glucose concentrations would be beneficial in many the additional experiments described below. Once a mechanism of action is determined for EphA/ephrin-A regulation of glucagon secretion, intermediates in this pathway can be tracked with glucose to reveal if additional non EphA/ephrin-A pathways are convoluting glucagon secretion at high glucose. If the activation of intermediates changes with glucose similar to how glucagon tracks with glucose upon EphA5-Fc and ephrin-A5-Fc treatment, then the effective glucose dependent change is likely within the EphA/ephrin-A signaling pathway. However, if the intermediates are unaffected by glucose then there is likely an outside confounding factor that is affecting glucagon secretion independent of EphA/ephrin-A regulated glucagon secretion. Alternatively, EphA/ephrin-A regulation of glucagon secretion could occur through separate pathways at low and high glucose.

### 5.3.2 EphA/ephrin-A Mechanism of Action

EphA forward signaling-mediated changes in glucagon secretion are correlated with changes in F-actin density. Stimulation of EphA forward signaling causes a decrease in glucagon secretion and an increase in F-actin density. Inhibition of EphA forward signaling causes an enhancement in glucagon secretion and a decrease in F-actin density. These results are suggestive, but are not conclusive of actin remodeling as the mechanism for EphA forward signaling-mediated inhibition of glucagon secretion. Further, EphA/ephrin-A regulation of F-actin has only been

investigated at low glucose. Further studies should be conducted to determine whether this correlation, and possible mechanism, holds true at high glucose. Additionally, causal data are required to determine whether or not EphA forward signaling-mediated inhibition of glucagon secretion works through changes in F-actin density. If actin remodeling is responsible for the glucagon secretion effects of EphA/ephrin-A modulation, then treatment of islets or α-cells with agents to prevent actin polymerization (Latrunculins or Cytochalasins) should prevent ephrin-A5-Fc induced inhibition of glucagon secretion.

The identification and modulation of additional intermediates between the modulation of EphA/ephrin-A signaling and changes in F-actin density will further support an F-actin-mediated mechanism of action. EphA forward signaling-mediated changes in F-actin are often mediated through the Rho family of small GTPases [190]. Specifically, EphA4 has been shown to signal through RhoA [273,274]. However, EphA forward signaling has also been associated with several other Rho family GTPases, primarily Cdc42 and Rac1 [193,194,275]. It would be useful to see if the activity of these Rho family GTPases was altered by modulation of EphA/ephrin-A signaling. One method for this would be the use of a two-chain FRET-based RhoA biosensor developed by Klaus Hann, Ph.D. (University of North Carolina-Chapel Hill, Department of Pharmacology). Alternatively, simple immunofluorescence (islets or sorted α-cells) or western blotting (sorted α-cells) using antibodies specific to total and activated Rho family GTPases could be used.

### 5.3.3 Further *In Vivo* Studies

More work is needed to synchronize the *in vivo* and *ex vivo* observations from the EphA4$^{-/-}$ mouse line. Islets isolated from EphA4$^{-/-}$ mice displayed an increase in glucagon secretion that is expected given the lack of EphA4 forward signaling in α-cells. *In vivo* however, the EphA4$^{-/-}$ mouse line displayed a decrease in fasting glucagon secretion. These discrepancies may be better resolved with additional *in vivo* experiments.

Previous studies that have demonstrated changes in glucagon secretion due to alterations in F-actin have only shown significant changes in glucagon secretion at low glucose, while glucagon secretion at high glucose was not affected [80]. Thus, EphA/ephrin-A regulation of glucagon secretion my only occur at low glucose and may not be relevant at high glucose. Studying EphA4$^{-/-}$ mice under hypoglycemic conditions using a hyperinsulinemia hypoglycemic clamp may provide better data on how the loss of EphA4 affects glucagon secretion. Given that EphA7 is more highly expressed in α-cells than EphA4 and that EphA7 expression is increased in response to the loss of EphA4, it may be worth generating a new glucagon iCRE knock-in promotor driven floxed EphA4/7 mouse line. This α-cell specific knockout of EphA4$^{-/-}$ and EphA7$^{-/-}$ would have increased penetrance (100% of α-cells) and would be expected to have a more significant enhancement of glucagon secretion. However, further compensation from additional α-cell EphA receptors remains a possibility that would conceivably detract from the increased signal of the EphA4/7$^{-/-}$ mouse line.

Separate from EphA receptor knockout mice, ephrin-A5-Fc-based treatment of a type-1 diabetes mouse model would demonstrate the possible therapeutic applications ephrin-A mediated inhibition of glucagon secretion and the benefits of inhibiting glucagon secretion in diabetes. A type-1 diabetes mouse model (without β-cells) would be necessary since ephrin-

A5-Fc treatment also inhibits insulin secretion form *ex vivo* islets, thus any direct effect on insulin secretion would be minimal in a type-1 diabetes mouse model. A number of previous *in* vivo studies have administered ephrin-Fc chimeric proteins via intraperitoneal injection [276–278]. Mice would be treated with exogenous insulin or exogenous insulin plus ephrin-A5-Fc (or a cocktail of multiple ephrin-A-Fc chimeric proteins). A number of markers for diabetes could be tracked over time, including blood glucose and plasma glucagon. Mice receiving ephrin-A5 in addition to insulin would be expected to have better controlled blood glucose due to a reduction in glucagon secretion.

### 5.3.4 EphB/ephrin-B Regulation of Glucagon Secretion

Previous studies [85] and the work described in (Chapter 2) establish a role for EphA/ephrin-A signaling in the regulation of hormone secretion from pancreatic islets. However, any role for EphB/ephrin-B signaling in the regulation of islet hormone secretion remains unknown. Transcriptional analysis shows that both α- and β-cells express a number of EphB receptors and ephrin-B ligands in addition to EphA receptors and ephrin-A ligands [203–205]. EphB receptors and ephrin-B ligands are closely related to their EphA and ephrin-A counterparts. They have both been shown to regulated similar processes through similar mechanisms.

Eph/ephrin signaling is incredibly complex. If I were to start a new project investigating EphB/ephrin-B regulation of islet hormone secretion I would do a number of things to simplify the project. I do not feel that identification of specific EphB receptors or ephrin-B ligands is essential for these initial studies, especially given the promiscuous binding between the various ephrin-B ligands and EphB receptors. Thus, I would use a cocktail of various EphB-Fc and

ephrin-B-Fc chimeric proteins to stimulate islets while assessing hormone secretion. I feel this strategy would provide a robust response and any loss in resolution caused by differential signaling between the various EphB receptors and ephrin-B ligands in islets would be inconsequential. I feel that this study done at 1, 4, and 11 mM glucose would be sufficient to establish the effect of EphB/ephrin-B signaling on islet hormone secretion. Additional efforts could then be channeled into determining and confirming a mechanism of action and then applying EphB/ephrin-B to a more physiologically relevant model.

### 5.3.5 EphA/ephrin-A Regulation of Somatostatin Secretion

EphA/ephrin-A regulation of glucagon secretion appears to be independent of both insulin and somatostatin inhibition of glucagon secretion. The paracrine receptor antagonist experiments provide good evidence that EphA/ephrin-A mediated glucagon secretion does not occur through changes in paracrine signaling. Thus, modulation of EphA/ephrin-A signaling acts directly on α- and β-cells to regulation hormone secretion. Less is known about δ-cell EphA/ephrin-A expression that α- or β-cell EphA/ephrin-A expression, but it based on general similarities between all of the islet-cell types, δ-cell may express EphA receptors and/or ephrin-A ligands. Thus, EphA/ephrin-A regulation of somatostatin secretion is a very plausible.

## 5.4 Future Directions and Experiments – Brown Adipose Tissue Secreted Factor Regulation of Glucagon Secretion

Described in Chapter 3, BAT has been shown to secrete an unknown factor that acts on islets to robustly inhibit glucagon secretion. Inhibition of glucagon secretion by this unknown factor appears to be independent of insulin secretion. Although the identity of this factor remains

unknown, we have been able to discern a few key pieces of information about it. Importantly, this unknown factor is less than 3 kDa and is also secreted by a brown adipocyte cell line (nbat9). Identification of this unknown factor is the major goal in moving this project forward.

### 5.4.1 Identification of BAT Secreted Factor

Size fractionation of BAT conditioned buffer suggests that the active BAT secreted factor is less than 3 kDa. However, preliminary mass spectrometry analysis of this active fraction suggests that the current fractionalization methods are insufficient. Far too many candidate molecules are still present in the less than 3 kDa fraction to have any chance at identifying the active factor. Identification of the BAT secreted factor will require additional fractionation steps to narrow down the pool of potential candidate molecules that can be identified with mass spectrometry. Chromatographic separation of BAT conditioned buffer into distinct fractions is a simple method for separating a complex mixture into several smaller fractions. Currently, BAT conditioned buffer has been separated into a number of fractions using ion exchange chromatography using diethylaminoethyl cellulose column and a NaCl gradient. However, a number of other chromatography and column options are available. Given that neither the aqueous nor the nonaqueous fractions following Folch extraction of BAT conditioned buffer were active, the active factor may be hydrophilic in nature and thus separation might benefit from normal-phase or HILIC chromatography. Following improved fractionation and identification of the active fraction(s) via glucagon secretion assays, the active fraction would need to be analyzed by mass spectrometry to discover the group of potential candidate active factors. These factors could be ranked based on prior known activity and tested individually, or pooled together for more efficient validation of activity.

Proteinase treatment and/or heat inactivation of BAT conditioned buffer would also provide valuable information on the identity of the unknown BAT secreted factor. These experiments should be able to determine whether or not the unknown factor is a small protein/peptide. Initial experiments were conducted with an immobilized proteinase K. However, there were challenges in inactivating and removing proteinase K from the conditioned buffer which disturbed the treatment of islets and the analysis of glucagon secretion. A gentler proteinase such as trypsin that can be effectively inactivated by serine protease inhibitors might be more effective.

### 5.4.2 Mechanism of Action

The mechanism of action of the BAT secreted factor is currently unknown. Although identification of the BAT secreted factor might narrow down the possible mechanisms of action, identification of the factor is not necessary for determining its mechanism of action. In fact, determining a mechanism of action first may aid in the identification of the BAT secreted factor. The current method for determining the activity of a BAT conditioned buffer fraction is a static glucagon secretion assay that is very time and resource intensive. The process requires two days, not including islet isolation. Additionally, each set of islets can only be used to test a single fraction. Depending on the specific mechanism of action, it may be possible to use readout of these signaling processes as a surrogate for glucagon secretion. This process might result in false positives, but this should be a relatively small amount that could be additionally tested with traditional static glucagon secretion experiments. Inhibition of α-cell metabolism and $Ca^{2+}$ activity are prime examples of potential mechanisms that are both robust regulators

of glucagon secretion and easily assessed as surrogate readouts for glucagon secretion. α-cell metabolism can be easily assessed by NAD(P)H autofluorescence and α-cell $Ca^{2+}$ activity can be easily assessed using the calcium indicator Fluo-4. Currently, identifying a mechanism of action for the BAT secreted factor would be a process of trial and error of likely mechanisms, including α-cell cAMP levels and F-actin density along with α-cell metabolism and $Ca^{2+}$ activity. However, α-cell cAMP and F-actin cannot be easily used as readouts for BAT conditioned buffer activity. A cAMP FRET biosensor can be used to assess whether or not cAMP is affected by BAT conditioned buffer, but can be limited in its efficient delivery to α-cells. Fluorescently-tagged phalloidin and traditional immunofluorescence can be used to determine whether or not F-actin remodeling is involved in BAT conditioned buffer-mediated inhibition of glucagon secretion. However, this is would be even less time efficient than traditional glucagon secretion assays. Alternatively, islets could be transfected with EGFP-labeled actin to assess actin remodeling in live cells in a higher throughput manner. Without additional evidence or the identity of the BAT secreted factor testing other potential mechanisms of action besides those describe here may not be worthwhile.

## 5.5 Future Directions and Experiments – General α-cell Physiology

### 5.5.1 Long-term Study of α-cell $Ca^{2+}$ Activity at Low and High Glucose

Previous long-term studies of α-cell $Ca^{2+}$ activity (described in 4.6) were limited to 2 hours due to conflicts between tracking individual α-cell activity and the time and reloading limitations of Fluo-4 staining. Longer studies, possibly for several hours at a time over a few days, at both low and high glucose might provide additional insight into the $Ca^{2+}$ activity patterns observed in the

previous study. Additionally, it would be interesting to see whether the differences in $Ca^{2+}$ activity pattern (oscillations vs single bursts) could be correlated with α-cells position of proximity to δ-cell in addition to its correlation with consistent activity over time. These experiments could be accomplished through the use of genetic calcium sensor mice, specifically GCaMP6 expressing mice on a glucagon promoter. These α-cell specific GCaMP6 islets could be loaded into a simple single-chamber microfluidic device for extended imaging. Following imaging, islets could be fixed within the microfluidic device and islet additional islet cell types (specifically δ-cells) could be identified after the imaging protocol through immunofluorescence.

## REFERENCES


1. Gerich JE. Physiology of glucose homeostasis. *Diabetes, Obes Metab*. 2000;2(6):345-350. doi:10.1046/j.1463-1326.2000.00085.x.

2. Owen OE, Morgan a. P, Kemp HG, Sullivan JM, Herrera MG, Cahill GF. Brain metabolism during fasting. *J Clin Invest*. 1967;46(10):1589-1595. doi:10.1172/JCI105650.

3. Mitrakou a, Ryan C, Veneman T, et al. Hierarchy of glycemic thresholds for counterregulatory hormone secretion, symptoms, and cerebral dysfunction. *Am J Physiol*. 1991;260(1 Pt 1):E67-E74.

4. Cryer PE. Hypoglycemia, functional brain failure, and brain death. *J Clin Invest*. 2007;117(4):868-870. doi:10.1172/JCI31669.

5. Sheetz MJ, King GL. Molecular understanding of hyperglycemia's adverse effects for diabetic complications. *JAMA*. 2002;288(20):2579-2588. doi:10.1001/jama.288.20.2579.

6. Brownlee M. The pathobiology of diabetic complications. *Diabetes*. 2005;54(6):1615. doi:10.2337/diabetes.54.6.1615.

7. Scarlett JM, Schwartz MW. Gut-brain mechanisms controlling glucose homeostasis. *F1000Prime Rep*. 2015;7(January). doi:10.12703/P7-12.

8. Kowalski GM, Bruce CR. The regulation of glucose metabolism: implications and considerations for the assessment of glucose homeostasis in rodents. *AJP Endocrinol Metab*. 2014;307(10):E859-E871. doi:10.1152/ajpendo.00165.2014.

9. Schwartz MW, Seeley RJ, Tschöp MH, et al. Cooperation between brain and islet in glucose homeostasis and diabetes. *Nature*. 2013;503(7474):59-66. doi:10.1038/nature12709.

10. Meyer C, Dostou JM, Welle SL, Gerich JE. Role of human liver, kidney, and skeletal muscle in postprandial glucose homeostasis. *Am J Physiol Endocrinol Metab*. 2002;282(2):E419-E427. doi:10.1152/ajpendo.00032.2001.

11. Steiner DF, Chan SJ, Welsh JM, Kwok SC. Structure and evolution of the insulin gene. *Annu Rev Genet*. 1985;19(10):463-484. doi:10.1146/annurev.ge.19.120185.002335.

12. Warram J, Krolewski A. Joslin's Diabetes Mellitus: Edited by C. Ronald Kahn ... [et Al.]. In: *Epidemiology of Diabetes Mellitus*.; 2005:344-352.

13. Smith GD, Swenson DC, Dodson EJ, Dodson GG, Reynolds CD. Structural stability in the 4-zinc human insulin hexamer. *Proc Natl Acad Sci U S A*. 1984;81(22):7093-7097. doi:10.1073/pnas.81.22.7093.

14. Belfiore A, Frasca F, Pandini G, Sciacca L, Vigneri R. Insulin receptor isoforms and insulin receptor/insulin-like growth factor receptor hybrids in physiology and disease. *Endocr Rev*. 2009;30(6):586-623. doi:10.1210/er.2008-0047.

15. Baron V, Kaliman P, Gautier N, Van Obberghen E. The insulin receptor activation process involves localized conformational changes. *J Biol Chem*. 1992;267(32):23290-23294.

16. Shepherd PR, Withers DJ, Siddle K. Phosphoinositide 3-kinase: the key switch mechanism in insulin signalling. *Biochem J*. 1998;333 ( Pt 3:471-490.

17. Cheatham B, Vlahos CJ, Cheatham L, Wang L, Blenis J, Kahn CR. Phosphatidylinositol 3-kinase activation is required for insulin stimulation of pp70 S6 kinase, DNA synthesis, and glucose transporter translocation. *Mol Cell Biol*. 1994;14(7):4902-4911. doi:10.1128/MCB.14.7.4902.Updated.

18. Lawrence Jr. JC, Roach PJ. New insights into the role and mechanism of gycogen synthase activation by insulin. *Diabetes*. 1997;46(4):541-547.

19. Sun Y, Bilan PJ, Liu Z, Klip A. Rab8A and Rab13 are activated by insulin and regulate GLUT4 translocation in muscle cells. *Proc Natl Acad Sci U S A*. 2010;107(46):19909-19914. doi:10.1073/pnas.1009523107.

20. Chang L, Chiang S-H, Saltiel AR. Insulin Signaling and the Regulation of Glucose Transport. *Mol Med*. 2004;10(7-12):65-71. doi:10.2119/2005-00029.Saltiel.

21. Pilkis SJ, Granner DK. Molecular physiology of the regulation of hepatic gluconeogenesis and glycolysis. *Annu Rev Physiol*. 1992;54:885-909. doi:10.1146/annurev.ph.54.030192.004321.

22. Barthel A, Schmoll D. Novel concepts in insulin regulation of hepatic gluconeogenesis. *Am J Physiol Endocrinol Metab*. 2003;285(4):E685-E692. doi:10.1152/ajpendo.00253.2003.

23. Hall RK, Granner DK. Insulin regulates expression of metabolic genes through divergent signaling pathways. *J Basic Clin Physiol Pharmacol*. 1999;10(2):119-133. doi:10.1515/JBCPP.1999.10.2.119.

24. Furuta M, Zhou A, Webb G, et al. Severe Defect in Proglucagon Processing in Islet A-cells of Prohormone Convertase 2 Null Mice. *J Biol Chem*. 2001;276(29):27197-27202. doi:10.1074/jbc.M103362200.

25. Mojsov S, Heinrich G, Wilson IB, Ravazzola M, Orci L, Habener JF. Preproglucagon gene expression in pancreas and intestine diversifies at the level of post-translational processing. *J Biol Chem*. 1986;261(25):11880-11889.

26. Hers HG, Hue L. Gluconeogenesis and related aspects of glycolysis. *Annu Rev Biochem*. 1983;52:617-653. doi:10.1146/annurev.bi.52.070183.003153.

27. Morishige WK. *Endocrine Metabolism III: Adrenal Glands*. III.; 2002. doi:10.1016/b978-012095440-7/50034-2.

28. Morishige WK. *Endocrine Metabolism IV: Thyroid Gland*.; 2002. doi:10.1016/B978-012095440-7/50035-4.

29. Jolles S. Paul Langerhans. *J Clin Pathol*. 2002;55(4):243. doi:10.1136/jcp.55.4.243.

30. Kim A, Miller K, Jo J, Kilimnik G, Wojcik P, Hara M. Islet architecture: A comparative study. *Islets*. 2009;1(2):129-136. doi:10.4161/isl.1.2.9480.

31. Brissova M, Fowler MJ, Nicholson WE, et al. Assessment of human pancreatic islet architecture and composition by laser scanning confocal microscopy. *J Histochem Cytochem*. 2005;53(9):1087-1097. doi:10.1369/jhc.5C6684.2005.

32. Cabrera O, Berman DM, Kenyon NS, Ricordi C, Berggren P-O, Caicedo A. The unique cytoarchitecture of human pancreatic islets has implications for islet cell function. *Proc Natl Acad Sci U S A*. 2006;103(7):2334-2339. doi:10.1073/pnas.0510790103.

33. Wang X, Misawa R, Zielinski MC, et al. Regional Differences in Islet Distribution in the Human Pancreas - Preferential Beta-Cell Loss in the Head Region in Patients with Type 2 Diabetes. *PLoS One*. 2013;8(6):1-9. doi:10.1371/journal.pone.0067454.

34. Trimble ER, Renold a E. Ventral and dorsal areas of rat pancreas: islet hormone content and secretion. *Am J Physiol*. 1981;240(4):E422-E427.

35. Yaginuma N, Takahashi T, Saito K, Kyoguku M. *The Microvasculature of the Human Pancreas and Its Relation to Langerhans Islets and Lobules.* Pathology, research and practice 181, 77-84 (1986). doi:10.1016/S0344-0338(86)80191-1.

36. Ballian N, Brunicardi FC. Islet vasculature as a regulator of endocrine pancreas function. *World J Surg*. 2007;31(4):705-714. doi:10.1007/s00268-006-0719-8.

37. Nyman LR, Wells KS, Head WS, et al. Real-time, multidimensional in vivo imaging used to investigate blood flow in mouse pancreatic islets. *J Clin Invest*. 2008;118(11):3790-3797. doi:10.1172/JCI36209.

38. Nyman LR, Ford E, Powers AC, Piston DW. Glucose-dependent blood flow dynamics in murine pancreatic islets in vivo. *Am J Physiol Endocrinol Metab*. 2010;298(4):E807-E814. doi:10.1152/ajpendo.00715.2009.

39. Hellman B, Salehi A, Grapengiesser E, Gylfe E. Isolated mouse islets respond to glucose with an initial peak of glucagon release followed by pulses of insulin and somatostatin in antisynchrony with glucagon. *Biochem Biophys Res Commun*. 2012;417(4):1219-1223. doi:10.1016/j.bbrc.2011.12.113.

40. Hellman B, Salehi A, Gylfe E, Dansk H, Grapengiesser E. Glucose generates coincident insulin and somatostatin pulses and antisynchronous glucagon pulses from human pancreatic islets. *Endocrinology*. 2009;150(12):5334-5340. doi:10.1210/en.2009-0600.

41. Zhao F-Q, Keating AF. Functional properties and genomics of glucose transporters. *Curr Genomics*. 2007;8(2):113-128. doi:10.2174/138920207780368187.

42. De Vos a., Heimberg H, Quartier E, et al. Human and rat beta cells differ in glucose transporter but not in glucokinase gene expression. *J Clin Invest*. 1995;96(5):2489-2495. doi:10.1172/JCI118308.

43. Matschinsky FM, Ellerman JE. Metabolism of glucose in the islets of Langerhans. *J Biol Chem*. 1968;243(10):2730-2736.

44. Hellman B, Sehlin J, Täljedal IB. Evidence for mediated transport of glucose in mammalian pancreatic -cells. *Biochim Biophys Acta*. 1971;241(1):147-154. doi:10.1016/0005-2736(71)90312-9.

45. Matschinsky F, Liang Y, Kesavan P, et al. Glucose Sensor. *J Clin Investig*. 1993;92:2092-2098. doi:10.1172/JCI116809.

46. Matschinsky FM. Banting Lecture 1995. 2014:223-241.

47. Matschinsky FM, Klee P. Perspectives in Diabetes Glucokinase as Glucose Sensor and Metabolic Signal Generator in Pancreatic p-Cells and Hepatocytes. 1990;39(June):647-652.

48. Sener a., Malaisse WJ. Nutrient metabolism in islet cells. *Experientia*. 1984;40(10):1026-1035. doi:10.1007/BF01971448.

49. Schuit F, De Vos A, Farfari S, et al. Metabolic fate of glucose in purified islet cells. Glucose-regulated anaplerosis in β cells. *J Biol Chem*. 1997;272(30):18572-18579. doi:10.1074/jbc.272.30.18572.

50. Cook DL, Hales CN. Intracellular ATP directly blocks K+ channels in pancreatic B-cells. *Nature*. 311(5983):271-273. doi:10.1038/311271a0.

51. Henquin JC. D-glucose inhibits potassium efflux from pancreatic islet cells. *Nature*. 1978;271(5642):271-273. doi:10.1038/271271a0.

52. Ashcroft FM, Rorsman P. Electrophysiology of the pancreatic beta-cell. *Prog Biophys Mol Biol*. 1989;54(2):87-143. doi:10.1016/0079-6107(89)90013-8.

53. Cerasi E, Luft R, Efendic S. Decreased sensitivity of the pancreatic beta cells to glucose in prediabetic and diabetic subjects. A glucose dose-response study. *Diabetes*. 1972;21(4):224-234.

54. Curry DL, Bennett LL, Grodsky GM. Dynamics of insulin secretion by the perfused rat pancreas. *Endocrinology*. 1968;83(3):572-584. doi:10.1210/endo-83-3-572.

55. O'Connor MD, Landahl H, Grodsky GM. Comparison of storage- and signal-limited models of pancreatic insulin secretion. *Am J Physiol*. 1980;238(5):R378-R389.

56. Santos RM, Rosario LM, Nadal A, Garcia-Sancho J, Soria B, Valdeolmillos M. Widespread synchronous [Ca2+]i oscillations due to bursting electrical activity in single pancreatic islets. *Pflugers Arch*. 1991;418(4):417-422.

57. MacDonald PE, Rorsman P. Oscillations, intercellular coupling, and insulin secretion in pancreatic beta cells. *PLoS Biol*. 2006;4(2):e49. doi:10.1371/journal.pbio.0040049.

58. Henquin JC. Triggering and amplifying pathways of regulation of insulin secretion by glucose. *Diabetes*. 2000;49(11):1751-1760.

59. Aizawa T, Komatsu M, Asanuma N, Sato Y, Sharp GW. Glucose action "beyond ionic events" in the pancreatic beta cell. *Trends Pharmacol Sci*. 1998;19(12):496-499.

60. Zhang M, Houamed K, Kupershmidt S, Roden D, Satin LS. Pharmacological properties and functional role of Kslow current in mouse pancreatic beta-cells: SK channels contribute to Kslow tail current and modulate insulin secretion. *J Gen Physiol*. 2005;126(4):353-363. doi:10.1085/jgp.200509312.

61. Kanno T, Rorsman P, Göpel SO. Glucose-dependent regulation of rhythmic action potential firing in pancreatic β-cells by k ATP -channel modulation. *J Physiol*. 2002;545(2):501-507. doi:10.1113/jphysiol.2002.031344.

62. Ravier MA, Güldenagel M, Charollais A, et al. Loss of connexin36 channels alters beta-cell coupling, islet synchronization of glucose-induced Ca2+ and insulin oscillations, and basal insulin release. *Diabetes*. 2005;54(6):1798-1807.

63. Benninger RKP, Zhang M, Head WS, Satin LS, Piston DW. Gap junction coupling and calcium waves in the pancreatic islet. *Biophys J*. 2008;95(11):5048-5061. doi:10.1529/biophysj.108.140863.

64. Bergsten P, Grapengiesser E, Gylfe E, Tengholm A, Hellman B. Synchronous oscillations of cytoplasmic Ca2+ and insulin release in glucose-stimulated pancreatic islets. *J Biol Chem*. 1994;269(12):8749-8753.

65. Gylfe E, Tengholm a. Neurotransmitter control of islet hormone pulsatility. *Diabetes, Obes Metab*. 2014;16(S1):102-110. doi:10.1111/dom.12345.

66. Hellman B. Pulsatility of insulin release--a clinically important phenomenon. *Ups J Med Sci*. 2009;114(4):193-205. doi:10.3109/03009730903366075.

67. Schwetz T a, Ustione A, Piston DW. Neuropeptide Y and somatostatin inhibit insulin secretion through different mechanisms. *Am J Physiol Endocrinol Metab*. 2013;304(2):E211-E221. doi:10.1152/ajpendo.00374.2012.

68. Kawai K, Yokota C, Ohashi S, Watanabe Y, Yamashita K. Evidence that glucagon stimulates insulin secretion through its own receptor in rats. *Diabetologia*. 1995;38(3):274-276.

69. Persaud SJ, Asare-Anane H, Jones PM. Insulin receptor activation inhibits insulin secretion from human islets of Langerhans. *FEBS Lett*. 2002;510(3):225-228.

70. Khan FA, Goforth PB, Zhang M, Satin LS. Insulin activates ATP-sensitive K(+) channels in pancreatic beta-cells through a phosphatidylinositol 3-kinase-dependent pathway. *Diabetes*. 2001;50(10):2192-2198.

71. Elahi D, Nagulesparan M, Hershcopf RJ, et al. Feedback inhibition of insulin secretion by insulin: relation to the hyperinsulinemia of obesity. *N Engl J Med*. 1982;306(20):1196-1202. doi:10.1056/NEJM198205203062002.

72. Aspinwall CA, Lakey JR, Kennedy RT. Insulin-stimulated insulin secretion in single pancreatic beta cells. *J Biol Chem*. 1999;274(10):6360-6365.

73. Aspinwall C a, Qian WJ, Roper MG, Kulkarni RN, Kahn CR, Kennedy RT. Roles of insulin receptor substrate-1, phosphatidylinositol 3-kinase, and release of intracellular Ca2+ stores in insulin-stimulated insulin secretion in beta -cells. *J Biol Chem*. 2000;275(29):22331-22338. doi:10.1074/jbc.M909647199.

74. Kulkarni RN, Brüning JC, Winnay JN, Postic C, Magnuson MA, Kahn CR. Tissue-specific knockout of the insulin receptor in pancreatic beta cells creates an insulin secretory defect similar to that in type 2 diabetes. *Cell*. 1999;96(3):329-339.

75. Turcot-Lemay L, Lacy PE. Effect of glucose and anti-insulin serum on insulin released from adult rat isolated islets of Langerhans in long-term organ culture (fourteen days). *Diabetes*. 1975;24(7):658-663.

76. Schatz H, Pfeiffer EF. Release of immunoreactive and radioactively prelabelled endogenous (pro)-insulin from isolated islets of rat pancreas in the presence of exogenous insulin. *J Endocrinol*. 1977;74(2):243-249.

77. Stagner J, Samols E, Polonsky K, Pugh W. Lack of direct inhibition of insulin secretion by exogenous insulin in the canine pancreas. *J Clin Invest*. 1986;78(5):1193-1198. doi:10.1172/JCI112702.

78. Paulmann N, Grohmann M, Voigt J-P, et al. Intracellular serotonin modulates insulin secretion from pancreatic beta-cells by protein serotonylation. *PLoS Biol*. 2009;7(10):e1000229. doi:10.1371/journal.pbio.1000229.

79. Ustione A, Piston DW. Dopamine synthesis and D3 receptor activation in pancreatic β-cells regulates insulin secretion and intracellular [Ca(2+)] oscillations. *Mol Endocrinol*. 2012;26(11):1928-1940. doi:10.1210/me.2012-1226.

80. Olofsson CS, Håkansson J, Salehi A, et al. Impaired insulin exocytosis in neural cell adhesion molecule-/- mice due to defective reorganization of the submembrane F-actin network. *Endocrinology*. 2009;150(7):3067-3075. doi:10.1210/en.2008-0475.

81. Jaques F, Jousset H, Tomas A, et al. Dual effect of cell-cell contact disruption on cytosolic calcium and insulin secretion. *Endocrinology*. 2008;149(5):2494-2505. doi:10.1210/en.2007-0974.

82. Rogers GJ, Hodgkin MN, Squires PE. E-cadherin and cell adhesion: A role in architecture and function in the pancreatic islet. *Cell Physiol Biochem*. 2007;20(6):987-994. doi:10.1159/000110459.

83. Johansson JK, Voss U, Kesavan G, et al. N-cadherin is dispensable for pancreas development but required for beta-cell granule turnover. *Genesis*. 2010;48(6):374-381. doi:10.1002/dvg.20628.

84. Tyrberg B, Miles P, Azizian KT, et al. T-cadherin (Cdh13) in association with pancreatic β-cell granules contributes to second phase insulin secretion. *Islets*. 2011;3(6):327-337. doi:10.4161/isl.3.6.17705.

85. Konstantinova I, Nikolova G, Ohara-Imaizumi M, et al. EphA-Ephrin-A-mediated beta cell communication regulates insulin secretion from pancreatic islets. *Cell*. 2007;129(2):359-370. doi:10.1016/j.cell.2007.02.044.

86. Miao H, Wang B. EphA receptor signaling--complexity and emerging themes. *Semin Cell Dev Biol*. 2012;23(1):16-25. doi:10.1016/j.semcdb.2011.10.013.

87. Tolhurst G, Reimann F, Gribble FM. Nutritional regulation of glucagon-like peptide-1 secretion. *J Physiol*. 2009;587(Pt 1):27-32. doi:10.1113/jphysiol.2008.164012.

88. Moens K, Heimberg H, Flamez D, et al. Expression and functional activity of glucagon, glucagon-like peptide I, and glucose-dependent insulinotropic peptide receptors in rat pancreatic islet cells. *Diabetes*. 1996;45(2):257-261. doi:10.2337/diabetes.45.2.257.

89. Perley MJ, Kipnis DM. Plasma insulin responses to oral and intravenous glucose: studies in normal and diabetic sujbjects. *J Clin Invest*. 1967;46(12):1954-1962. doi:10.1172/JCI105685.

90. Campfield L a, Smith FJ. Neural control of insulin secretion: interaction of norepinephrine and acetylcholine. *Am J Physiol*. 1983;244(5):R629-R634.

91. Henquin JC, Nenquin M. The muscarinic receptor subtype in mouse pancreatic B-cells. *FEBS Lett*. 1988;236(1):89-92. doi:10.1016/0014-5793(88)80290-4.

92. Thorens B. Brain glucose sensing and neural regulation of insulin and glucagon secretion. *Diabetes, Obes Metab*. 2011;13(SUPPL. 1):82-88. doi:10.1111/j.1463-1326.2011.01453.x.

93. Berthoud HR, Bereiter DA, Trimble ER, Siegel EG, Jeanrenaud B. Cephalic phase, reflex insulin secretion neuroanatomical and physiological characterization. *Diabetologia*. 1981;20(1 Supplement):393-401. doi:10.1007/BF00254508.

94. Poretsky L. Principles of diabetes mellitus. *Princ Diabetes Mellit*. 2010:1-887. doi:10.1007/978-0-387-09841-8.

95. Cheng H, Straub SG, Sharp GWG. Protein acylation in the inhibition of insulin secretion by norepinephrine, somatostatin, galanin, and PGE2. *Am J Physiol Endocrinol Metab*. 2003;285(2):E287-E294. doi:10.1152/ajpendo.00535.2002.

96. Levin SR, Karam JH, Hane S, Grodsky GM, Forsham PH. Enhancement of arginine-induced insulin secretion in man by prior administration of glucose. *Diabetes*. 1971;20(3):171-176.

97. Hellman B, Sehlin J, Täljedal IB. Effects of glucose and other modifiers of insulin release on the oxidative metabolism of amino acids in micro-dissected pancreatic islets. *Biochem J*. 1971;123(4):513-521.

98. Malaisse WJ, Blachier F, Mourtada A, et al. Stimulus-secretion coupling of arginine-induced insulin release. Metabolism of L-arginine and L-ornithine in pancreatic islets. *Biochim Biophys Acta*. 1989;1013(2):133-143. doi:10.1016/0303-7207(89)90233-5.

99. Henquin JC, Meissner HP. Effects of amino acids on membrane potential and 86Rb+ fluxes in pancreatic beta-cells. *Am J Physiol*. 1981;240(3):E245-E252.

100. Charles S, Tamagawa T, Henquin JC. A single mechanism for the stimulation of insulin release and 86Rb+ efflux from rat islets by cationic amino acids. *Biochem J*. 1982;208(2):301-308.

101. Heimberg H, De Vos a, Pipeleers D, Thorens B, Schuit F. Differences in glucose transporter gene expression between rat pancreatic alpha- and beta-cells are correlated to differences in glucose transport but not in glucose utilization. *J Biol Chem*. 1995;270(15):8971-8975.

102. Heimberg H, De Vos A, Moens K, et al. The glucose sensor protein glucokinase is expressed in glucagon-producing alpha-cells. *Proc Natl Acad Sci U S A*. 1996;93(14):7036-7041.

103. Bokvist K, Olsen HL, Høy M, et al. Characterisation of sulphonylurea and ATP-regulated K+ channels in rat pancreatic A-cells. *Pflugers Arch*. 1999;438(4):428-436.

104. Gromada J, Bokvist K, Ding WG, et al. Adrenaline stimulates glucagon secretion in pancreatic A-cells by increasing the Ca2+ current and the number of granules close to the L-type Ca2+ channels. *J Gen Physiol*. 1997;110(3):217-228.

105. MacDonald PE, De Marinis YZ, Ramracheya R, et al. A K ATP channel-dependent pathway within alpha cells regulates glucagon release from both rodent and human islets of Langerhans. *PLoS Biol*. 2007;5(6):e143. doi:10.1371/journal.pbio.0050143.

106. Le Marchand SJ, Piston DW. Glucose decouples intracellular ca(2+) activity from glucagon secretion in mouse pancreatic islet alpha-cells. *PLoS One*. 2012;7(10):e47084. doi:10.1371/journal.pone.0047084.

107. Shiota C, Rocheleau J V, Shiota M, Piston DW, Magnuson M a. Impaired glucagon secretory responses in mice lacking the type 1 sulfonylurea receptor. *Am J Physiol Endocrinol Metab*. 2005;289(4):E570-E577. doi:10.1152/ajpendo.00102.2005.

108. Quoix N, Cheng-Xue R, Mattart L, et al. Glucose and pharmacological modulators of ATP-sensitive K+ channels control [Ca2+]c by different mechanisms in isolated mouse ??-cells. *Diabetes*. 2009;58(2):412-421. doi:10.2337/db07-1298.

109. Le Marchand SJ, Piston DW. Glucose suppression of glucagon secretion: metabolic and calcium responses from alpha-cells in intact mouse pancreatic islets. *J Biol Chem*. 2010;285(19):14389-14398. doi:10.1074/jbc.M109.069195.

110. Ishihara H, Maechler P, Gjinovci A, Herrera P-L, Wollheim CB. Islet beta-cell secretion determines glucagon release from neighbouring alpha-cells. *Nat Cell Biol*. 2003;5(4):330-335. doi:10.1038/ncb951.

111. Rorsman P, Braun M, Zhang Q. Regulation of calcium in pancreatic α- and β-cells in health and disease. *Cell Calcium*. 2012;51(3-4):300-308. doi:10.1016/j.ceca.2011.11.006.

112. Rorsman P, Salehi SA, Abdulkader F, Braun M, MacDonald PE. K(ATP)-channels and glucose-regulated glucagon secretion. *Trends Endocrinol Metab*. 2008;19(8):277-284. doi:10.1016/j.tem.2008.07.003.

113. Walker JN, Ramracheya R, Zhang Q, Johnson PR V, Braun M, Rorsman P. Regulation of glucagon secretion by glucose: paracrine, intrinsic or both? *Diabetes Obes Metab*. 2011;13 Suppl 1:95-105. doi:10.1111/j.1463-1326.2011.01450.x.

114. Salehi A, Vieira E, Gylfe E. Paradoxical stimulation of glucagon secretion by high glucose concentrations. *Diabetes*. 2006;55(8):2318-2323. doi:10.2337/db06-0080.

115. Ravier M a, Rutter G a. Glucose or insulin, but not zinc ions, inhibit glucagon secretion from mouse pancreatic alpha-cells. *Diabetes*. 2005;54(6):1789-1797.

116. Hauge-Evans AC, King AJ, Carmignac D, et al. Somatostatin secreted by islet delta-cells fulfills multiple roles as a paracrine regulator of islet function. *Diabetes*. 2009;58(2):403-411. doi:10.2337/db08-0792.

117. Egefjord L, Petersen AB, Rungby J. Zinc, alpha cells and glucagon secretion. *Curr Diabetes Rev*. 2010;6(1):52-57.

118. Wendt A, Birnir B, Buschard K, et al. Glucose inhibition of glucagon secretion from rat alpha-cells is mediated by GABA released from neighboring beta-cells. *Diabetes*. 2004;53(4):1038-1045.

119. Robertson RP, Zhou H, Slucca M. A role for zinc in pancreatic islet β-cell cross-talk with the α-cell during hypoglycaemia. *Diabetes Obes Metab*. 2011;13 Suppl 1:106-111. doi:10.1111/j.1463-1326.2011.01448.x.

120. Rorsman P, Berggren P-O, Bokvist K, et al. Glucose-inhibition of glucagon secretion involves activation of GABAA-receptor chloride channels. *Nature*. 1989;341:233-236.

121. Franklin I, Gromada J, Gjinovci A, Theander S, Wollheim CB. β-cell secretory products activate α-cell ATP-dependent potassium channels to inhibit glucagon release. *Diabetes*. 2005;54(6):1808-1815. doi:10.2337/diabetes.54.6.1808.

122. Prost A-L, Bloc A, Hussy N, Derand R, Vivaudou M. Zinc is both an intracellular and extracellular regulator of KATP channel function. *J Physiol*. 2004;559(Pt 1):157-167. doi:10.1113/jphysiol.2004.065094.

123. Bloc a, Cens T, Cruz H, Dunant Y. Zinc-induced changes in ionic currents of clonal rat pancreatic -cells: activation of ATP-sensitive K+ channels. *J Physiol*. 2000;529 Pt 3:723-734.

124. Strowski MZ, Parmar RM, Blake a D, Schaeffer JM. Somatostatin inhibits insulin and glucagon secretion via two receptors subtypes: an in vitro study of pancreatic islets from somatostatin receptor 2 knockout mice. *Endocrinology*. 2000;141(1):111-117.

125. Kawamori D, Kurpad AJ, Hu J, et al. Insulin signaling in alpha cells modulates glucagon secretion in vivo. *Cell Metab*. 2009;9(4):350-361. doi:10.1016/j.cmet.2009.02.007.

126. Elliott AD, Ustione A, Piston DW. Somatostatin and insulin mediate glucose-inhibited glucagon secretion in the pancreatic α-cell by lowering cAMP. *Am J Physiol - Endocrinol Metab*. 2015;308(2):E130-E143. doi:10.1152/ajpendo.00344.2014.

127. Unger RH, Orci L. Paracrinology of islets and the paracrinopathy of diabetes. *Proc Natl Acad Sci U S A*. 2010;107(37):16009-16012. doi:10.1073/pnas.1006639107.

128. Hardy a B, Serino a S, Wijesekara N, Chimienti F, Wheeler MB. Regulation of glucagon secretion by zinc: lessons from the β cell-specific Znt8 knockout mouse model. *Diabetes Obes Metab*. 2011;13 Suppl 1:112-117. doi:10.1111/j.1463-1326.2011.01451.x.

129. Braun M, Wendt A, Birnir B, et al. Regulated exocytosis of GABA-containing synaptic-like microvesicles in pancreatic beta-cells. *J Gen Physiol*. 2004;123(3):191-204. doi:10.1085/jgp.200308966.

130. Bailey SJ, Ravier M a, Rutter G a. Glucose-dependent regulation of gamma-aminobutyric acid (GABA A) receptor expression in mouse pancreatic islet alpha-cells. *Diabetes*. 2007;56(2):320-327. doi:10.2337/db06-0712.

131. Ma X, Zhang Y, Gromada J, et al. Glucagon stimulates exocytosis in mouse and rat pancreatic alpha-cells by binding to glucagon receptors. *Mol Endocrinol*. 2005;19(1):198-212. doi:10.1210/me.2004-0059.

132. Orci L, Malaisse-Lagae F, Ravazzola M, et al. A morphological basis for intercellular communication between alpha- and beta-cells in the endocrine pancreas. *J Clin Invest*. 1975;56(4):1066-1070. doi:10.1172/JCI108154.

133. Michaels RL, Sheridan JD. Islets of Langerhans: dye coupling among immunocytochemically distinct cell types. *Science*. 1981;214(4522):801-803. doi:10.1126/science.6117129.

134. Meda P, Santos RM, Atwater I. Direct identification of electrophysiologically monitored cells within intact mouse islets of Langerhans. *Diabetes*. 1986;35(2):232-236. doi:10.2337/diabetes.35.2.232.

135. Göpel S, Kanno T, Barg S, Galvanovskis J, Rorsman P. Voltage-gated and resting membrane currents recorded from B-cells in intact mouse pancreatic islets. *J Physiol*. 1999;521 Pt 3:717-728. doi:10.1111/j.1469-7793.1999.00717.x.

136. Nadal A, Quesada I, Soria B. Homologous and heterologous asynchronicity between identified α-, β- and δ-cells within intact islets of Langerhans in the mouse. *J Physiol*. 1999;517(1):85-93. doi:10.1111/j.1469-7793.1999.0085z.x.

137. Tian G, Sandler S, Gylfe E, Tengholm A. Glucose- and hormone-induced cAMP oscillations in α- and β-cells within intact pancreatic islets. *Diabetes*. 2011;60(5):1535-1543. doi:10.2337/db10-1087.

138. Gromada J, Franklin I, Wollheim CB. Alpha-cells of the endocrine pancreas: 35 years of research but the enigma remains. *Endocr Rev*. 2007;28(1):84-116. doi:10.1210/er.2006-0007.

139. Quesada I, Tudurí E, Ripoll C, Nadal A. Physiology of the pancreatic alpha-cell and glucagon secretion: role in glucose homeostasis and diabetes. *J Endocrinol*. 2008;199(1):5-19. doi:10.1677/JOE-08-0290.

140. Hong J, Jeppesen PB, Nordentoft I, Hermansen K. Fatty acid-induced effect on glucagon secretion is mediated via fatty acid oxidation. *Diabetes Metab Res Rev*. 2007;23(3):202-210. doi:10.1002/dmrr.663.

141. Heller RS, Kieffer TJ, Habener JF. Insulinotropic glucagon-like peptide I receptor expression in glucagon-producing alpha-cells of the rat endocrine pancreas. *Diabetes*. 1997;46(5):785-791. doi:10.2337/diabetes.46.5.785.

142. Tornehave D, Kristensen P, Rømer J, Knudsen LB, Heller RS. Expression of the GLP-1 receptor in mouse, rat, and human pancreas. *J Histochem Cytochem*. 2008;56(9):841-851. doi:10.1369/jhc.2008.951319.

143. De Heer J, Rasmussen C, Coy DH, Holst JJ. Glucagon-like peptide-1, but not glucose-dependent insulinotropic peptide, inhibits glucagon secretion via somatostatin (receptor subtype 2) in the perfused rat pancreas. *Diabetologia*. 2008;51(12):2263-2270. doi:10.1007/s00125-008-1149-y.

144. Meier JJ, Gallwitz B, Siepmann N, et al. Gastric inhibitory polypeptide (GIP) dose-dependently stimulates glucagon secretion in healthy human subjects at euglycaemia. *Diabetologia*. 2003;46(6):798-801. doi:10.1007/s00125-003-1103-y.

145. Chia CW, Carlson OD, Kim W, et al. *Exogenous Glucose-Dependent Insulinotropic Polypeptide Worsens Post Prandial Hyperglycemia in Type 2 Diabetes.*; 2009. doi:10.2337/db08-0958.

146. Holst JJ, Schaffalitzky de Muckadell OB, Fahrenkrug J. Nervous control of pancreatic exocrine secretion in pigs. *Acta Physiol Scand*. 1979;105(1):33-51. doi:10.1111/j.1748-1716.1979.tb06312.x.

147. Ahrén B. Autonomic regulation of islet hormone secretion--implications for health and disease. *Diabetologia*. 2000;43(4):393-410. doi:10.1007/s001250051322.

148. Bloom SR, Edwards a V. Pancreatic endocrine responses to stimulation of the peripheral ends of the vagus nerves in conscious calves. *J Physiol*. 1981;315:31-41.

149. Berts a, Gylfe E, Hellman B. Cytoplasmic Ca2+ in glucagon-producing pancreatic alpha-cells exposed to carbachol and agents affecting Na+ fluxes. *Endocrine*. 1997;6(1):79-83. doi:10.1007/BF02738806.

150. Godoy-Matos AF. The role of glucagon on type 2 diabetes at a glance. *Diabetol Metab Syndr*. 2014;6(1):91. doi:10.1186/1758-5996-6-91.

151. Mitrakou A, Kelley D, Mokan M, et al. Role of reduced suppression of glucose production and diminished early insulin release in impaired glucose tolerance. *N Engl J Med*. 1992;326(1):22-29. doi:10.1056/NEJM199201023260104.

152. Shah P, Vella A, Basu A, Basu R, Schwenk WF, Rizza R a. Lack of suppression of glucagon contributes to postprandial hyperglycemia in subjects with type 2 diabetees mellitus. *J Clin Endocrinol Metab*. 2000;85(11):4053-4059. doi:10.1210/jc.85.11.4053.

153. Classification I. Standards of medical care in diabetes-2014. *Diabetes Care*. 2014;37(SUPPL.1):14-80. doi:10.2337/dc14-S014.

154. Diabetes DOF. Diagnosis and classification of diabetes mellitus. *Diabetes Care*. 2010;33(SUPPL. 1). doi:10.2337/dc10-S062.

155. American Diabetes Association. National Diabetes Statistics Report , 2014 Estimates of Diabetes and Its Burden in the Epidemiologic estimation methods. *Natl Diabetes Stat Rep*. 2014:2009-2012.

156. Boyle JP, Thompson TJ, Gregg EW, Barker LE, Williamson DF. Projection of the year 2050 burden of diabetes in the US adult population: dynamic modeling of incidence, mortality, and prediabetes prevalence. *Popul Health Metr*. 2010;8(1):29. doi:10.1186/1478-7954-8-29.

157. Economic costs of diabetes in the U.S. In 2007. *Diabetes Care*. 2008;31(3):596-615. doi:10.2337/dc08-9017.

158. Xu J, Kochanek KD, Murphy SL, Tejada-Vera B. National Vital Statistics Reports Deaths: Final Data for 2007. *Statistics (Ber)*. 2010;58(19):135.

159. Gale E a M. The rise of childhood type 1 diabetes in the 20th century. *Diabetes*. 2002;51(12):3353-3361. doi:10.2337/diabetes.51.12.3353.

160. Tanaka S, Kobayashi T, Momotsu T. A novel subtype of type 1 diabetes mellitus. *N Engl J Med*. 2000;342(24):1835-1837. doi:10.1056/NEJM200006153422413.

161. Joslin EP. *The Treatment of Diabetes Mellitus with Observations Upon the Disease Based Upon Thirteen Hundred Cases*. 2nd Editio. Philadelphia and New York: Lea & Febiger; 1917.

162. Bliss M. Rewriting medical history: Charles best and the banting and best myth. *J Hist Med Allied Sci*. 1993;48(3):253-274. doi:10.1093/jhmas/48.3.253.

163. Skyler JS. Effects of Glycemic Control on Diabetes Complications and on the Prevention of Diabetes. *Clin Diabetes*. 2004;22(4):162-166. doi:10.2337/diaclin.22.4.162.

164. *The Effect of Intensive Treatment of Diabetes on the Development and Progression of Long-Term Complications in Insulin-Dependent Diabetes Mellitus. The Diabetes Control and Complications Trial Research Group.*; 1993. doi:10.1056/NEJM199309303291401.

165. Schiller JS, Lucas JW, Peregoy J a. Summary health statistics for U.S. adults: National Health Interview Survey, 2011. *Vital Health Stat 10*. 2012;10(256).

166. Weyer C, Bogardus C, Mott DM, Pratley RE. The natural history of insulin secretory dysfunction and insulin resistance in the pathogenesis of type 2 diabetes mellitus. *J Clin Invest*. 1999;104(6):787-794. doi:10.1172/JCI7231.

167. Prentki M, Nolan CJ. Islet β cell failure in type 2 diabetes. *J Clin Invest*. 2006;116(7):1802-1812. doi:10.1172/JCI29103.

168. Donath MY, Ehses JA, Maedler K, et al. Mechanisms of β-cell death in type 2 diabetes. *Diabetes*. 2005;54(SUPPL. 2):S97-S107. doi:10.2337/diabetes.54.suppl_2.S108.

169. Rifkin H, Porte D, Gallon DJ. Ellenberg and Rifkin's Diabetes Mellitus. *Endocrinologist*. 1992;2(2):139-140. doi:10.1097/00019616-199203000-00013.

170. Barnett AH, Eff C, Leslie RD, Pyke DA. Diabetes in identical twins. A study of 200 pairs. *Diabetologia*. 1981;20(2):87-93. doi:10.1007/BF00262007.

171. Carter JS, Pugh J a, Monterrosa a. Non-insulin-dependent diabetes mellitus in minorities in the United States. *Ann Intern Med*. 1996;125(3):221-232.

172. Harris MI, Flegal KM, Cowie CC, et al. Prevalence of diabetes, impaired fasting glucose, and impaired glucose tolerance in U.S. adults. The Third National Health and Nutrition Examination Survey, 1988-1994. *Diabetes Care*. 1998;21(4):518-524. doi:10.2337/diacare.21.4.518.

173. Sladek R, Rocheleau G, Rung J, et al. A genome-wide association study identifies novel risk loci for type 2 diabetes. *Nature*. 2007;445(7130):881-885. doi:10.1038/nature05616.

174. Sullivan PW, Morrato EH, Ghushchyan V, Wyatt HR, Hill JO. Obesity, inactivity, and the prevalence of diabetes and diabetes-related cardiovascular comorbidities in the U.S. 2000-2002. *Diabetes Care*. 2005;28(7):1599-1603. doi:10.2337/diacare.28.7.1599.

175. Shoelson SE, Lee J, Goldfine AB. Inflammation and insulin resistance. *J Clin Invest*. 2006;116(7):1793-1801. doi:10.1172/JCI29069.

176. Kirpichnikov D, McFarlane SI, Sowers JR. Metformin: An update. *Ann Intern Med*. 2002;137(1):25-33. doi:10.1054/jcaf.2003.36.

177. Aronoff SL, Berkowitz K, Shreiner B, Want L. Glucose Metabolism and Regulation: Beyond Insulin and Glucagon. *Diabetes Spectr*. 2004;17(3):183-190. doi:10.2337/diaspect.17.3.183.

178. Unger RH, Orci L. Glucagon and the A cell: physiology and pathophysiology (first two parts). *N Engl J Med*. 1981;304(25):1518-1524. doi:10.1056/NEJM198106183042504.

179. Unger RH, Orci L. Glucagon and the A cell: physiology and pathophysiology (second of two parts). *N Engl J Med*. 1981;304(26):1575-1580. doi:10.1056/NEJM198106183042504.

180. Unger RH, Aguilar-Parada E, Müller W a, Eisentraut a M. Studies of pancreatic alpha cell function in normal and diabetic subjects. *J Clin Invest*. 1970;49(4):837-848. doi:10.1172/JCI106297.

181. Unger RH, Orci L. The essential role of glucagon in the pathogenesis of diabetes mellitus. *Lancet*. 1975;1(7897):14-16. doi:10.1016/S0140-6736(75)92375-2.

182. Gosmanov NR, Szoke E, Israelian Z, et al. Role of the decrement in intraislet insulin for the glucagon response to hypoglycemia in humans. *Diabetes Care*. 2005;28(5):1124-1131. doi:10.2337/diacare.28.5.1124.

183. Raju B, Cryer PE. Loss of the decrement in intraislet insulin plausibly explains loss of the glucagon response to hypoglycemia in insulin-deficient diabetes: Documentation of the intraislet insulin hypothesis in humans. *Diabetes*. 2005;54(3):757-764. doi:10.2337/diabetes.54.3.757.

184. Lee Y, Wang M-Y, Du XQ, Charron MJ, Unger RH. Glucagon receptor knockout prevents insulin-deficient type 1 diabetes in mice. *Diabetes*. 2011;60(2):391-397. doi:10.2337/db10-0426.

185. Yu X, Park B-H, Wang M-Y, Wang Z V, Unger RH. Making insulin-deficient type 1 diabetic rodents thrive without insulin. *Proc Natl Acad Sci U S A*. 2008;105(37):14070-14075. doi:10.1073/pnas.0806993105.

186. Wang M, Chen L, Clark GO, et al. Leptin therapy in insulin-deficient type I diabetes. *Proc Natl Acad Sci U S A*. 2010;107(11):4813-4819. doi:10.1073/pnas.0909422107.

187. Gunawardana SC, Piston DW. Reversal of type 1 diabetes in mice by brown adipose tissue transplant. *Diabetes*. 2012;61(3):674-682. doi:10.2337/db11-0510.

188. Christensen M, Bagger JI, Vilsbøll T, Knop FK. The alpha-cell as target for type 2 diabetes therapy. *Rev Diabet Stud*. 2011;8(3):369-381. doi:10.1900/RDS.2011.8.369.

189. Hirai H, Maru Y, Hagiwara K, Nishida J, Takaku F. A novel putative tyrosine kinase receptor encoded by the eph gene. *Science*. 1987;238(4834):1717-1720. doi:10.1126/science.2825356.

190. Boyd AW, Bartlett PF, Lackmann M. Therapeutic targeting of EPH receptors and their ligands. *Nat Rev Drug Discov*. 2014;13(1):39-62. doi:10.1038/nrd4175.

191. Pasquale EB. Eph receptors and ephrins in cancer: bidirectional signalling and beyond. *Nat Rev Cancer*. 2010;10(3):165-180. doi:10.1038/nrc2806.

192. Flanagan JG, Vanderhaeghen P. The ephrins and Eph receptors in neural development. *Annu Rev Neurosci*. 1998;21:309-345. doi:10.1146/annurev.neuro.21.1.309.

193. Lai K-O, Ip NY. Synapse development and plasticity: roles of ephrin/Eph receptor signaling. *Curr Opin Neurobiol*. 2009;19(3):275-283. doi:10.1016/j.conb.2009.04.009.

194. Pitulescu ME, Adams RH. Eph/ephrin molecules--a hub for signaling and endocytosis. *Genes Dev*. 2010;24(22):2480-2492. doi:10.1101/gad.1973910.

195. Arvanitis D, Davy A. Eph/ephrin signaling: networks. *Genes Dev*. 2008;22(4):416-429. doi:10.1101/gad.1630408.

196. Nikolov DB, Xu K, Himanen JP. Eph/ephrin recognition and the role of Eph/ephrin clusters in signaling initiation. *Biochim Biophys Acta - Proteins Proteomics*. 2013;1834(10):2160-2165. doi:10.1016/j.bbapap.2013.04.020.

197. Freywald A, Sharfe N, Roifman CM. The kinase-null EphB6 receptor undergoes transphosphorylation in a complex with EphB1. *J Biol Chem*. 2002;277(6):3823-3828. doi:10.1074/jbc.M108011200.

198. Janes PW, Griesshaber B, Atapattu L, et al. Eph receptor function is modulated by heterooligomerization of A and B type Eph receptors. *J Cell Biol*. 2011;195(6):1033-1045. doi:10.1083/jcb.201104037.

199. Wimmer-Kleikamp SH, Janes PW, Squire A, Bastiaens PIH, Lakmann M. Recruitment of Eph receptors into signaling clusters does not require ephrin contact. *J Cell Biol*. 2004;164(5):661-666. doi:10.1083/jcb.200312001.

200. Gerlai R. Eph receptors and neural plasticity. *Nat Rev Neurosci*. 2001;2(3):205-209. doi:10.1038/35058582.

201. Quoix N, Cheng-Xue R, Guiot Y, Herrera PL, Henquin J-C, Gilon P. The GluCre-ROSA26EYFP mouse: a new model for easy identification of living pancreatic alpha-cells. *FEBS Lett*. 2007;581(22):4235-4240. doi:10.1016/j.febslet.2007.07.068.

202. Bowe JE, Franklin ZJ, Hauge-Evans a. C, King a. J, Persaud SJ, Jones PM. METABOLIC PHENOTYPING GUIDELINES: Assessing glucose homeostasis in rodent models. *J Endocrinol*. 2014;222(3):G13-G25. doi:10.1530/JOE-14-0182.

203. Dorrell C, Schug J, Lin CF, et al. Transcriptomes of the major human pancreatic cell types. *Diabetologia*. 2011;54(11):2832-2844. doi:10.1007/s00125-011-2283-5.

204. Ku GM, Kim H, Vaughn IW, et al. Research resource: RNA-Seq reveals unique features of the pancreatic β-cell transcriptome. *Mol Endocrinol*. 2012;26(10):1783-1792. doi:10.1210/me.2012-1176.

205. Blodgett DM, Nowosielska A, Afik S, et al. Novel Observations from Next Generation RNA Sequencing of Highly Purified Human Adult and Fetal Islet Cell Subsets. *Diabetes*. 2015:db150039. doi:10.2337/db15-0039.

206. Noberini R, Koolpe M, Peddibhotla S, et al. Small molecules can selectively inhibit ephrin binding to the EphA4 and EphA2 receptors. *J Biol Chem*. 2008;283(43):29461-29472. doi:10.1074/jbc.M804103200.

207. Tomas A, Yermen B, Min L, Pessin JE, Halban PA. Regulation of pancreatic beta-cell insulin secretion by actin cytoskeleton remodelling: role of gelsolin and cooperation with the MAPK signalling pathway. *J Cell Sci*. 2006;119(Pt 10):2156-2167. doi:10.1242/jcs.02942.

208. Orci L, Gabbay KH, Malaisse WJ. Pancreatic beta-cell web: its possible role in insulin secretion. *Science*. 1972;175(26):1128-1130.

209. Olsen HL, Theander S, Bokvist K, Buschard K, Wollheim CB, Gromada J. Glucose stimulates glucagon release in single rat alpha-cells by mechanisms that mirror the stimulus-secretion coupling in beta-cells. *Endocrinology*. 2005;146(11):4861-4870. doi:10.1210/en.2005-0800.

210. Quesada I, Nadal a, Soria B. Different effects of tolbutamide and diazoxide in alpha, beta-, and delta-cells within intact islets of Langerhans. *Diabetes*. 1999;48(12):2390-2397. doi:10.2337/diabetes.48.12.2390.

211. Quesada I, Todorova MG, Alonso-Magdalena P, et al. Glucose induces opposite intracellular Ca2+ concentration oscillatory patterns in identified {alpha}- and β-cells within intact human islets of Langerhans. *Diabetes*. 2006;55(9):2463-2469. doi:10.2337/db06-0272.

212. Gylfe E, Gilon P. Glucose regulation of glucagon secretion. *Diabetes Res Clin Pract*. 2014;103(1):1-10. doi:10.1016/j.diabres.2013.11.019.

213. Del Prato S, Castellino P, Simonson DC, DeFronzo R a. Hyperglucagonemia and insulin-mediated glucose metabolism. *J Clin Invest*. 1987;79(2):547-556. doi:10.1172/JCI112846.

214. Cannon B. Brown Adipose Tissue: Function and Physiological Significance. *Physiol Rev*. 2004;84(1):277-359. doi:10.1152/physrev.00015.2003.

215. Cinti S. The adipose organ: morphological perspectives of adipose tissues. *Proc Nutr Soc*. 2001;60(3):319-328. doi:10.1079/PNS200192.

216. Diaz MB, Herzig S, Vegiopoulos A. Thermogenic adipocytes: From cells to physiology and medicine. *Metabolism*. 2014;63(10):1238-1249. doi:10.1016/j.metabol.2014.07.002.

217. Lidell ME, Betz MJ, Enerbäck S. Brown adipose tissue and its therapeutic potential. *J Intern Med*. 2014. doi:10.1111/joim.12255.

218. Heaton JM. The distribution of brown adipose tissue in the human. *J Anat*. 1972;112(Pt 1):35-39.

219. Nedergaard J, Bengtsson T, Cannon B. Unexpected evidence for active brown adipose tissue in adult humans. *Am J Physiol Endocrinol Metab*. 2007;293:444-452. doi:10.1152/ajpendo.00691.2006.

220. Cypess AM, Lehman S, Williams G, et al. Identification and importance of brown adipose tissue in adult humans. *N Engl J Med*. 2009;360(15):1509-1517. doi:10.1097/OGX.0b013e3181ac8aa2.

221. Virtanen KA, Lidell ME, Orava J, et al. *Functional Brown Adipose Tissue in Healthy Adults.*; 2009. doi:10.1056/NEJMoa0808949.

222. Ruth M. Cold-Activated Brown Adipose Tissue in Healthy Men. *Yearb Endocrinol*. 2010;2010:115-117. doi:10.1016/S0084-3741(10)79546-9.

223. Kozak LP. Brown Fat and the Myth of Diet-Induced Thermogenesis. *Cell Metab*. 2010;11(4):263-267. doi:10.1016/j.cmet.2010.03.009.

224. Rothwell NJ, Stock MJ. A role for brown adipose tissue in diet-induced thermogenesis. *Obes Res*. 1997;5(6):650-656. doi:10.1038/281031a0.

225. Weitzel JM, Iwen KAH, Seitz HJ. Regulation of mitochondrial biogenesis by thyroid hormone. *Exp Physiol*. 2003;88(1):121-128. doi:10.1113/eph8802506.

226. Wu J, Boström P, Sparks LM, et al. Beige adipocytes are a distinct type of thermogenic fat cell in mouse and human. *Cell*. 2012;150(2):366-376. doi:10.1016/j.cell.2012.05.016.

227. Rosenwald M, Wolfrum C. The origin and definition of brite versus white and classical brown adipocytes. *Adipocyte*. 2014;3(1):4-9. doi:10.4161/adip.26232.

228. Park A, Kim WK, Bae K-H. Distinction of white, beige and brown adipocytes derived from mesenchymal stem cells. *World J Stem Cells*. 2014;6(1):33-42. doi:10.4252/wjsc.v6.i1.33.

229. Vázquez-Vela MEF, Torres N, Tovar AR. White Adipose Tissue as Endocrine Organ and Its Role in Obesity. *Arch Med Res*. 2008;39(8):715-728. doi:10.1016/j.arcmed.2008.09.005.

230. Rosell M, Kaforou M, Frontini A, et al. Brown and white adipose tissues: intrinsic differences in gene expression and response to cold exposure in mice. *Am J Physiol Endocrinol Metab*. 2014;306(8):E945-E964. doi:10.1152/ajpendo.00473.2013.

231. Wang G-X, Zhao X-Y, Lin JD. The brown fat secretome: metabolic functions beyond thermogenesis. *Trends Endocrinol Metab*. 2015;(II):1-7. doi:10.1016/j.tem.2015.03.002.

232. Hondares E, Iglesias R, Giralt A, et al. Thermogenic activation induces FGF21 expression and release in brown adipose tissue. *J Biol Chem*. 2011;286(15):12983-12990. doi:10.1074/jbc.M110.215889.

233. Badman MK, Pissios P, Kennedy AR, Koukos G, Flier JS, Maratos-Flier E. Hepatic Fibroblast Growth Factor 21 Is Regulated by PPARα and Is a Key Mediator of Hepatic Lipid Metabolism in Ketotic States. *Cell Metab*. 2007;5(6):426-437. doi:10.1016/j.cmet.2007.05.002.

234. Owen BM, Ding X, Morgan DA, et al. FGF21 Acts Centrally to Induce Sympathetic Nerve Activity, Energy Expenditure, and Weight Loss. *Cell Metab*. 2014;20(4):670-677. doi:10.1016/j.cmet.2014.07.012.

235. Tseng Y-H, Kokkotou E, Schulz TJ, et al. New role of bone morphogenetic protein 7 in brown adipogenesis and energy expenditure. *Nature*. 2008;454(7207):1000-1004. doi:10.1038/nature07221.

236. Zamani N, Brown CW. Emerging roles for the transforming growth factor-β superfamily in regulating adiposity and energy expenditure. *Endocr Rev*. 2011;32(3):387-403. doi:10.1210/er.2010-0018.

237. Qian S-W, Tang Y, Li X, et al. BMP4-mediated brown fat-like changes in white adipose tissue alter glucose and energy homeostasis. *Proc Natl Acad Sci U S A*. 2013;110(9):E798-E807. doi:10.1073/pnas.1215236110.

238. Petruzzelli M, Schweiger M, Schreiber R, et al. A Switch from White to Brown Fat Increases Energy Expenditure in Cancer-Associated Cachexia. *Cell Metab*. 2014;20(3):433-447. doi:10.1016/j.cmet.2014.06.011.

239. Wallenius V, Wallenius K, Ahrén B, et al. Interleukin-6-deficient mice develop mature-onset obesity. *Nat Med*. 2002;8(1):75-79. doi:10.1038/nm0102-75.

240. Yore MM, Syed I, Moraes-vieira PM, et al. Discovery of a Class of Endogenous Mammalian Lipids with Anti-Diabetic and Anti-inflammatory Effects. *Cell*. 2014;159(2):318-332. doi:10.1016/j.cell.2014.09.035.

241. Stanford KI, Middelbeek RJW, Townsend KL, et al. Brown adipose tissue regulates glucose homeostasis and insulin sensitivity. *J Clin Invest*. 2013;123(1):215-223. doi:10.1172/JCI62308DS1.

242. Conarello SL, Jiang G, Mu J, et al. Glucagon receptor knockout mice are resistant to diet-induced obesity and streptozotocin-mediated beta cell loss and hyperglycaemia. *Diabetologia*. 2007;50(1):142-150. doi:10.1007/s00125-006-0481-3.

243. Tudurí E, Marroquí L, Soriano S, et al. Inhibitory effects of leptin on pancreatic alpha-cell function. *Diabetes*. 2009;58(7):1616-1624. doi:10.2337/db08-1787.

244. Lipton JM, Glyn JR. Central administration of peptides alters thermoregulation in the rabbit. *Peptides*. 1980;1(1):15-18. doi:10.1016/0196-9781(80)90029-7.

245. Billington CJ, Briggs JE, Link JG, Levine AS. Glucagon in physiological concentrations stimulates brown fat thermogenesis in vivo. *Am J Physiol*. 1991;261(2 Pt 2):R501-R507.

246. Kinoshita K, Ozaki N, Takagi Y, Murata Y, Oshida Y, Hayashi Y. Glucagon is essential for adaptive thermogenesis in brown adipose tissue. *Endocrinology*. 2014;155(August):en20141175. doi:10.1210/en.2014-1175.

247. Billington CJ, Bartness TJ, Briggs J, Levine a S, Morley JE. Glucagon stimulation of brown adipose tissue growth and thermogenesis. *Am J Physiol*. 1987;252(1 Pt 2):R160-R165.

248. Dicker A, Zhao J, Cannon B, et al. Apparent thermogenic effect of injected glucagon is not due to a direct effect on brown fat cells Apparent thermogenic effect of injected glucagon is not due to a direct effect on brown fat cells. 2013.

249. Filali-Zegzouti Y, Abdelmelek H, Rouanet JL, Cottet-Emard JM, Pequignot JM, Barré H. Role of catecholamines in glucagon-induced thermogenesis. *J Neural Transm*. 2005;112(4):481-489. doi:10.1007/s00702-004-0199-7.

250. Joel CD. Stimulation of metabolism of rat brown adipose tissue by addition of lipolytic hormones in vitro. *J Biol Chem*. 1966;241(4):814-821.

251. Chiamolera MI, Wondisford FE. Minireview: Thyrotropin-releasing hormone and the thyroid hormone feedback mechanism. *Endocrinology*. 2009;150(3):1091-1096. doi:10.1210/en.2008-1795.

252. Kaneto a., Kosaka K. Stimulation of glucagon secretion by oxytocin. *Endocrinology*. 1970;87(2):439-444.

253. Rocheleau J V, Walker GM, Head WS, McGuinness OP, Piston DW. Microfluidic glucose stimulation reveals limited coordination of intracellular Ca2+ activity oscillations in pancreatic islets. *Proc Natl Acad Sci U S A*. 2004;101(35):12899-12903. doi:10.1073/pnas.0405149101.

254. Benninger RKP, Hutchens T, Head WS, et al. Intrinsic Islet Heterogeneity and Gap Junction Coupling Determine Spatiotemporal Ca2+ Wave Dynamics. *Biophys J*. 2014;107(11):2723-2733. doi:10.1016/j.bpj.2014.10.048.

255. Song KM, Lee S, Ban C. Aptamers and their biological applications. *Sensors*. 2012;12(1):612-631. doi:10.3390/s120100612.

256. E. Wang R, Zhang Y, Cai J, Cai W, Gao T. Aptamer-Based Fluorescent Biosensors. *Curr Med Chem*. 2011;18(27):4175-4184. doi:10.2174/092986711797189637.

257. Song S, Wang L, Li J, Fan C, Zhao J. Aptamer-based biosensors. *TrAC - Trends Anal Chem*. 2008;27(2):108-117. doi:10.1016/j.trac.2007.12.004.

258. Stoltenburg R, Reinemann C, Strehlitz B. FluMag-SELEX as an advantageous method for DNA aptamer selection. *Anal Bioanal Chem*. 2005;383(1):83-91. doi:10.1007/s00216-005-3388-9.

259. Vater A, Sell S, Kaczmarek P, et al. A mixed mirror-image DNA/RNA aptamer inhibits glucagon and acutely improves glucose tolerance in models of type 1 and type 2 diabetes. *J Biol Chem*. 2013;288(29):21136-21147. doi:10.1074/jbc.M112.444414.

260. D'Agata R, Spoto G. Artificial DNA and surface plasmon resonance. *Artif DNA PNA XNA*. 2012;3(2):45-52. doi:10.4161/adna.21383.

261. Huang K, Martí A a. Recent trends in molecular beacon design and applications. *Anal Bioanal Chem*. 2012;402(10):3091-3102. doi:10.1007/s00216-011-5570-6.

262. Brinton LT, Sloane HS, Kester M, Kelly K a. Formation and role of exosomes in cancer. *Cell Mol Life Sci*. 2014;72(4):659-671. doi:10.1007/s00018-014-1764-3.

263. Frydrychowicz M, Kolecka-Bednarczyk a., Madejczyk M, Yasar S, Dworacki G. Exosomes - Structure, Biogenesis and Biological Role in Non-Small-Cell Lung Cancer. *Scand J Immunol*. 2015;81(1):2-10. doi:10.1111/sji.12247.

264. Yamashita T, Kamada H, Kanasaki S, et al. Epidermal growth factor receptor localized to exosome membranes as a possible biomarker for lung cancer diagnosis. *Pharmazie*. 2013;68(12):969-973. doi:10.1691/ph.2013.3599.

265. Higginbotham JN, Demory Beckler M, Gephart JD, et al. Amphiregulin exosomes increase cancer cell invasion. *Curr Biol*. 2011;21(9):779-786. doi:10.1016/j.cub.2011.03.043.

266. Wahren J, Larsson C. C-peptide: New findings and therapeutic possibilities. *Diabetes Res Clin Pract*. 2015;107(3):309-319. doi:10.1016/j.diabres.2015.01.016.

267. Yosten GLC, Maric-Bilkan C, Luppi P, Wahren J. Physiological effects and therapeutic potential of proinsulin C-peptide. *AJP Endocrinol Metab*. 2014;307(11):E955-E968. doi:10.1152/ajpendo.00130.2014.

268. Tomoda H, Kishimoto Y, Lee YC. Temperature effect on endocytosis and exocytosis by rabbit alveolar macrophages. *J Biol Chem*. 1989;264(26):15445-15450.

269. Bittner MA, Holz RW. A temperature-sensitive step in exocytosis. *J Biol Chem*. 1992;267(23):16226-16229.

270. Nouvian R. Temperature enhances exocytosis efficiency at the mouse inner hair cell ribbon synapse. *J Physiol*. 2007;584(Pt 2):535-542. doi:10.1113/jphysiol.2007.139675.

271. Nlend RN, Michon L, Bavamian S, et al. Connexin36 and pancreatic beta-cell functions. *Arch Physiol Biochem*. 2006;112(2):74-81. doi:10.1080/13813450600712019.

272. Gucciardo E, Sugiyama N, Lehti K. Eph- and ephrin-dependent mechanisms in tumor and stem cell dynamics. *Cell Mol Life Sci*. 2014:3685-3710. doi:10.1007/s00018-014-1633-0.

273. Winning RS, Ward EK, Scales JB, Walker GK. EphA4 catalytic activity causes inhibition of RhoA GTPase in Xenopus laevis embryos. *Differentiation*. 2002;70(1):46-55. doi:10.1046/j.1432-0436.2002.700105.x.

274. Jellinghaus S, Poitz DM, Ende G, et al. Ephrin-A1/EphA4-mediated adhesion of monocytes to endothelial cells. *Biochim Biophys Acta - Mol Cell Res*. 2013;1833(10):2201-2211. doi:10.1016/j.bbamcr.2013.05.017.

275. Lisabeth EM, Falivelli G, Pasquale EB. Eph receptor signaling and ephrins. *Cold Spring Harb Perspect Biol*. 2013;5(9). doi:10.1101/cshperspect.a009159.

276. Dries JL, Kent SD, Virag J a I. Intramyocardial administration of chimeric ephrinA1-Fc promotes tissue salvage following myocardial infarction in mice. *J Physiol*. 2011;589(Pt 7):1725-1740. doi:10.1113/jphysiol.2010.202366.

277. Månsson-Broberg A, Siddiqui AJ, Genander M, et al. Modulation of ephrinB2 leads to increased angiogenesis in ischemic myocardium and endothelial cell proliferation. *Biochem Biophys Res Commun*. 2008;373(3):355-359. doi:10.1016/j.bbrc.2008.06.036.

278. Noren NK, Foos G, Hauser C a, Pasquale EB. The EphB4 receptor suppresses breast cancer cell tumorigenicity through an Abl-Crk pathway. *Nat Cell Biol*. 2006;8(8):815-825. doi:10.1038/ncb1438.